ISTANBUL TECHNICAL UNIVERSITY ★ GRADUATE SCHOOL OF SCIENCE ENGINEERING AND TECHNOLOGY

COMPARISON OF SCALED REAL STRONG MOTIONS AND TURKISH EARTHQUAKE DESIGN SPECTRUM FOR MODERN REINFORCED CONCRETE MINARETS

M.Sc. THESIS

Keyvan DEHGHANIAN
(501121028)

Department of Civil Engineering

Structure Engineering Programme

Thesis Advisor: Assoc.Prof. Dr.Mustafa Gençoğlu

October 2015

İSTANBUL TEKNİK ÜNİVERSİTESİ ★ FEN BİLİMLERİ ENSTİTÜSÜ

MODERN BETONARME MINARELER IÇIN ÖLÇEKLI GERÇEK DEPREM KAYITLARININ VE TÜRK DEPREM YÖNETMELIĞI (DBYBHY, 2007) TASARIM SPECTRUM KARŞILAŞTIRILMASI

YÜKSEK LİSANS TEZİ

Keyvan DEHGHANIAN
(501121028)

İnşaat Mühendisliği Anabilim Dalı

Yapı Mühendisliği Programı

Tez Danışmanı: Doç.Dr. Mustafa Gençoğlu

Ekim 2015

Keyvan Dehghanian, a **M.Sc.** student of ITU **Graduate School of Science and Technology** student ID **501121028,** successfully defended the **thesis/dissertation** entitled "**COMPARISON OF SCALED REAL STRONG MOTIONS ANDTURKISH EARTHQUAKE DESIGN SPECTRUM FOR MODERN REINFORCED CONCRETE MINARETS**", which he prepared after fulfilling the requirements specified in the associated legislations, before the jury whose signatures are below.

Thesis Advisor: **Asst.Prof. Dr.Mustafa Gençoğlu**
İstanbul Technical University

Jury Members: **Prof.Dr.KadirGüler**
İstanbul Technical University

Yrd.Doç.Dr. SemaAlacalı
Yıldız Technical University

Date of Submission: 8September 2015
Date of Defence: 8September 2015

To my family and spouse for their unrelenting support,

FOREWORD

Due to various Active fault lines in this region the risk of devastating earthquakes is a real time threat. Many experienced lives and property losses during large earthquakes that took place in the past. As the culture and the heritage of these lands Islamic architecture plays a crucial role and with that safety of these structures becomes a much more important topic.

The lack of specialized and detailed instructions for design of such structures in Turkish codes and reliance only on experience creates an uneasiness towards the newly built or under construction structures of this kind.

For this purpose a newly under construction minaret was chosen and designed and calculated separately to control and compare the results of scaled real strong motions effect on the structure with the results obtained from the guidelines provided by TEC 2007.

At the outset, I would like to present my deepest thanks for my first and dependable supporters, my family and following that all my respectable teachers in Istanbul Technical University who helped me change not only my vision of engineering but also of life and My advisor Assoc.Prof. Dr. Mustafa Gençoğlu for his support allowed me to overcome every possible problem in every step of my academic life and broadening my vision.

September 2015

Keyvan Dehghanian
(Civil Engineer)

TABLE OF CONTENTS

Page

ABBREVIATIONS

EMA : Experimental Modal Analysis
CVS : Comma Separated Variables
EFDD : Enhanced Frequency Domain Decomposition
FEM : Finite element model
NGA : Next Generation Attenuation
OMA : Operational Modal Analysis
PGMD : PEER Ground Motion Database
SSI : Stochastic Subspace Identification

LIST OF TABLES

Page

LIST OF FIGURES

COMPARISON OF SCALED REAL STRONG MOTIONS AND TURKISH EARTHQUAKE DESIGN SPECTRUM FOR MODERN REINFORCED CONCRETE MINARETS

SUMMARY

Due to rapid developments in structural analysis and computational facilities, using real Earthquake records for analysis is becoming more common in seismic analysis and design of structures. One of the crucial issues of such analysis is the selection of acceleration time histories to satisfy design code requirements and soil type at a specific site. In literature, there are three sources of acceleration time histories: design response spectrum compatible artificial records, synthetic records obtained from seismological models and Strong Motion Records recorded in real earthquakes. Due to the increase of available strong ground motion database, using and scaling real recorded Strong Motion Records is becoming one of the most contemporary research issues in this field.

Time history-analysis of building structures have been used for a quite long time for research at universities. Considering the advantage of time-history analysis relative to the equivalent static force method, the National Building of Turkey and other modern building codes around the world require the use of time-history analysis in the design of specified types of buildings located in seismic regions. One of the main issues in the use of time-history analysis is related to the selection and scaling of the seismic excitations (i.e., accelerograms) to be compatible with the design spectrum for the location considered. Currently, both recorded (i.e., "real") accelerograms and artificial accelerograms are used in the analysis.

The objective of this study is to determine the effects of the selection and scaling of seismic excitations on the response of reinforced concrete Minarets. Four cases of reinforced concrete Minaret with the total height of 90 and 71 meters, designed for Istanbul (high seismic zone) was used in this study. Four sets of seismic excitations

were used in the analysis – 4 set of “real” accelerograms, obtained by different methods. All sets were scaled to be compatible with the design spectrum for Istanbul. Drifts Along the height and Moments on transition sections were used as response parameters.

The results from the linear analysis show that the type of the excitation set affects both the Drifts Along the height and the Moments on transition sections significantly. Based on the results from this study, sets of scaled real records are preferred for use in time-history analysis of building structures. If such records are not available, then sets of simulated accelerograms based on the regional seismic characteristics should be used.

In this study, basic methodologies and criteria for selecting strong ground motion time histories are discussed and summarized as well as some scaled records are used for comparison with the Turkish code for the Modern day Reinforced concrete minarets. The time domain-scaling procedure is utilized to scale, the available real records to match the proposed elastic design spectrum given in the Turkish earthquake code (TEC, 2007) for different seismic regions and soil types. The best-fitted ground motion time histories are selected and classified taken into account the earthquake magnitude, focal mechanism and site conditions.

MODERN BETONARME MINARELER IÇIN ÖLÇEKLI GERÇEK DEPREMKAYITLARININ VE TÜRK DEPREM YÖNETMELIĞI (DBYBHY, 2007)TASARIM SPECTRUM KARŞILAŞTIRILMASI

ÖZET

Türkiye'nin deprem fay hatlarının yoğun olduğu bir coğrafyada bulunmaktadır. Bu yüzden olası bir depreme karsı her an hazırlıklı olmamız gerekmektedir. Türkiye'de belli aralıklarla deprem yönetmelikleri çıkarılmıştır. 1997 ABYYHY yönetmeliğinden önce yapılan binalar ve yüksek yapılar genellikle deprem performansı açısından yetersiz kalmaktadır. Depreme hazırlık açısından, ülke olarak, yapabileceğimiz en faydalı is, düşük deprem performanslı bu binaların performanslarını değerlendirmek ve gereken değişiklikleri tasarımlarında yapmaktır.

Yapısal analiz ve hesaba dayalı olanaklardaki hızlı gelişmeler sonucu zaman, tanım alanında hesap yöntemleri, sismik analizde ve yapıların tasarımında yaygın olarak kullanılmaktadır. Bu yöntemler kullanılırken ortaya çıkan en önemli sorunlardan biri, yönetmelik gereksinimlerini karşılayan deprem kayıtlarının teminidir. Deprem ivme kayıtları üç kaynaktan elde edilebilir: 1) Tasarım ivme spektrumu uyumlu yapay kayıtlar, 2) Simule edilmiş (benzeştirilmiş) kayıtlar ve 3) Deprem esnasında kaydedilen ivme kayıtlarıdır. Mevcut olan kuvvetli yer hareketi veri bankalarının her geçen gün zenginleşmesi ve bunlara ulaşmanın ilerleyen teknoloji ile birlikte daha da kolaylaşması, gerçek depremlerden alınan kayıtların kullanılması ve ölçeklenmesini en güncel araştırma konularından biri haline getirmiştir. Bu çalışmada, uygun kuvvetli yer hareketi kayıtlarının seçilmesi için önerilen temel yöntemler ve kriterler ortaya konulmaktadır.

Türkiye Deprem Yönetmeliği'nde (DBYBHY, 2007) tanımlanan uyum kriterlerine ve yerel zemin sınıflarına göre seçilen kayıtlar, zaman tanım alanında ölçekleme yöntemleri kullanılarak önerilen tasarım ivme spektrumlarıyla eşleştirilmeye

çalışılmakta ve farklı zemin tipleri için en iyi uyumu sağlayan gerçek kayıtlar seçilmektedir.
Yapısal analiz ve hesaplama cihazların hızlı gelişmeler nedeniyle, analiz için gerçek deprem kayıtlarını kullanımı, sismik analiz ve yapıların tasarımında daha yaygın hale gelmektedir. Böyle bir analizin en önemli konulardan biri, tasarım kod gereklerinin ve zemin tipini karşılayan uygun ivme kayıtlarının seçilmesidir. Mevcut kuvvetli yer hareketi veri tabanı artışı nedeniyle, Gerçek Güçlü kaydedilen ölçeklenmiş kuvvetli yer hareketi kullanımı en güncel araştırma konularından biri haline gelmiştir.

Bina yapılarının analizinde zaman tanım alanında hesap yöntemi üniversitelerde araştırma için oldukça uzun bir süredir kullanılmaktadır. Zaman tanım alanı yönteminin Eşdeğer statik kuvvet yöntemine göre analiz karşılaştırıldığında avantajı göz önüne alınıp, Türkiye Ulusal Yapı ve dünyadaki diğer modern bina kodları sismik bölgelerde bulunan binaların belirtilen türde tasarımında zaman tanım alanı analizi kullanılmasını gerektirir. Zaman tanım alanı analizi kullanımında önemli konulardan biri olarak kabul konumu tasarım spektrumu ile uyumlu olacak şekilde sismik titreşim (yani, İvme) seçimi ve ölçekleme ile ilgilidir. Şu anda, iki kayıt (yani, "gerçek") ivme ve yapay ivme deprem analizlerinde kullanılır.
Bu çalışmanın amacı, sismik titreşim seçimi ve ölçekleme etkisini yeni bir betonarme Minare üzerinde araştırmaktır. Tasarlanmış toplam 90 metre yüksekliğinde betonarme Minare, İstanbul'da (yüksek sismik bölge) bulunmakta ve bu çalışmada kullanılmıştır.

Beş set sismik titreşim analizde kullanılmıştır - Farklı yöntemlerle elde edilen 5 set "gerçek" ivme. Tüm setleri İstanbul için tasarım spektrumu ile uyumlu olacak şekilde ölçeklendirildi ve hesaba dâhil edildi. Yüksekliğinde tepe noktasında yer değiştirme ve geçiş bölümlerinde momentler ve kesme küvetleri parametre olarak kullanılmıştır.
Bu çalışmanın sonuçlarına göre, ölçekli gerçek kayıt setlerinde bina yapılarının zaman alanı analizinde kullanım için tercih edilmesidir. Bu tür kayıtlar mevcut değilse, o zaman bölgesel sismik özelliklerine göre simüle edilmiş ivme setleri kullanılmalıdır.

Bu çalışmada, günümüzde yapılan modern betonarme minarelerin Türk deprem yönetmenliği tasarlanıp, gerçek ivme kayıtları ile karşılaştırılmasi için temel metodolojileri ve kriterleri özetlenmiştir. Zaman alanı ölçekleme işlemi farklı sismik

bölgelerde ve zemin tipleri için Türk deprem kodunda (DBYBHY, 2007) verilen önerilen elastik tasarım spektrumu ile uyumlu ölçeklenmiş gerçek kayıtları kullanılır. Deprem büyüklüğü, odak mekanizması ve saha koşullarına bakarak en iyi uyum sağlayan yer hareketleri seçilir ve analiz koşullarını sağlanmıştır ve minare performansı her kayıt için değerlendirilmiştir.

1. INTRODUCTION

Traditionally, the calculation of seismic loads acting on the structure of is done with either "Equivalent Static Seismic Load Method "or" Modal Analysis ".

In recent years, structural analysis with rapid increase in technology, the nonlinear-inelastic calculation method is widely used in the design and analysis of structures.
In the time domain linear or nonlinear elastic the most important issue in the realization of these analysis, is selection of appropriate seismic scalable records.

Dynamic analysis of structures is extensively used in research at universities.
Until recently, it has not been used in practical seismic design or evaluations of buildings. However, recent editions of modern building codes around the world require the use of the dynamic analysis method in the seismic design of buildings located in regions with high seismicity (e.g., NRCC 2005; ASCE 2006; European Committee for Standardization2004; Standards New Zealand 2004). The codes allow the use of linear and nonlinear dynamic analysis.

Linear dynamic analysis can be conducted using the response spectrum method orthe numerical integration linear time-history method. The response spectrum method is quite straightforward because the seismic forces according to this method are related directly to the design spectrum and the mode periods. For the numerical integration linear and nonlinear time-history analysis methods, however, acceleration time histories (i.e.,accelerograms) are needed. The codes require that these accelerograms be compatible with the design spectrum. An accelerogram is considered to be compatible with a given design spectrum if the 5% damped response spectrum of the accelerogram is close to the design spectrum within a specified period range, which is usually referred to as the period range of interest. Other important quantities related to the use of spectrum compatible accelerograms are the number of accelerograms for use in the analysis, and the degree of the compatibility of the accelerograms with the design spectrum (i.e., how much the spectra of the accelerograms should be close to the design spectrum).

It is possible to mention that earthquake records can be obtained from three different sources:

The design spectrum records is created using artificial ways(,By RSPMATCH The program developed by Abrahamson), source and wave propagation characteristics simulated physically (simulated) records (e.g.SMSMSwith the help of a program developed byBoora) and derived from the actual earthquake records. The number of entries received during the earthquake and their increasing day by day with developing technologies to facilitate access to data transfer time in the field definition in the analysis to be performed, has made the actual records the most preferred option.

The criteria used for selecting the records for real strong motions according to the design spectrum in a given area should include geological and seismological conditions. The magnitude of the earthquake, fault type, the distance to the fault of the study area, tearing direction, local soil conditions and spectral content are the most important of these conditions.

After determining the criteria to be used for matching and to be applied to the actual recordings, a scaling method should be determined for making an adequate approximation that is satisfactory. To obtain the linear scaling factor, spectral amplitude can be used. In some special cases a scaling can be done changing the frequency content and duration of the time axis without increasing the number of cycles. One of the most important issues to be considered in the records obtained after the scaling Process re is to protect the amplitude and intensity in the actual recording.

In this study, a general method and criteria for the selection of earthquake records detailed are considered to be used in our case study of the modern designed and constructed Reinforced concrete Minarets . In TEC (2007), located for each seismic zone and each ground class the appropriate records to the specified seismic design are chosen and faulting type and ground conditions taken into account. For the Selected real earthquake records, 5% damping ratio of a linear single degree of freedom system is calculated. The resulting spectrum is used in the Analysis of the mentioned case model of this study.

1.1 Purpose of Thesis

The objective of this study is to investigate the effects of the selection and scaling of seismic excitations on the response of modern reinforced concrete minarets and have a comparison between the results acquired from a linear analysis using the response spectrum from the Turkish earthquake code. The maximum interstorey drifts and story shears are used as response parameters. In order to achieve this objective, the tasks conducted and described in this thesis are as follows:

- Review of relevant literature,
- Design and modelling of the minaret used in the analysis,
- Selection and scaling of the seismic motions,
- Linear analysis of the structure
- Comparison between the results

1.2 Literature Review

Minarets are generally thin and tall engineering structures such as towers. The earliest mosques were built without minarets.

The tallest minaret in the world with 210 m is pertained Hassan II Mosque in Casablanca, Morocco.

Minarets have various architectural features of time and region, when and where they were built. For instance, in 13th century Syrian architecture, minarets were built with low square towers sitting at the four corners of mosques. In 15th century Egyptian architecture, minarets were built with an octagonal shape and generally had two balconies—the upper is smaller than the lower. Iraqi style minarets are a free standing conical shape surrounded by a spiral staircase. Moroccan style minarets are normally square, and many mosques generally have a single minaret. Finally, Ottoman style minarets are slim and have a circular shape.

(a) (b) (c)

Figure 1.1: Minaret styles related to regional architectures.(a) Persian style minarets; (b) Morocco style minarets; (c) Ottoman style minarets

Minarets basically consist of three parts such as base, shaft and gallery. The base is reached from soil to floor. The shaft is a thin body of the minaret and stairs are placed cylindrically in the shaft to provide the necessary structural support for highly elongated shafts. The gallery is a balcony which encircles the upper section where the muezzins call out to pray. It is covered by a roof-like canopy and adorned with ornaments such as decorative bricks, and decorated with painted tiles, cornices, arches and inscriptions. In Ottoman style, parts of a minaret are: (a) footing as a base; (b) pulpit, transition segment, cylindrical or polygonal body as a shaft; (c) balcony; (d) upper part of a minaret body; (e) spire; and (f) flag as shown in Figure 1.2. In many earthquake-prone or high strong wind areas, many of the minarets are partly or completely damaged. One reason for not designing minarets to better withstand these environmental loadings is that the dynamic behaviour of the minarets is not adequately known. The dynamic behaviour of the minarets is related to their modal characteristics, such as natural frequencies, mode shapes and damping ratios. This unknown behaviour is a result of assumptions in design criteria and construction, uncertainties in geometrical and material properties, or some modelling uncertainties related to the lack of information on the as-built structure such as boundary conditions. Therefore, the current behaviour of the minarets has to be determined to look like the other engineering structures, especially against dynamic loads such as earthquake and wind. However, it is difficult to determine the behaviour of these structures by theoretical studies because of the aforementioned reasons. To determine modal behaviour or the dynamic characteristics of the minarets, modal testing

including ambient vibration testing and experimental modal analysis is used, which removes these uncertainties.

Modal testing is a popular technique for studying the behaviour of a structure through a number of natural frequencies and mode shapes. Various methods, including both time and frequency domain based, are available for extracting modal information from the dynamic response of a structure and the corresponding input excitation. The process of establishing the dynamic characteristics of a system from an experimental model is known as system identification (Ewins, 1984; Juang, 1994; Ljung, 1987).

Modal testing of structures is not a recent practice, and many studies have been carried out in the past. Modal testing was originally developed in the more advanced mechanical and aerospace engineering disciplines (Maia and Silva, 1997), where modal parameter identification is based on both input and output measurements. After the modal testing procedure transferred to the civil engineering discipline, this procedure was successfully implemented on different types of civil engineering structures, such as bridges (Brownjohn et al., 1992; Deger et al., 1996; Brownjohn, 1997; Zivanovicet al., 2006; Bayraktar et al., 2007), buildings (Ventura et al., 2002; Sortis et al., 2005), historical masonry towers (Gentile and Saisi, 2007) and silos (Dooms et al., 2006).

In modal testing, there are basically two different methods available to experimentally identify the dynamic characteristics of a structure: Experimental Modal Analysis (EMA) and Operational Modal Analysis (OMA) (Cantieni, 2004). In EMA, the structure is excited by a known input force (such as impulse hammers, drop weights and electrodynamics shakers), and responses of the structure are measured. In OMA, the structure is excited by an unknown input force (ambient vibrations such as traffic, wind and earthquake loads), and responses of the structure are measured. Some heavy-force excitations become very expensive and sometimes may cause possible damage to the structure. But, ambient excitations such as traffic, wave, wind, earthquake and their combinations, are environmental or natural excitations. Therefore, the system identification techniques through ambient vibration measurements become very attractive. In this case, only the response data of ambient vibrations are measurable, although actual loading conditions are

unknown (Roeck et al., 2000). In OMA, some techniques in frequency and time domain are used to determine the dynamic characteristics of structures.

These techniques are: (a) Enhanced Frequency Domain Decomposition (EFDD) and Frequency Domain Subspace in frequency domain; and (b) Stochastic Subspace Identification (SSI), Poly reference Complex Exponential, Eigen system Realization Algorithm and Ibrahim Time Domain in time domain.

In the modern analysis of structures, much effort is devoted to the derivation of accurate models. These accurate models are used in many applications of civil engineering structures like damage detection, structural control, structural evaluation and assessment. In the development of the finite element model (FEM) of structures, it is common to make simplifying assumptions. The FEM of a structure is constructed on the basis of highly idealized engineering blueprints and designs that may or may not truly represent all the physical aspects of an actual structure. When field dynamic tests are performed to validate the analytical model, commonly natural frequencies and mode shapes do not coincide with the expected results from the analytical model. These discrepancies originate from the uncertainties in simplifying assumptions of structural geometry, materials, as well as inaccurate boundary conditions. The problem of how to modify the analytical model from the dynamic measurements is known as the model updating in structural dynamics. The main purpose of the model updating procedure is to minimize the differences between the analytically and experimentally obtained modal properties. The updating process typically consists of manual tuning and automatic model updating.

The manual tuning involves manual changes of the model geometry and modelling parameters by trial and error, guided by engineering judgment. The aim of this is to bring the numerical model closer to the experimental one. Often, in this process, an analyst is able to improve the initial structural idealization typically related to boundary conditions and non-structural elements. This process usually includes only a small number of key parameters manageable manually. The aim of automatic updating is to improve further the correlation between the numerical and experimental modal properties by taking into account most of the uncertain parameters. Over the last decade, there have been some model updating techniques used in the literature from mechanical and aerospace engineering to civil structural

engineering (Baruch and Bar Itzhac, 1978; Caesar, 1986; Larsson and Sas, 1992; Imregun et al., 1995; Modak et al., 2002). Although the whole is more difficult to implement in civil engineering, some successful examples of updating in civil engineering can be seen in bridges (Jaishi and Ren, 2005; Zivanovic et al., 2007), buildings (Lord et al., 2004) and high-rise structures (Wu and Li,2004).

Although many studies can be found in the literature for civil engineering structures, there are few articles related to both modal testing, FEM updating and earthquake behavior that are specifically concerned with minarets. In this thesis, a particular minaret is introduced shortly, and the initial FEM and main assumptions made during its development are presented. After that, modal testing of the minaret is explained. Then, the FEM of the minaret is manually updated. Lastly, earthquake behaviour of the minaret is examined before and after model updating, and the results of the study are discussed.

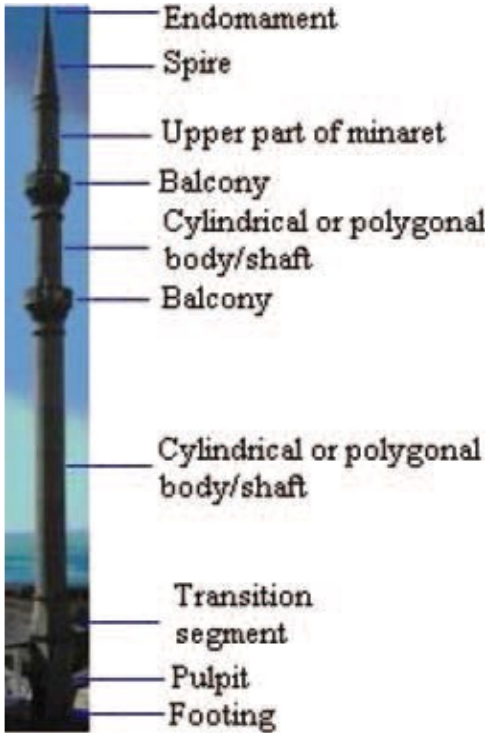

Figure 1.2: Main parts of an Ottoman style minaret.

Earthquakes occurred in Turkey and Turkey Earthquake Map are shown in the figures below. (Figure 1.3 and Figure 1.4)

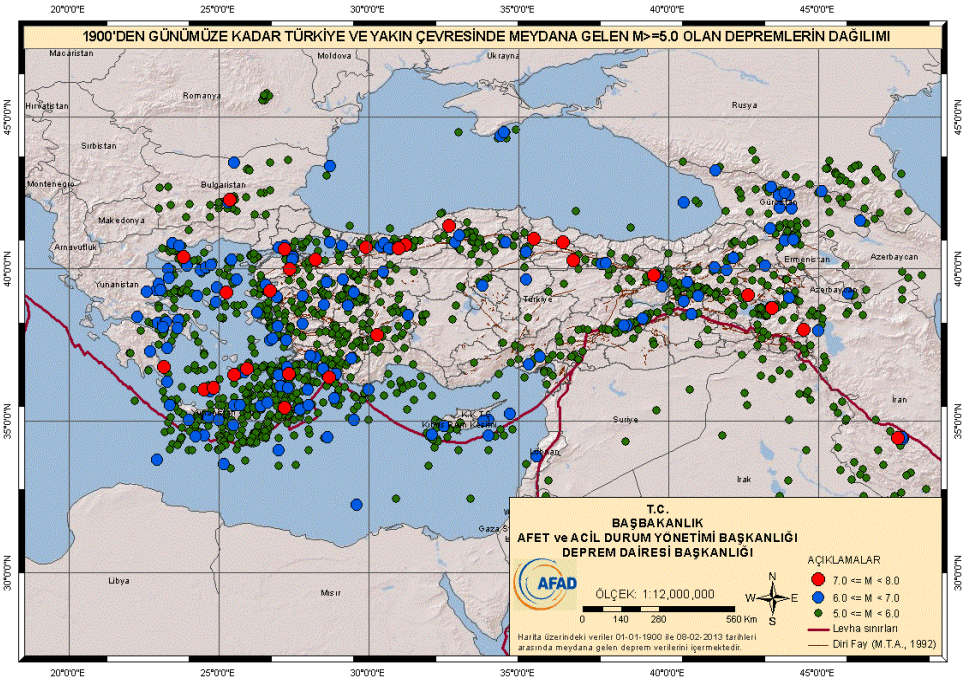

Figure 1.3: Earthquakes occurred in Turkey and in the immediate vicinity.

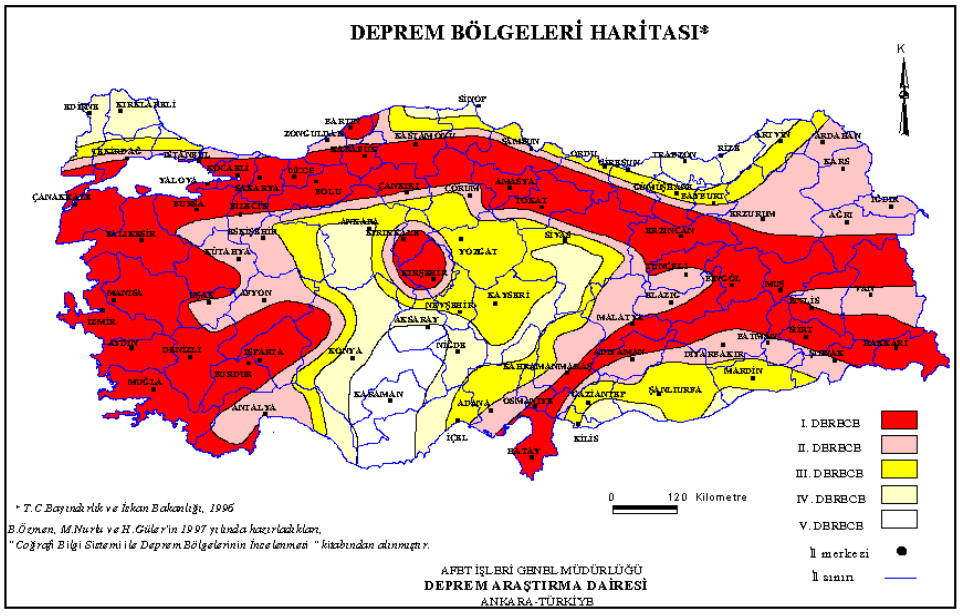

Figure 1.4: Earthquake Zones Map

1.3 Description of the RC minaret

A reinforced concrete (RC) minaret located in Istanbul, Turkey is selected as an application. This minaret was constructed recently through 2014-15. A picture of the mosque and its RC minaret under construction is shown in Figure 1.5(a) and (b).As can be seen in Figures, the minaret is very slim and tall, and has two balconies on its body. In Figure 1.12, the approximate geometrical properties as well as the foreseen reinforcement detail of the minaret can be seen.

Figure 1.5(a)-(b): The minaret.

A minaret is a slender tower built next to a mosque. While most historical minarets were constructed using reinforced or unreinforced stone or brick masonry, the majority of minarets recently constructed in Turkey are reinforced concrete (RC) structures. A typical minaret structure comprises a base or boot on top of its foundation, a tapered transition segment, a circular body or shaft with one or more balconies, and a spire at the top. The base or boot is usually square or polygonal, and is sometimes called the pulpit by architects. The minaret can be free standing or the boot may be attached to the mosque structure.

The minaret contains interior spiral stairs running all the way up to the highest balcony level which are not externally visible. Historically the balconies are built so that someone could climb up the stairs and call for prayer. With the advent of loudspeakers, these balconies are not needed; however, one or more balconies are built in each minaret mainly for architectural reasons. Balconies create mass concentrations along the minaret's height and affect its dynamic structural response.

Currently, there are no structural code requirements or guidelines for the design of reinforced concrete minarets, or minarets in general, in Turkey. As a result, experienced contractors and construction workers with no engineering knowledge have built these slender structures, for the most part. In most cases, each contractor constructs a typical minaret with the same structural and architectural features regardless of the local soil conditions or seismicity of the region.

Turkey is located in one of the most seismically active regions of the world. Fifty-seven destructive earthquakes have struck Turkey in the twentieth century, resulting in the destruction of infrastructure and more than 90.000deaths. During these earthquakes, many minarets were damaged or have collapsed. Sezen et al. documents and discusses vulnerabilities and damages to 64 masonry and RC minarets after the 1999 Kocaeli (Mw7.4) and Duzce(Mw7.2) earthquakes. As a result of these two earthquakes, the collapse of 115 minarets in the city of Duzce alone was reported. Sezen et al. reports that approximately 70% of the RC and masonry minarets surveyed in Duzce sustained severe damage or collapsed. Even though the minarets are hardly ever occupied, they are located mostly in residential areas or shopping districts, and their collapse sometimes causes loss of life. It is extremely important to regulate the construction and design of these slender structures for safety reasons in anticipation of future earthquakes.

This study attempts to identify the structural vulnerabilities of minarets based on their past seismic performance. In addition to widespread earthquake damage and collapses, some reported failures of minarets due to wind loading indicate that most of these tower structures are vulnerable to lateral loads. A large number of research studies investigating the seismic response of historical masonry minarets and towers are available. However, there are only a few studies investigating the lateral response of RC minarets. Dogangun et al. investigate the architectural and structural properties

of these slender structures. The description of each minaret segment and the associated observed damage are presented below.

1.4 Observed damage and implications

The type and distribution of damage in a structure varies greatly depending on many factors, including the detailing and properties of the structure and its components, soil properties, and the magnitude of the earthquake. Acar et al. investigate the effect of local soil conditions on the seismic response of RC minarets. Observations from recent earthquakes suggest that the damage in the minarets is usually concentrated in a few specific locations. These observed local damage concentrations and vulnerabilities of minarets are presented here. Fig. 1.7. Damage to the transition segment.

The relatively stiff boot or base of the minaret normally suffers no damage. The stiffness and strength of the minaret are reduced over the height of the tapered transition segment with a larger square or polygonal shape near its bottom and circular shape near the top. In a few cases, damage over the transition segment was observed. Fig. 1.6 shows two such cases where the concrete cracking or spalling was either spread over the segment or concentrated near the top just below the cylindrical body.

Horizontal circumferential cracks and concrete spalling near the bottom of the minaret cylinder or body were the most common types of damage, leading to the collapse of RC minarets (Fig. 1.7). There are two main reasons for this type of failure.

Figure 1.6:Damage to the transition segment (photos by (a) Firatand (b) Scawthorn).

First, the cross section size becomes smaller, which results in reduced lateral and flexural strength. Second, as shown in Fig. 1.9 in most cases at that location all longitudinal steel bars were lap spliced, creating a discontinuity. Prior to1999, smooth reinforcing bars were commonly used in Turkey because they are less expensive, more readily available than ribbed bars, and easier to bend and cut on site compared with ribbed bars. Considering that the anchorage length required for the smooth longitudinal bars is significantly larger than that of deformed bars, it is most likely that the lap spliced longitudinal bars failed before the full flexural strength could be developed. However, many other minaret collapses, e.g., top two pictures in Fig. 1.7, suggest that failure may have occurred simply because of insufficient flexural strength near the bottom of the cylinder.

The minaret shown in Fig.1.8 survived after the August 17, 1999 Kocaeli earthquake with some apparent distress causing light cracks and concrete spalling near the cylinder base. After nearly three months, during the November 12 Duzce event, the minaret collapsed at the section near the bottom of the cylinder where the smooth longitudinal reinforcing bars had been spliced. The lap splice length was approximately 800 mm. The ends of the longitudinal bars had 180_ hooks (Fig. 1.9).

It appears that the combination of smooth bars with 180end hooks, and the existence of short lap splices created a vulnerable region near the bottom of the cylinder.

Figure 1.7: Minaret failures near the bottom of the cylinder bodies.

Figure 1.8: Minaret in Kocaeli after the August 17 earthquake (minor cracks) and November 12 earthquake (collapse).

At that location, light or insignificant damage was observed after the first earthquake, and collapse occurred after the second event. Anecdotal evidence and the picture of the survived minaret (Fig. 1.8) indicate no significant damage or permanent deformation after the Kocaeli event. This shows that the minaret probably stayed elastic during that earthquake. The typical failure mode (as in Fig. 1.7) after the second event suggests that the minaret was vulnerable near the bottom of its cylindrical body and had very little or no inelastic strength and deformation capacity to resist strong lateral forces during the latter event.

Many similar post-earthquake reconnaissance observations provided evidence for the probable cause of failure, which is typically a result of sudden lateral and flexural strength reduction due to a combination of several factors, including the use of smooth rebar leading to weaker bond between concrete and steel, transverse hoops with hooks rather than continuous spiral reinforcement, short longitudinal lap splices, and the choice of lap splice location where the cross section is reduced to a circle with a smaller size. Furthermore, discontinued longitudinal rebar with 180end hooks seemed to contribute to the sudden stiffness and strength change near the bottom of the cylinder.

Figure 1.9: Splicing of transverse reinforcement and longitudinal bars with 180end hooks.

The collapsed minaret shown in Fig.1.9 is a good example illustrating that the transverse reinforcement had 180_ end hooks and all smooth longitudinal bars with 180_ end hooks were cut at the same location where the failure occurred. At this cross section, due to longitudinal bar end hooks, the amount or effective area of concrete is reduced with both possible poor concrete confinement and potential unnecessary steel congestion. The current Turkish Standards Code (TS 500, 2000) does not allow 180end hooks at the end of longitudinal bars in RC components or

structures. Similarly, the 180hooks at the end of the transverse reinforcement or hoops open up under cyclic loads, and do not confine concrete as effectively as spirals. In minarets which have a ring shaped cross section, the effective confinement of concrete is a challenge. The use of 180 hooks at the end of both longitudinal and transverse steel exacerbates the problem near the bottom of the minaret cylinder where the longitudinal rebar is usually lap spliced.

Structural failure or damage to the upper portion of the cylindrical body of the minarets was observed less frequently. If and when structural damage occurs, it is typically associated with some irregularities such as larger mass or stiffness concentrations around balconies.

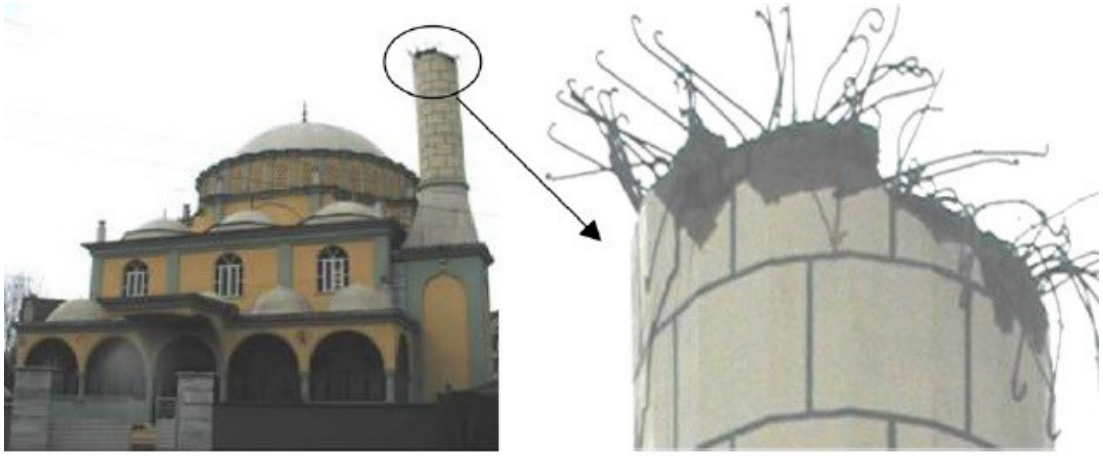

Figure 1.10: Failure around mid-height of a minaret.

Longitudinal rebar often may be lap spliced and not anchored well at those locations. Fig. 6 shows one such case where lap spliced longitudinal rebar with 180_ end hooks exist. No sign of distress or damage at other locations, including the bottom of the cylinder, suggests that longitudinal reinforcement discontinuity created by the lap splices may have been the primary cause of this specific failure.

No damage was reported to the spires that are RC and monolithically connected to the minaret body. Metal sheet is commonly used for spires because of its lightweight and easy installation. There were few instances of metal spire failure over the virtually undamaged minaret body. If the metal spire is anchored to the top of the minaret body properly, no damage should be expected. In almost all cases, as shown in Figs. 1.6through 1.10, the stiffer minaret base or boot is not damaged. Also, the boot is usually attached to the mosque structure, making it relatively rigid.

However, if the boot is not attached to the mosque or if nearby structures of part of the mosque structure hit the boot, the rigid body rotation of the boot and minaret failures may be observed.

The above discussion of minaret failures focused on how and why minarets may have failed during the recent earthquakes in Turkey. In many cases minarets fell on top of the mosque creating a potential structural hazard and causing casualties. It is also possible that the minaret may fall on nearby buildings. During the 17 August earthquake one minaret fell on an otherwise virtually undamaged building causing damage in the upper stories. It is recommended that there should be a safe distance between the minaret and surrounding buildings. To the authors' knowledge, no safe distance requirement exists in the current Turkish design and construction regulations. A practical safe distance from the minaret to the nearest structure could be the cylindrical body length between the top of the transition region and spire.

This assumes that the minaret is not going to fall on the mosque structure and the spire is made up of light metal sheet material.

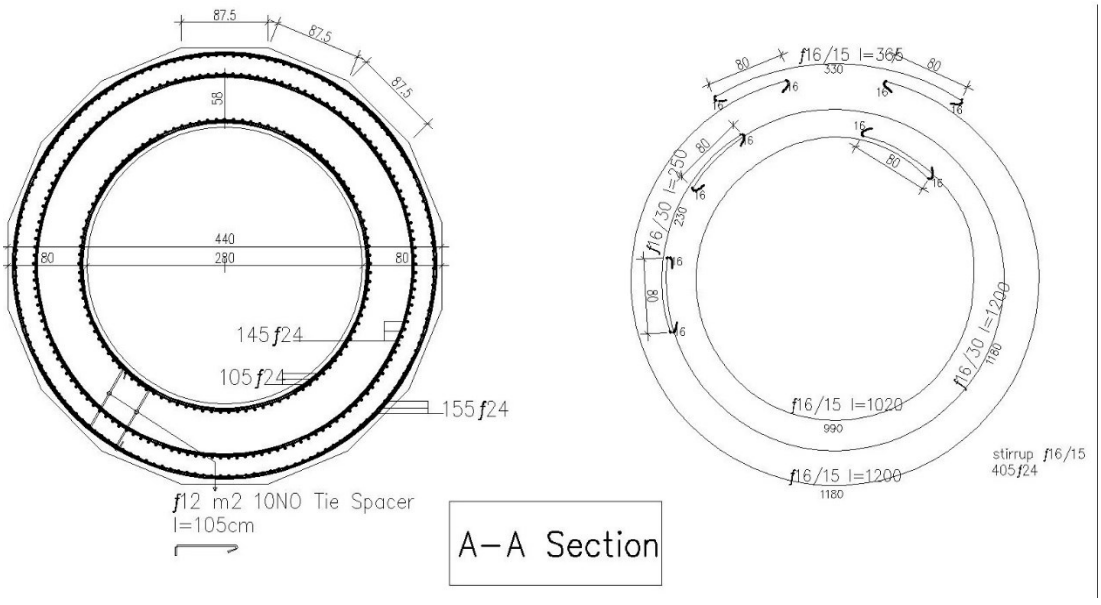

Figure 1.11.1: Geometrical properties of the minaret (Section A-A)

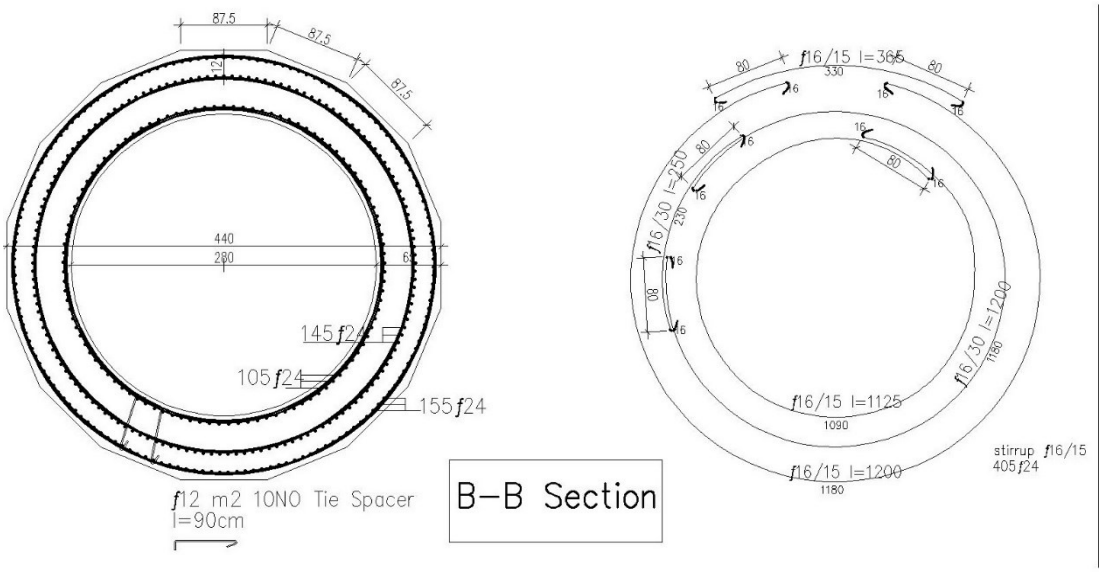

Figure 1.11.2: Geometrical properties of the minaret (Section B-B)

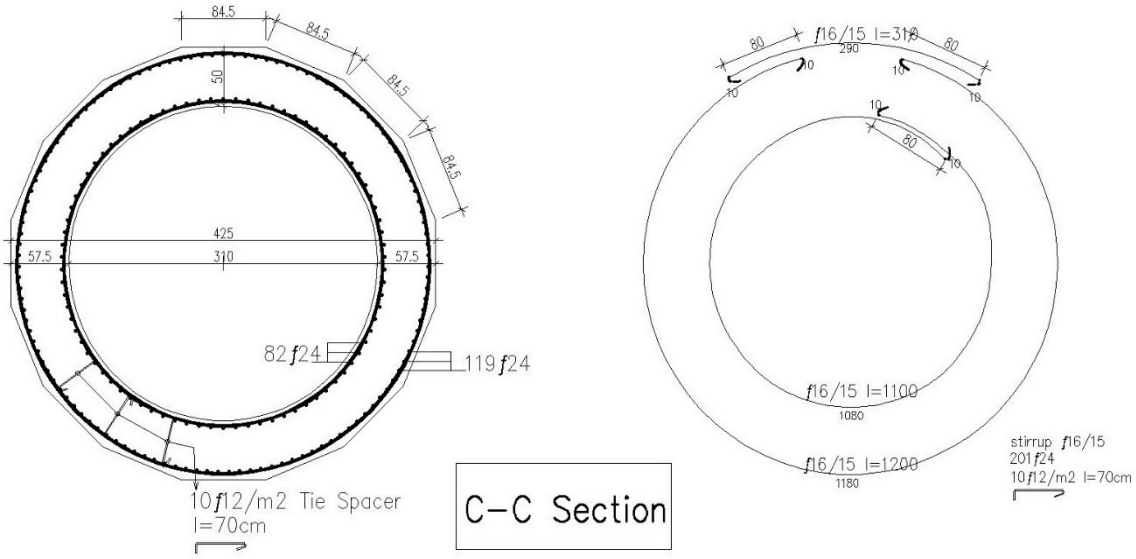

Figure 1.11.3: Geometrical properties of the minaret (Section C-C)

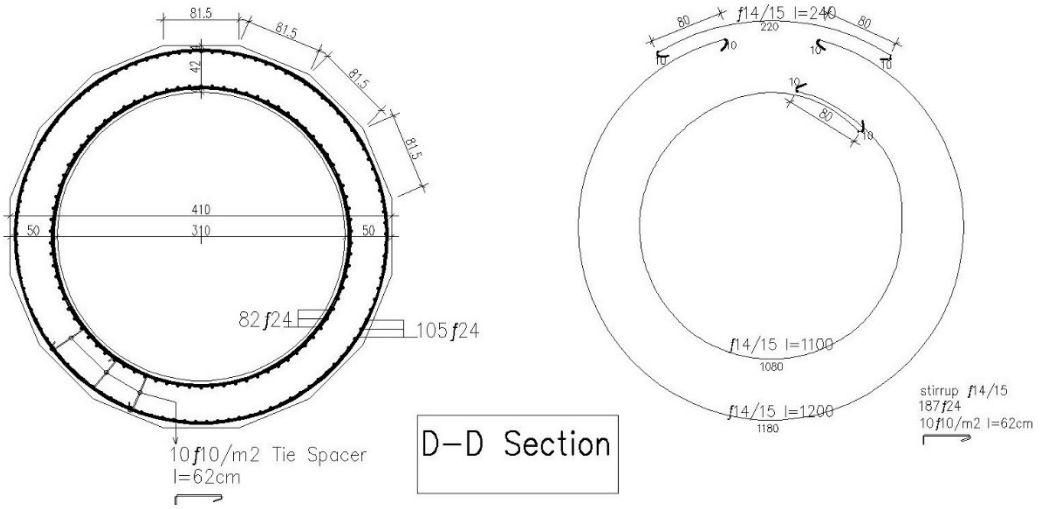

Figure 1.11.4: Geometrical properties of the minaret (Section D-D)

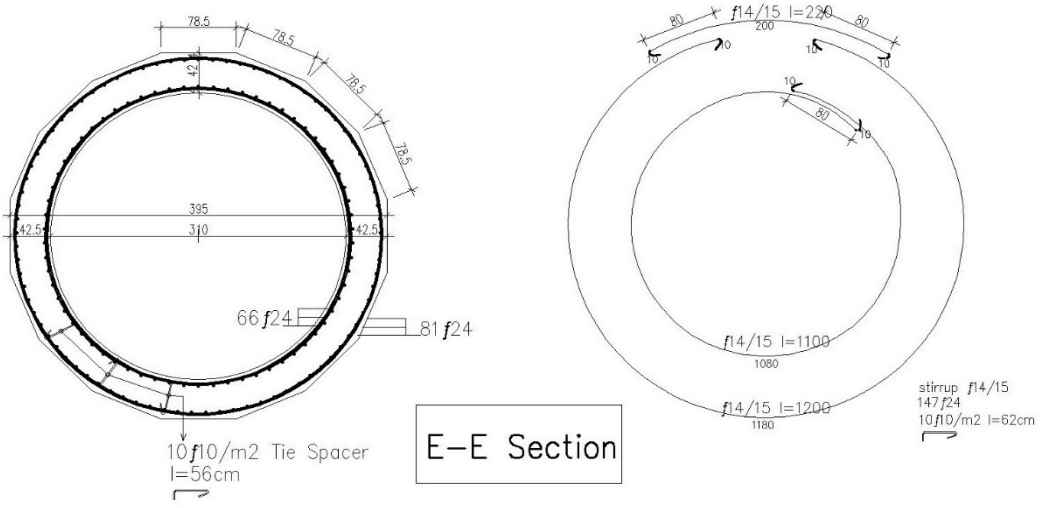

Figure 1.11.5: Geometrical properties of the minaret (Section E-E)

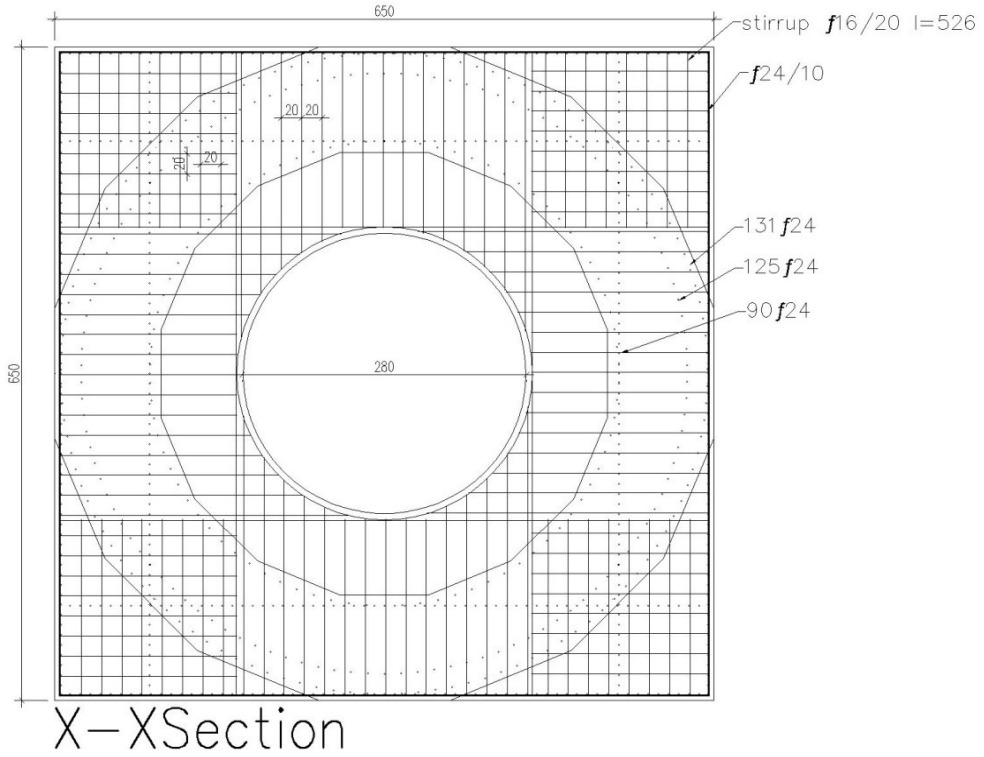

Figure 1.11.6: Geometrical properties of the minaret (Section X-X)

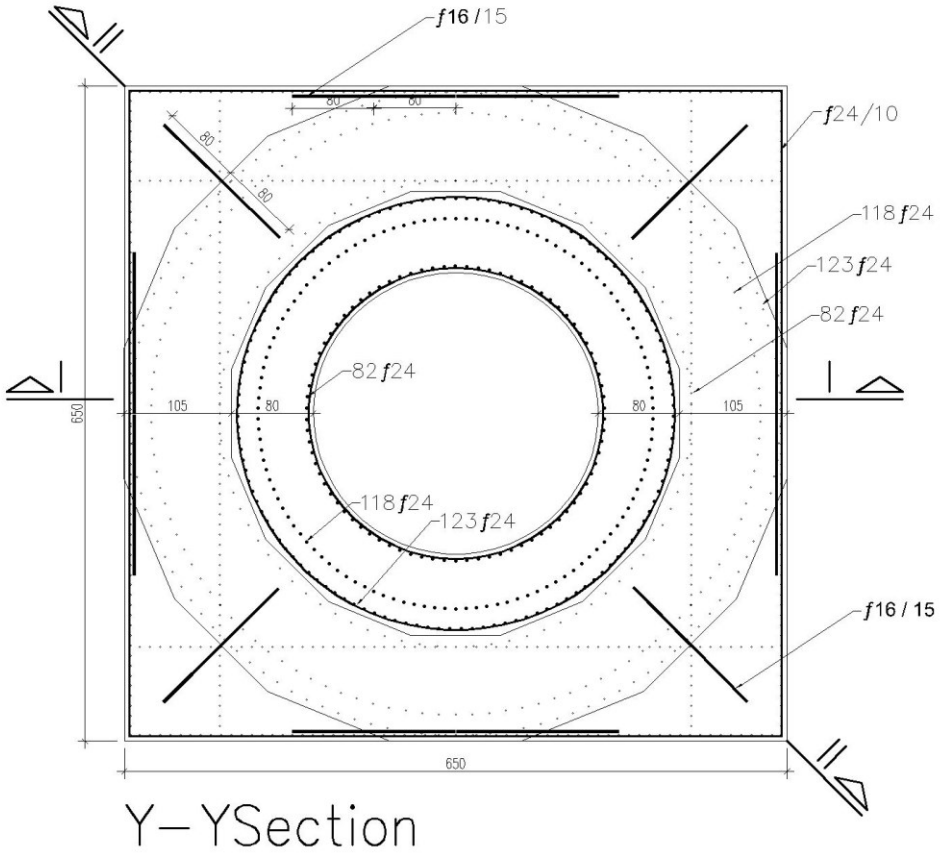

Figure 1.11.7: Geometrical properties of the minaret (Section Y-Y)

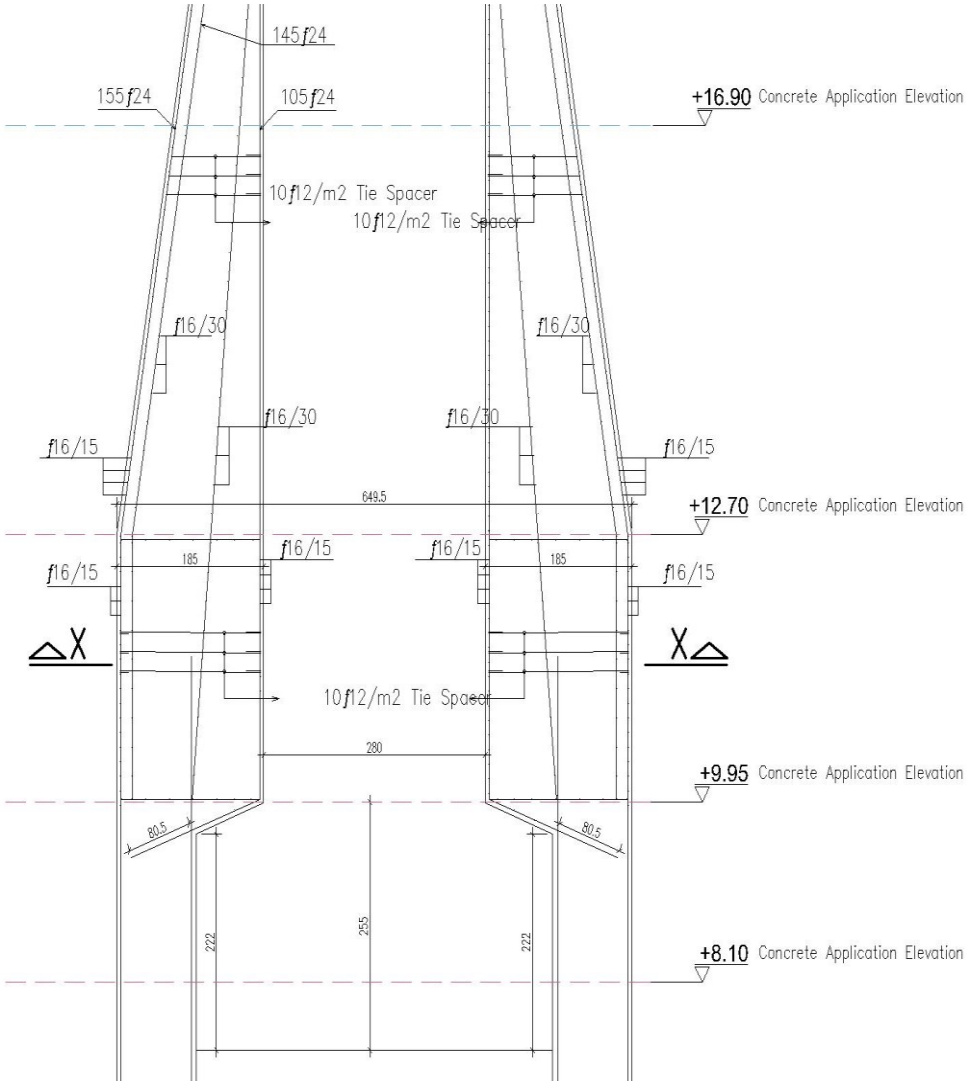

Figure 1.11.8: Geometrical and reinforcement properties of the minaret (Transition segment section)

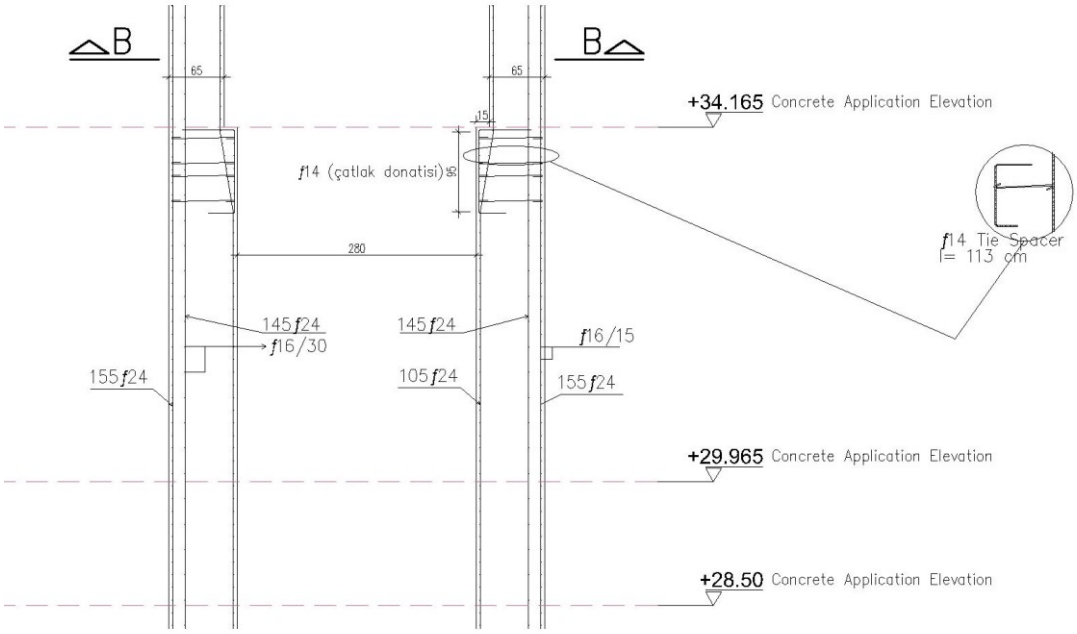

Figure 1.11.9: Geometrical and reinforcement properties of the minaret (Altering Cross-sections)

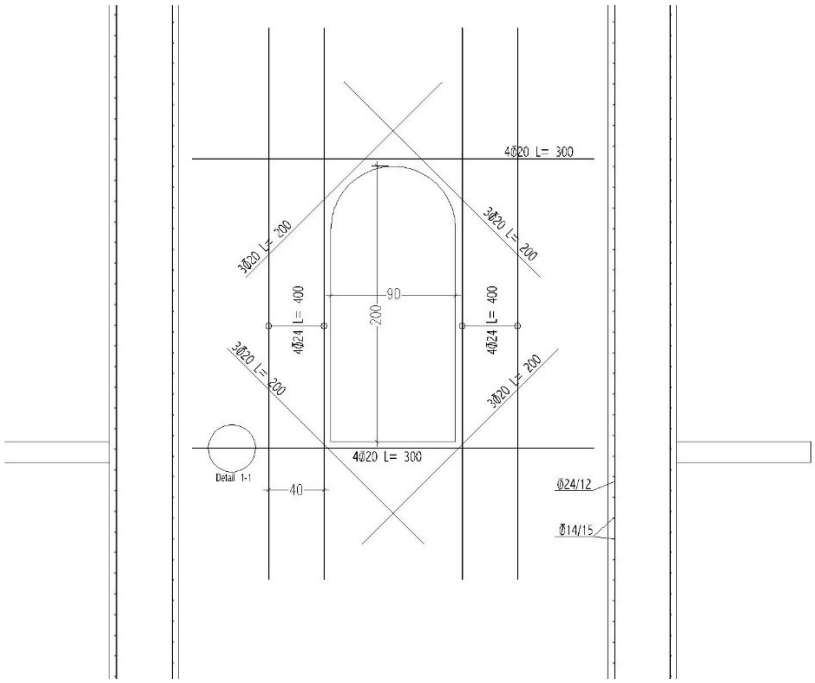

Figure 1.11.10: Geometrical and reinforcement properties of the minaret (Void reinforcement details)

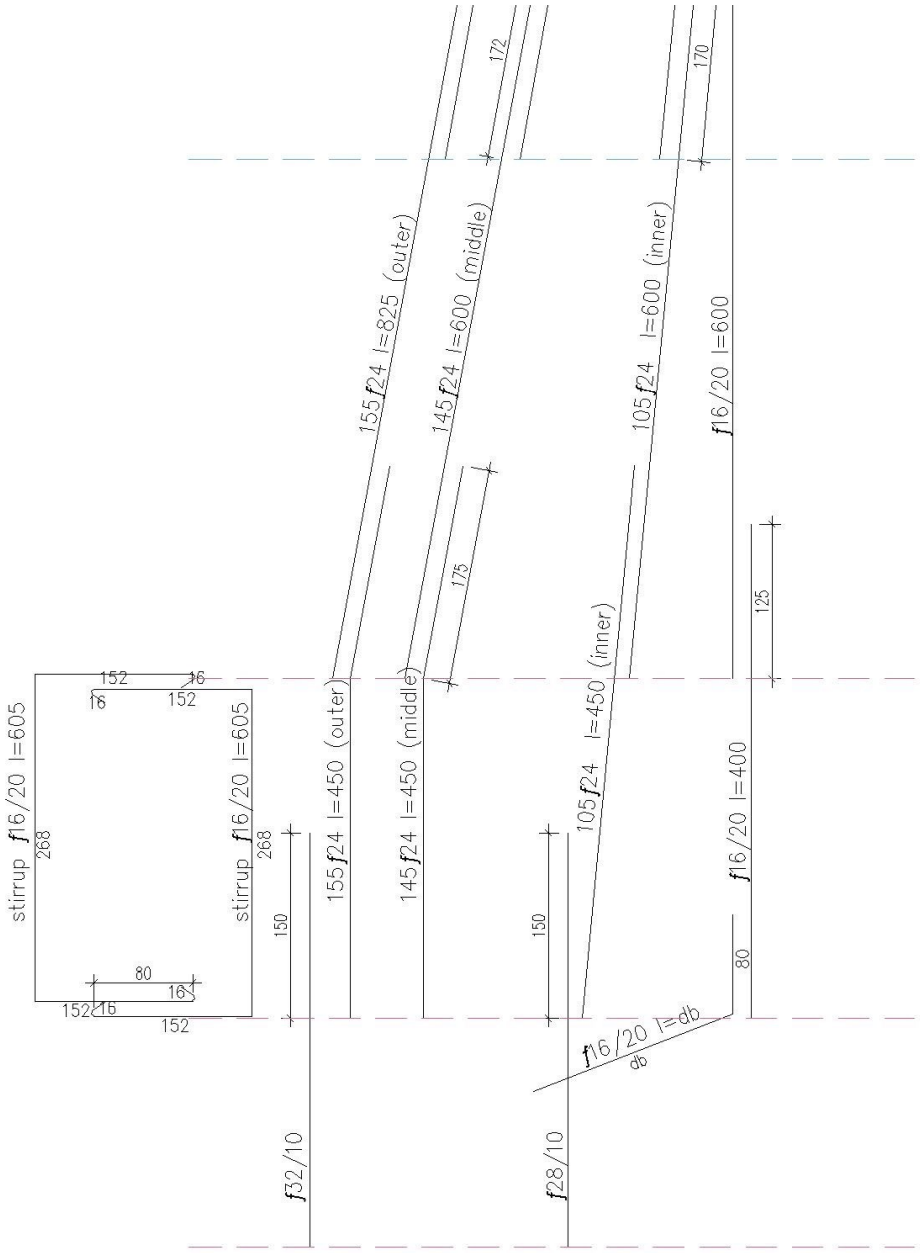

Figure 1.11.11: Geometrical and reinforcement properties of the minaret (transition segment rebar details)

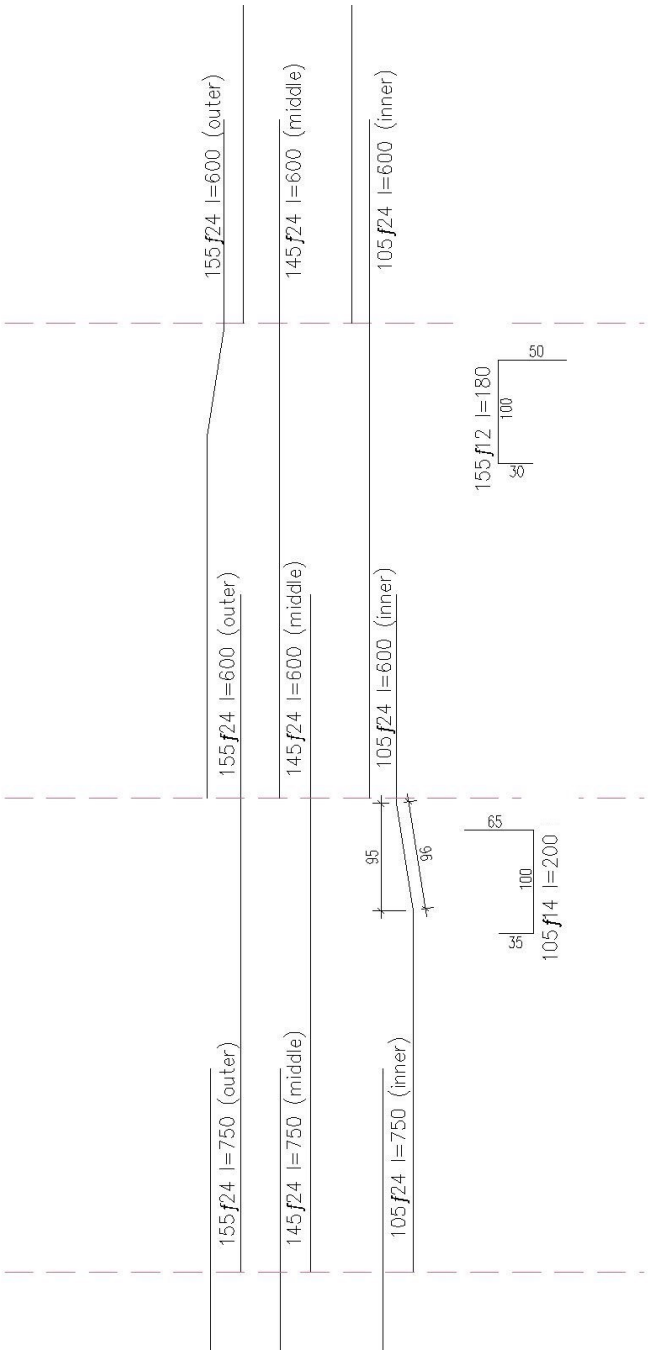

Figure 1.11.12: Geometrical and reinforcement properties of the minaret (altering cross-sections rebar details)

2. FINITE ELEMENT MODELLING OF THE MINARET

2.1 Material properties

The first and most important details in modelling the minaret is the material details of the necessary components used during the construction process. The general weight of the concrete was decided 24.5 KN/m³, the modulus of elasticity (E)37000 MPa and the compression strength for the C50 Concrete as 32 MPa, the tensile strength was assumed as 10% of that value (3.2MPa). These values are only indicative and were used to evaluate qualitatively the results obtained through the computer models.

The details for material modelling of the rebar components was as follows. The general weight 76.9 KN/m³, modulus of elasticity (E) 200000 MPa and a Minimum Yield stress of 434 MPa and Minimum Tensile strength of 500 MPa were determined for the FEM Models.

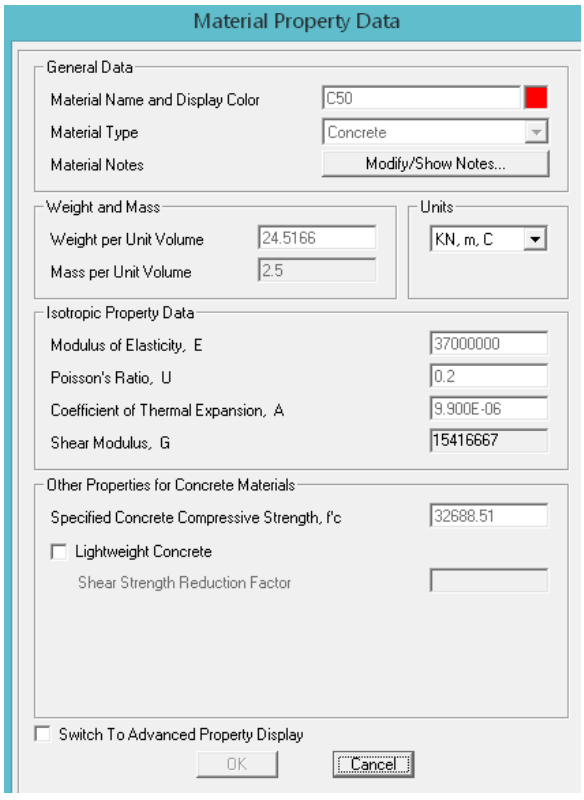

Figure 2.1: Concrete properties for the components of the minaret

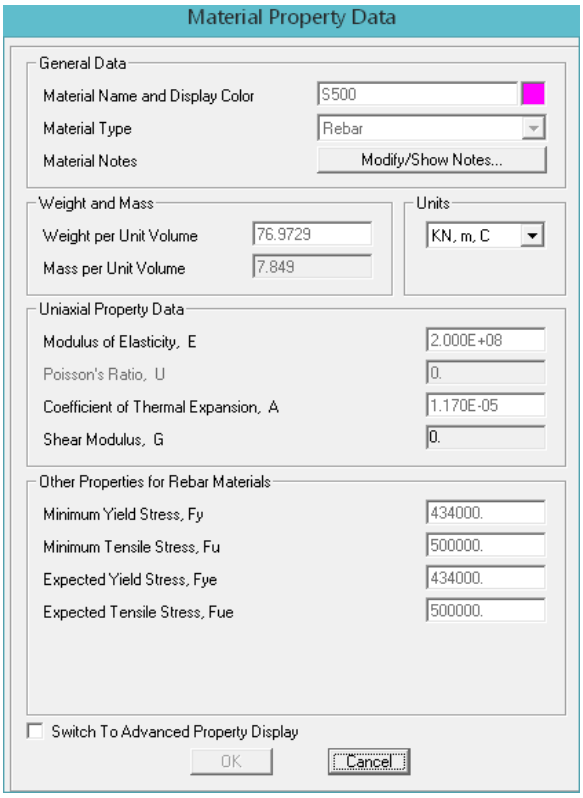

Figure 2.2: Steel Rebar properties for the components of the minaret

2.2 Frame Elements

During the FEM SAP 2000 modelling of the Minaret the frame, sections were designed. Using the Section Designer feature in SAP 2000, the frame elements were formed as pipe elements. Based upon the customary architecture of the ottomans the section of the minaret get slimmer to decrease the weight over height of the minaret. Following that same custom the sections get thinner by 7.5 cm on each different sections in our case.

A total of eight different sections and a transition segment was used in designing the minaret. The First number in The XX/YYY Format is the thickness of the pipe element and the Second number represents the inner diameter of the pipe.

Frame Properties and Moment Curvature and Interaction surfaces of some of the elements can be seen through figures 2.3 to 2.10.

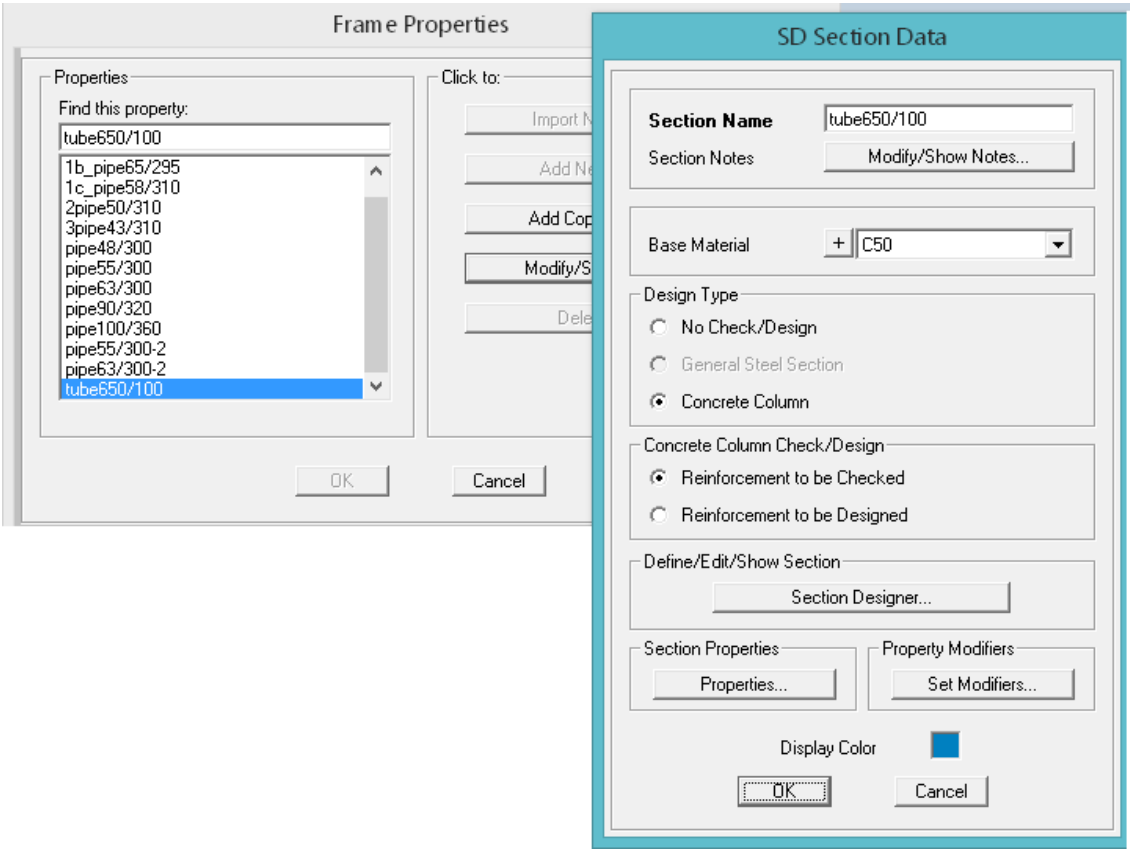

Figure 2.3: Defining Frame Properties for the minaret

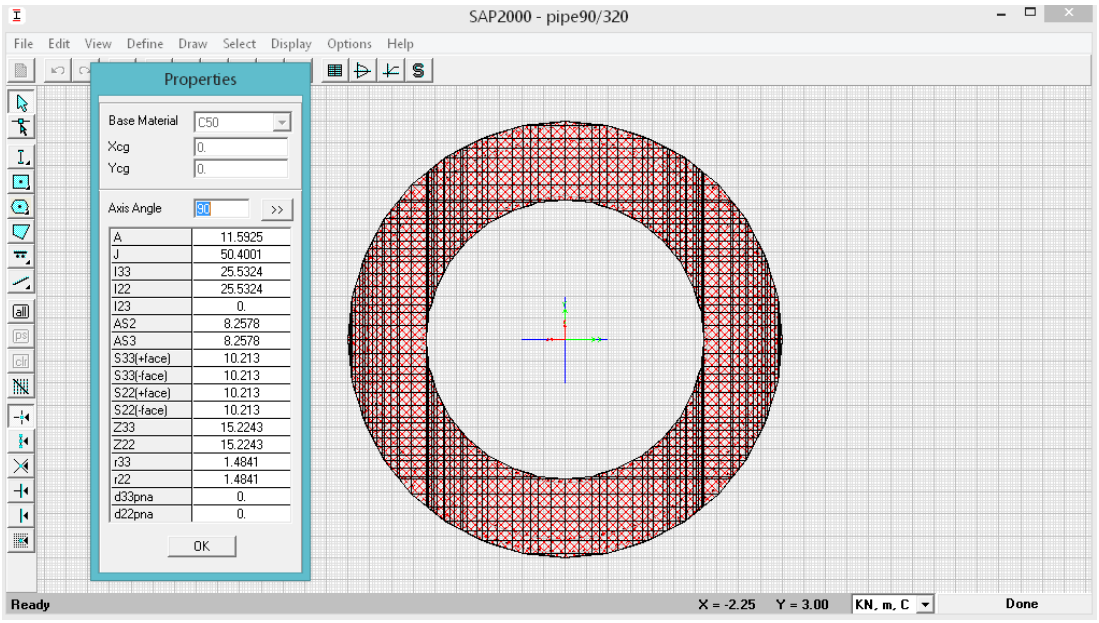

Figure 2.4: Section Designer Properties of the Pipe Element

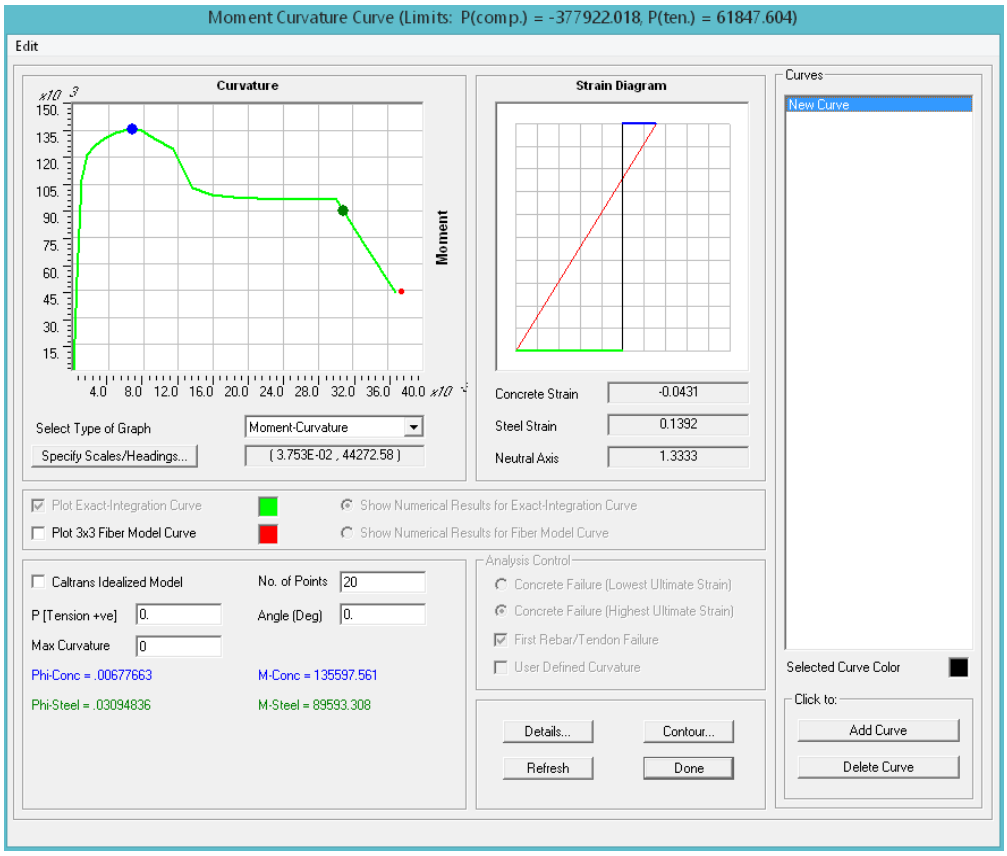

Figure 2.5: Moment Curvature curve for Pipe Element 90/320

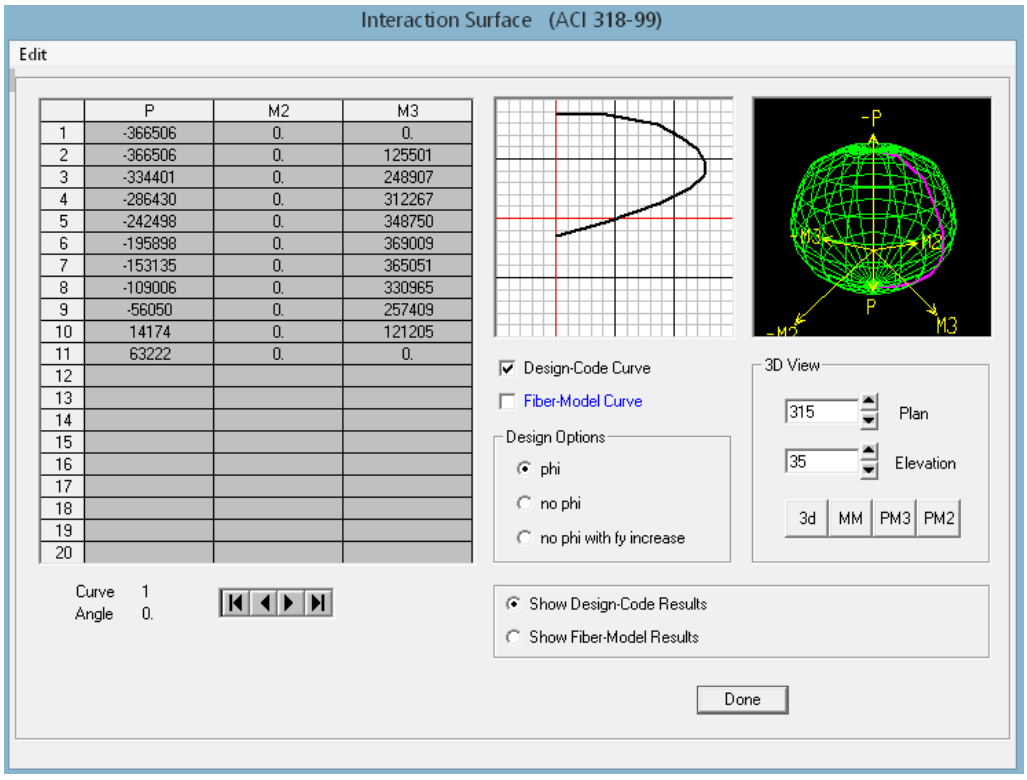

Figure 2.6: Interaction Surface for the Pipe Element 90/320

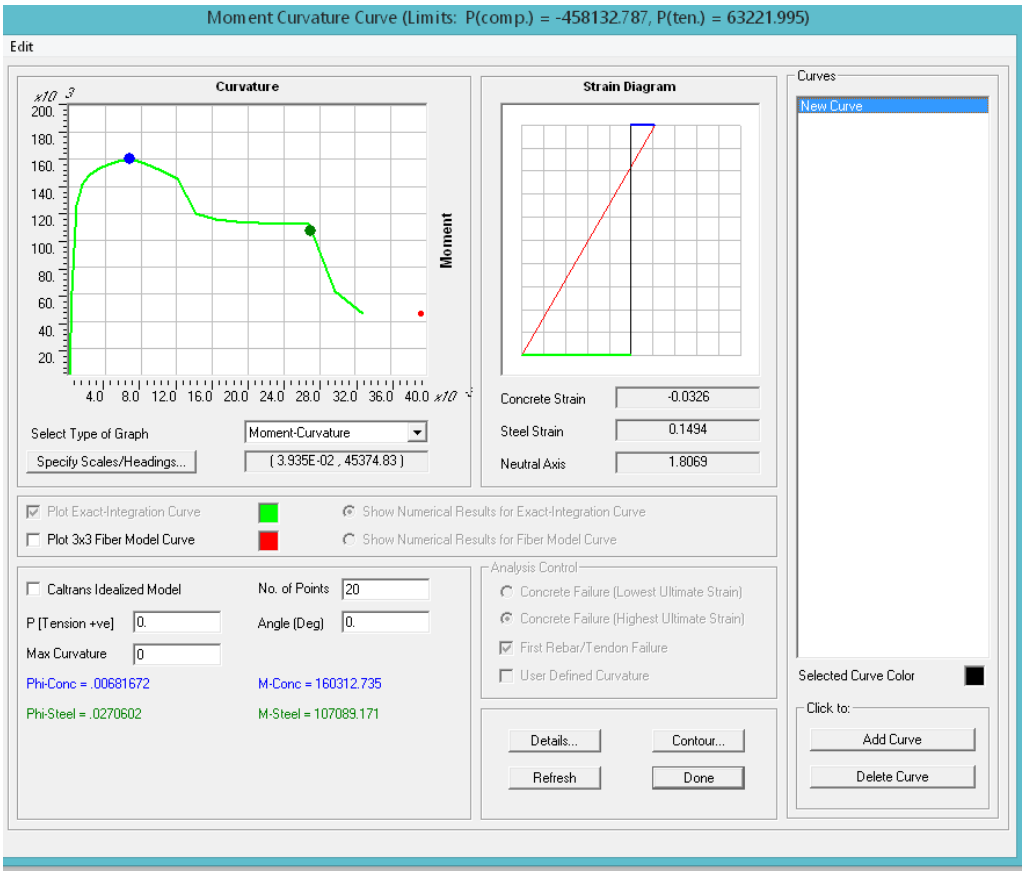

Figure 2.7: Moment Curvature curve for the Pipe Element 100/360

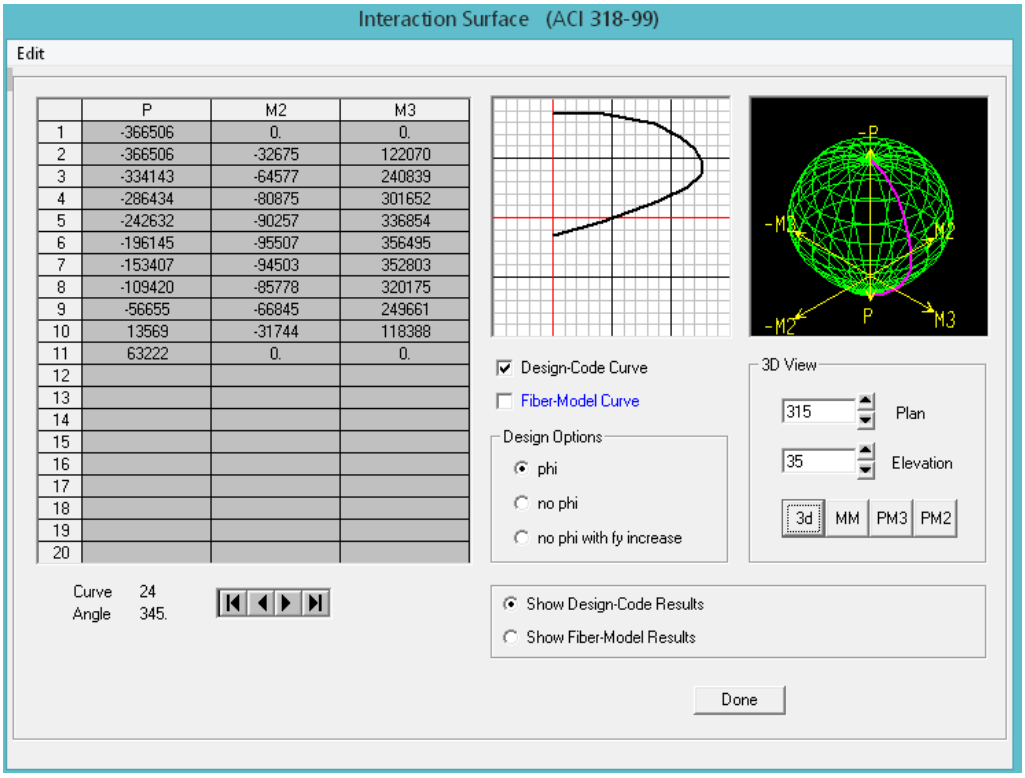

Figure 2.8: Interaction Surface for the Pipe Element 90/360

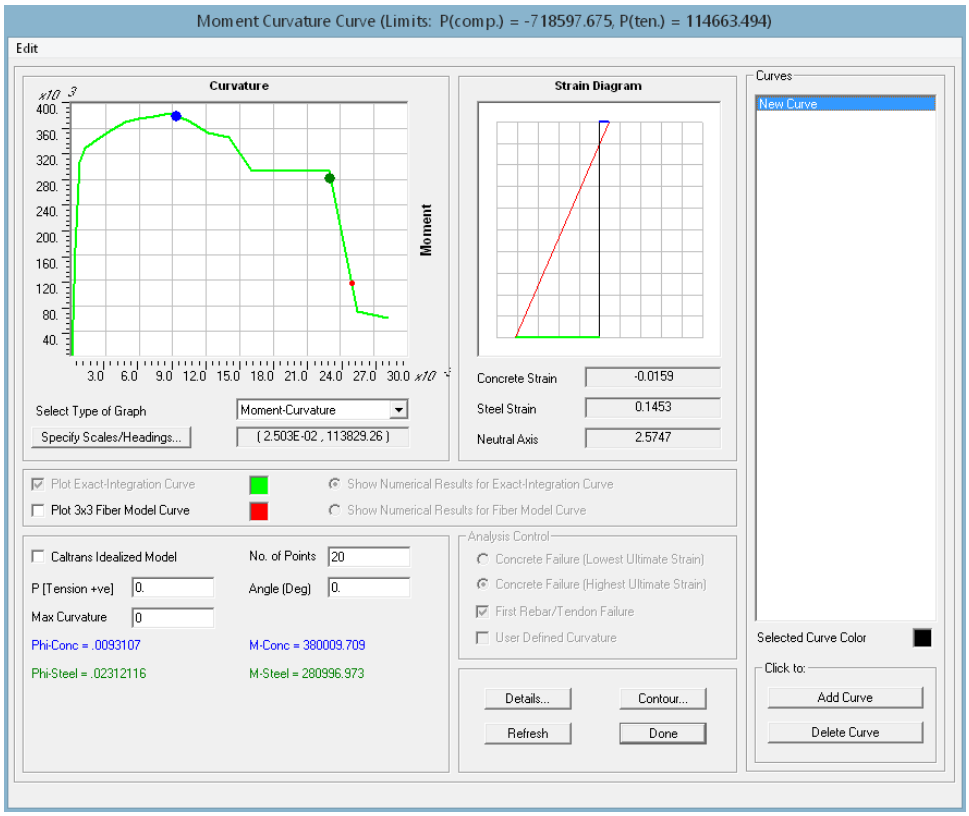

Figure 2.9: Moment Curvature curve for the Tube Element (Base Element of the Minaret)

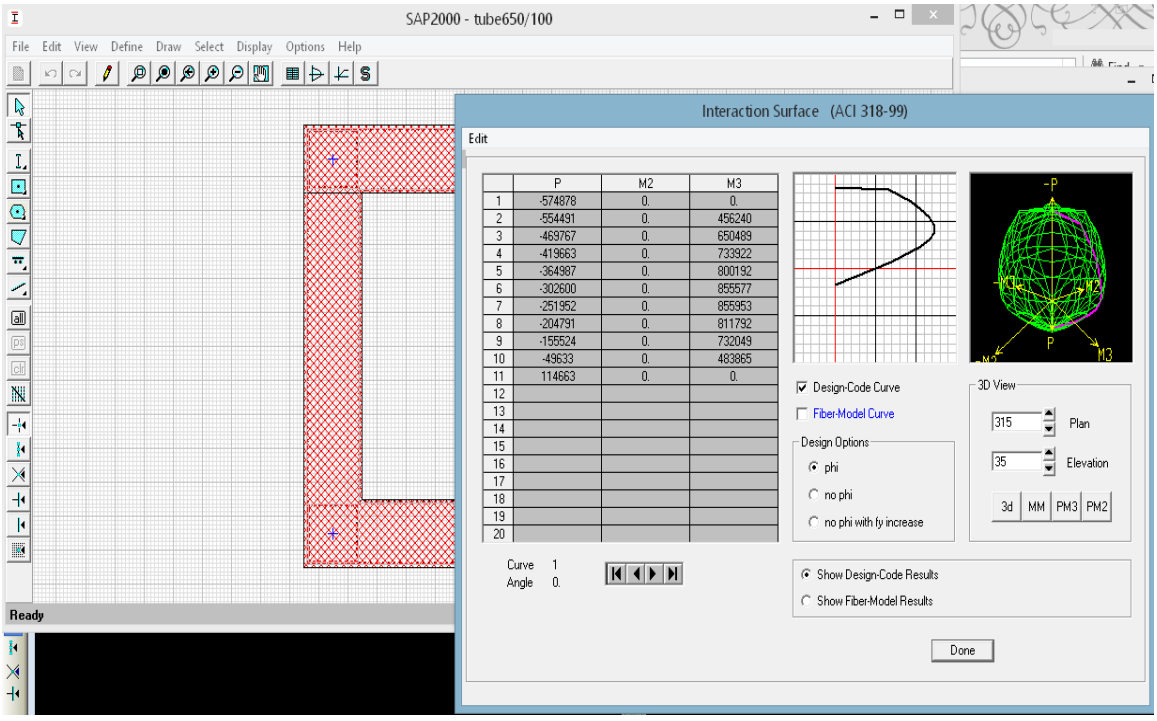

Figure 2.10: Interaction Surface for the Tube Element (Base Element of the Minaret)

2.3 Staircase and Its Implication on The Behaviour of The Minaret

During the stage of calibration of the model, several hypotheses were tested to evaluate the contribution of each structural element. The removal of the stairs has had little effect on the modes of vibration dealing with translation. The Stairs were constructed as an independent steel structure consisted of a system to carry the weight of the system and as for the other joints, their link to the body of minaret does not cause any significant change in the behaviour of the minaret.

When the pulpit was part of the mosque, the restrain of the pulpit until the height of the building was tested. The Results and the behavioural differences can be seen in the following chapters.

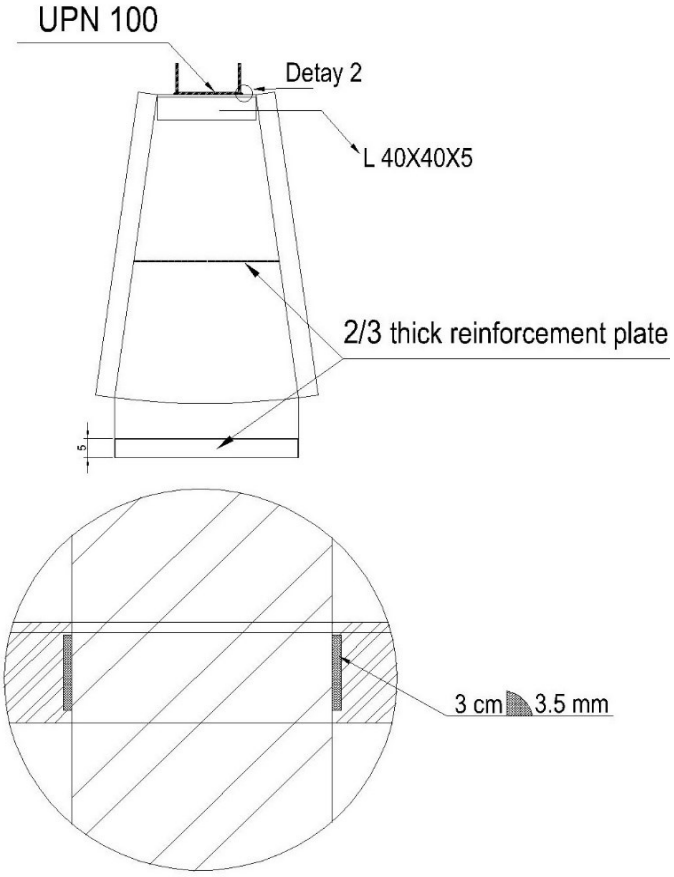

Figure 2.11: Stair construction details

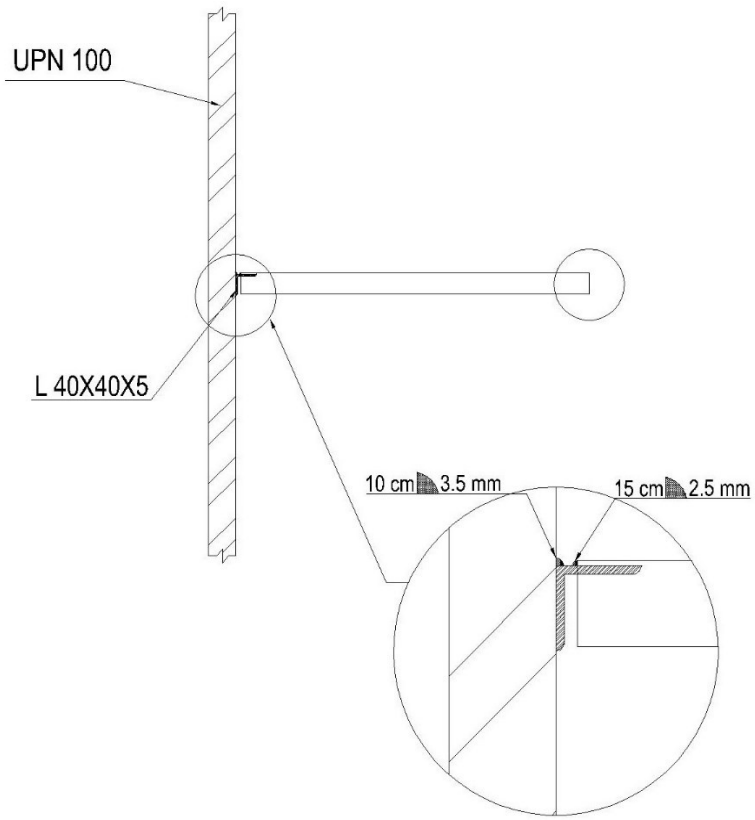

Figure 2.12: Stair link details to minaret body

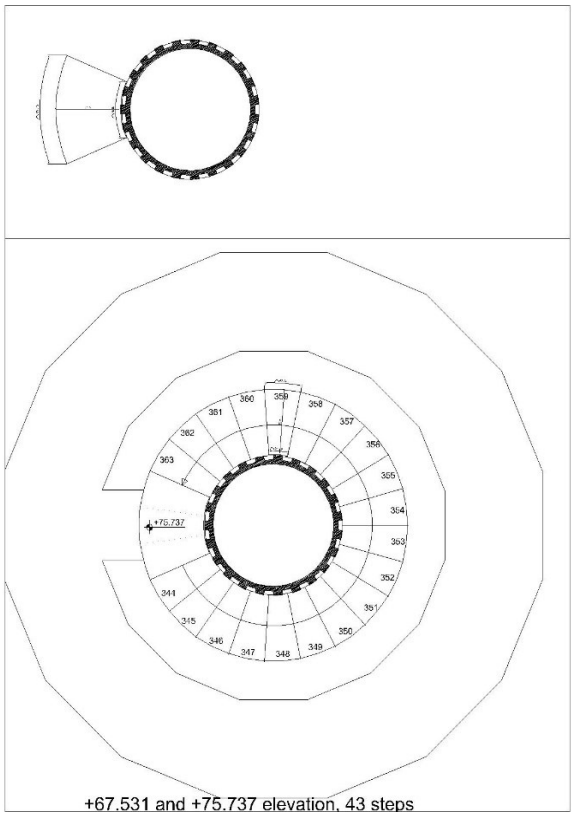

Figure 2.13: Stair arrangements

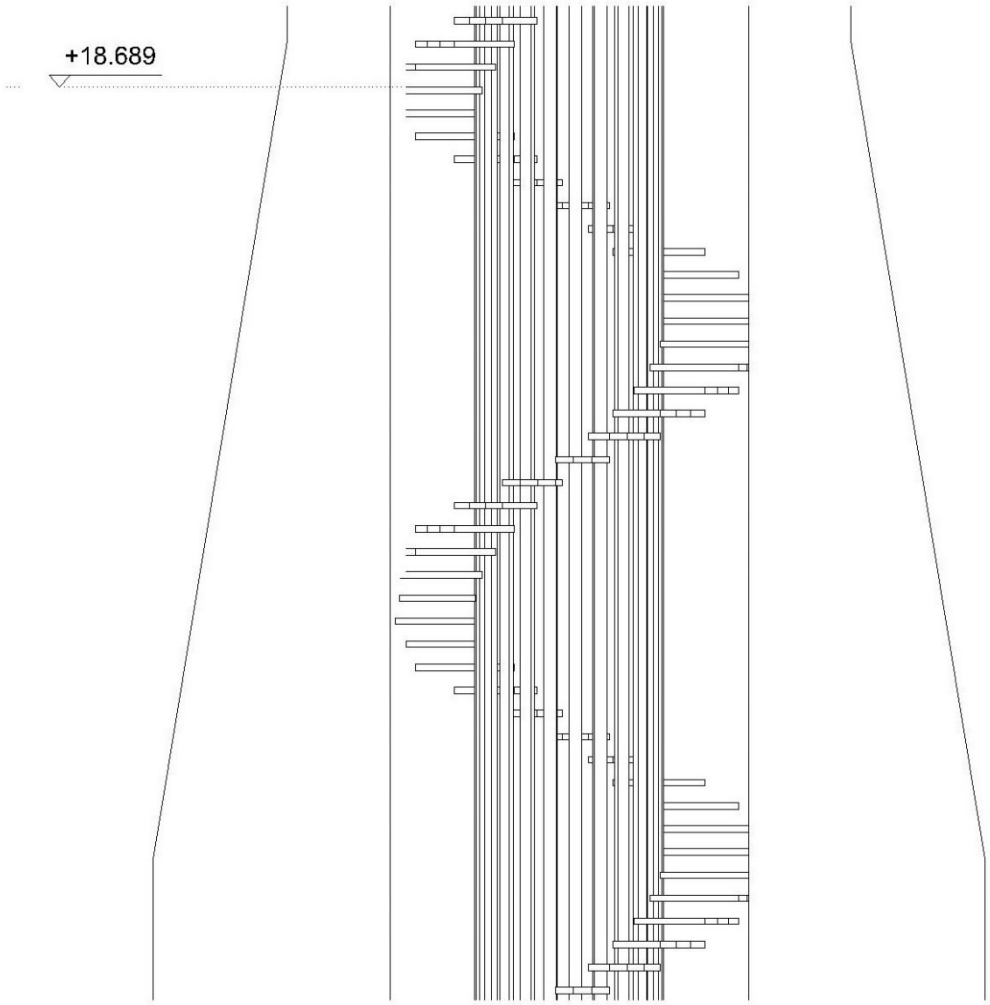

Figure 2.14: Staircase section

As it can be seen in the pictures 2.11 through 2.14 Staircase is designed independent of the main body and causes insignificant effect on the behaviour of the minaret.

2.4 Analytical Modal Parameters

The Sap2000 (Sap 2000, 14.2) finite element program is used to obtain analytical modal parameters. In the FEM of the minaret, three-dimensional (3D) elements, which exhibit quadratic displacement behaviour, are used. The element has three degrees of freedom, translations in the nodal x, y, and z directions. The3D FEM of the minaret and the concrete block with stairs are shown in Figure 2.15.

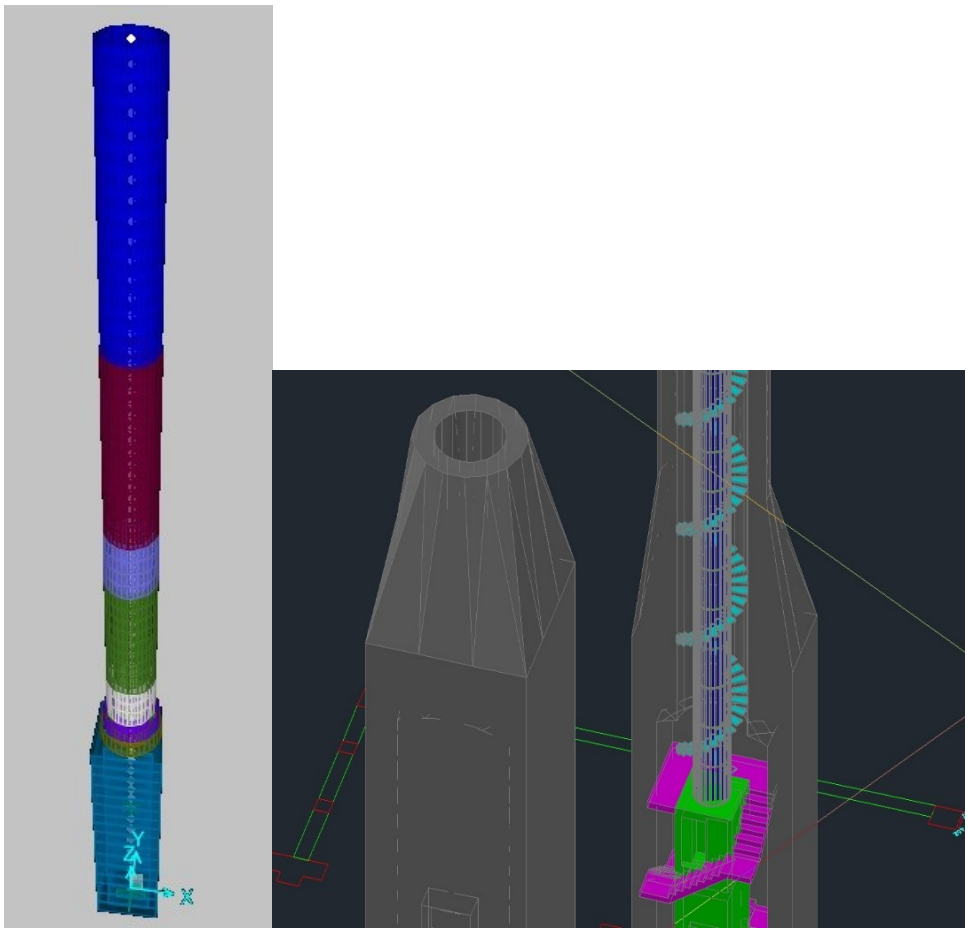

Figure 2.15: 3D finite element model of the RC minaret: (a) the finite element model of the minaret (b) concrete block and stairs.

Determination of material properties and boundary conditions, which must be taken into accounting the analytical analysis, is very important for thin and tall structures such as minarets. In this Study, to obtain the dynamic characteristics of the minaret, the elasticity modulus, Poisson ratio and mass per unit volume are specified as 2·4E4 MPa, 0·2, and 2500 kg/m3, respectively, as initial material properties. As initial boundary conditions, all of the degrees of freedoms under the footing part of the minaret are fixed. The term 'initial' is used to suggest that the FEM could be inaccurate due to various modelling and parametric uncertainties, and that the model is the basis for the model updating. In Figure 2.16, the first six mode shapes and natural frequencies obtained from analytical modal analysis are illustrated. As shown in Figure 2.16, the first six modes are bending modes and the other modes are torsional modes.

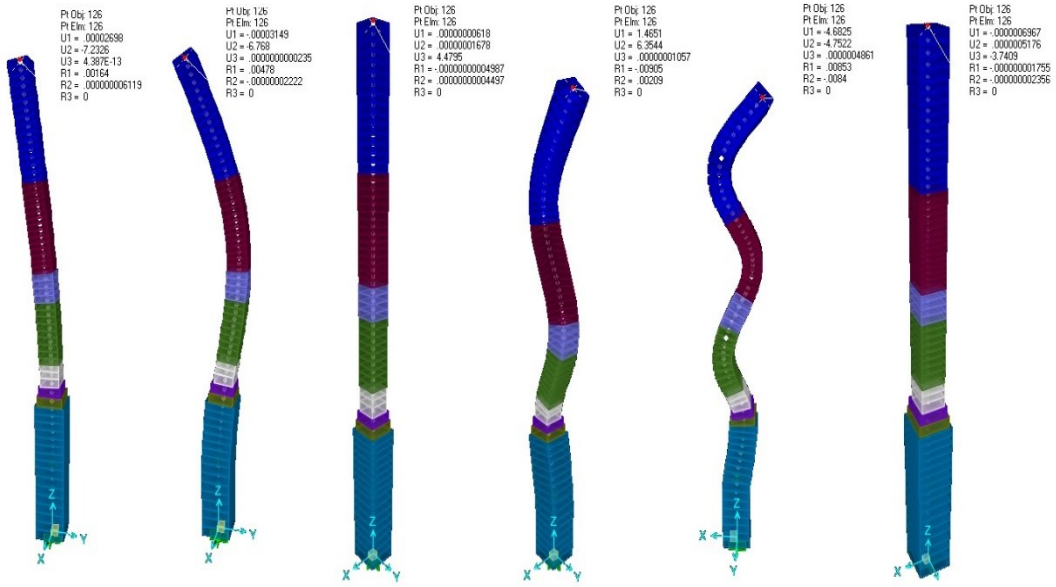

Figure 2.16: The first six mode shapes obtained From Operational Modal Analysis and their relative displacement on the last node of the Minaret, Node no 126.

Table 2.1: The first six modes and natural frequencies of the first model

Mode	1st	2nd	3rd	4th	5th	6th
Period (S)	1.134	0.24	0.107	0.065	0.0607	0.0376
Frequency(Hz)	0.8816	4.1406	9.3434	15.277	16.459	26.563

\

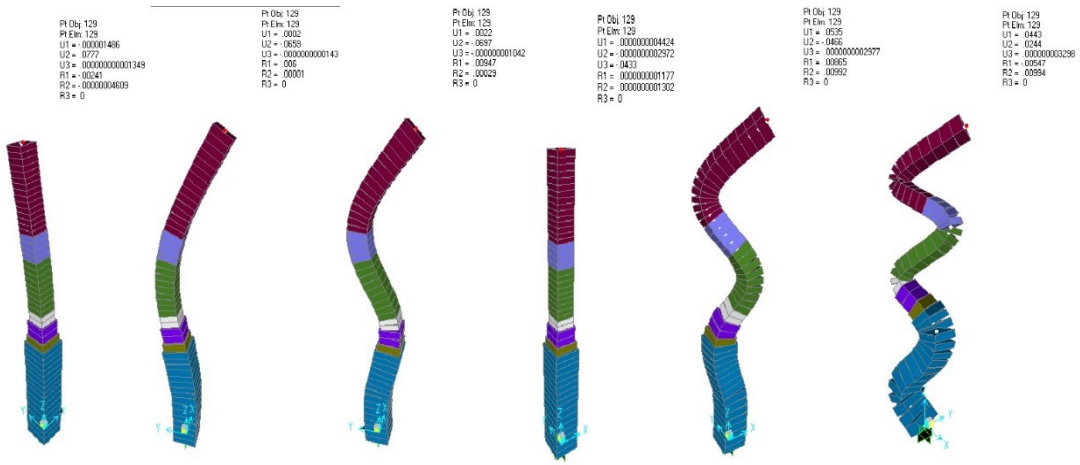

Figure 2.17: The first six mode shapes obtained From Operational Modal Analysis and their relative displacement on the last node of the second model of the Minaret, Node no 129.

Table 2.2: The first six modes and natural frequencies of the second model

Mode	1st	2nd	3rd	4th	5th	6th
Period (S)	0.58	0.14	0.063	0.0522	0.0336	0.0220
Frequency(Hz)	1.72	6.992	15.657	19.147	29.760	45.435

The Figure 2.17 and table 2.2 belong to the second model, which has the 71-Meter RC minaret and is used to compare the results obtained for the first model in the process.

2.5 Special Acceleration Response Spectra (TEC, 2007)

Symbol List:

A(T): Spectral Acceleration coefficient
A_0: Effective Ground Acceleration Coefficient
S(T): Spectrum Coefficient
I: Building Importance Factor
R: Structural Behaviour Factor
T: Building natural vibration period [s]
In this method first base shear is calculated according to regulations. The calculation for the base shear force uses the Eq. (2.1.)

$$Vt=\lambda\ W\ S(T)\ A_o\ I \qquad \textbf{(2.1.)}$$

According to earthquake Code [23] According to W, the total weight of the building Eq. (2.2.) is calculated according to. Floor weights, Eq. (2.3.), Each floor in a certain fixed charge varying according to the type structure of the moving load factor (the factor) and is obtained by multiplying the addition. Live load reduction during the recent earthquake is because there is unlikely that all of the moving load on all floors. Housing is taken at n = 0.3.

Spectrum coefficient, S (T), is calculated considering the natural period of the structure, T, according to local soil conditions.

$$S(T)=1+1.5\cdot T/T_A \qquad (0\leq T\leq T_A) \qquad \textbf{(2.2.)}$$

$$S(T)=2.50 \qquad (T_A\leq T\leq T_B) \qquad \textbf{(2.3.)}$$

$$S(T)=2.5\cdot (T_B/ T)^{0.8} \qquad (T>T_B) \qquad \textbf{(2.4.)}$$

TA and TB, located in the regulation of local ground class is used in determining the spectral characteristic periods Table 2.3.

Table2.3: Spectrum Characteristics Periods, $T_A$and T_B.

Local Ground Class	T_A (s)	T_B (s)
Z1	0.10	0.30
Z2	0.15	0.40
Z3	0.15	0.60
Z4	0.20	0.90

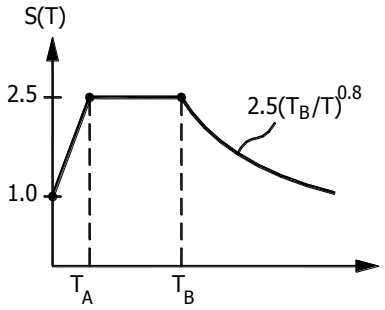

Figure 2.18: Special design acceleration spectra.

Effective ground acceleration coefficient, A_0, is taken into account according to the Table 2.13 in the regulations. Building importance factor, I, is taken 1.2 for buildings where People are concentrations of short Period.

Table 2.4: Effective ground acceleration coefficient

Earthquake Region	A_0
1	0.40
2	0.30
3	0.20
4	0.10

The case for this study is located In Istanbul, Turkey and the local ground class is Z2 and According to earthquake Code for structures which their Mass is piled up the top, move independently and are supported on one vertical element and their behaviour is like inverted pendulum type structures, R, Structural Behaviour Factor is considered equal to 2.

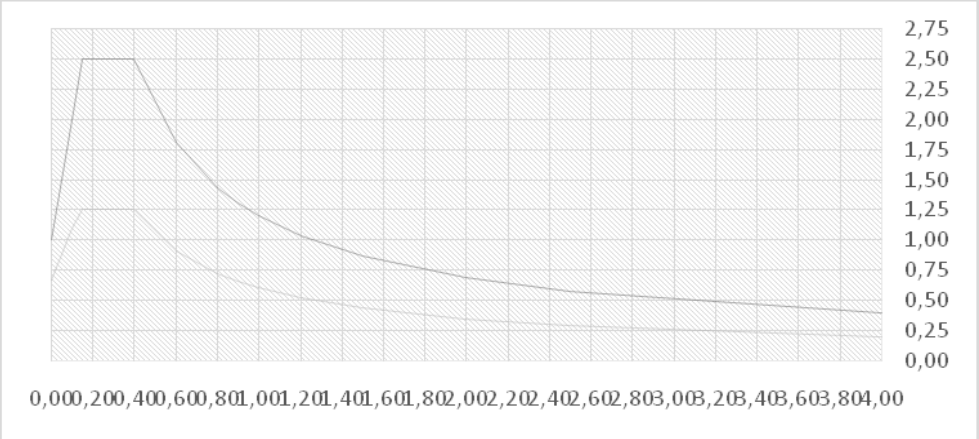

Figure 2.19: Design acceleration spectra For Z2 and R=2

Table 2.5: Design Period vs acceleration For Z2 and R=2

Period	Acceleration	Accel/R	R
0.00	1.00	0.67	1.50
0.10	2.00	1.09	1.83
0.15	2.50	1.25	2.00
0.20	2.50	1.25	2.00
0.40	2.50	1.25	2.00
0.60	1.81	0.90	2.00
0.80	1.44	0.72	2.00
1.00	1.20	0.60	2.00
1.20	1.04	0.52	2.00
1.50	0.87	0.43	2.00
2.00	0.69	0.34	2.00
2.50	0.58	0.29	2.00

In Figure 2.19 and table 2.5, it can be

seen that due to the regulations of TEC2007 S_{Ae} (T), Elastic Spectral acceleration [m / s^2]Reduced to be taken into account in any nth vibration mode acceleration spectrum. Eq. (2.6.) and used instead of Special design acceleration spectra.

$$SaR(Tn) = \frac{Sae(Tn)}{Ra(Tn)} \qquad \textbf{(2.5.)}$$

For Time history analysis seismic analysis source and wave propagation characteristics of physically simulated ground motions can be used. This type of motions are built while the local soil conditions are taken into account. The use of recorded or simulated ground motions will be produced in the event of earthquake ground motionand at least three, after satisfying the conditions of the regulations, shall be used throughout the analysis.

In the Time History domain when a nonlinear method is used, the load bearing system the internal forces representing the dynamic behaviour of the system components under cyclic loads with relations, theoretical and experimental validation proven to record will be identified utilizing the relevant literature. Linear or non-linear account, the result is the maximum of the three places in the use of movement, at least seven places when using the motion will be based on the average of the results for the design.

(TEC 2007) is developed mainly for building structures, similarly its basic provisions couldbe used to design or evaluate the adequacy of the minarets. The Turkish earthquake code specifies the following maximum relative displacement requirement for building structures.

$$\Delta i\,max \square \leq \frac{0.02\,.\,hi}{R} \qquad \textbf{(2.6.)}$$

Whereh_i is the story height and R is the behaviour factor related to the ductility of structure. Ifthis requirement is applied to the 90, and 71m tall minarets, thecorresponding maximumallowable top displacements are 0.90 and 0.71m, respectively. Assuming the equationgives an indication of extend of lateral

displacements for slender cantilever structures, thecode specified displacement limit is not exceeded for the minarets analysed.

3. SCALING THE STRONG GROUND MOTIONS

3.1 Introduction

The PEER Ground Motion Database – Beta Version is an interactive web based application that allows the user to select sets of strong ground motion acceleration time series that are representative of design ground motions. The user specifies the design ground motions in terms of a target response spectrum and the desired characteristics of the earthquake ground motions in terms of earthquake magnitude, source-to-site distance and other general characteristics. The PGMD tool then selects acceleration time series from the PEER-NGA database for rotated fault-normal and fault-parallel acceleration time series that satisfy the user-specified selection criteria and provide good fits to the target response spectrum.

Table 3.1: Explanation for the Terms used in PEER Ground Motion Database

Data Field	Explanations
Magnitude	Restrict range of moment magnitude, input in the format of [min, max] or leave as blank for no restriction.
Fault Type	Types of fault mechanism. Options are: (1) All types of fault; (2) Strike Slip; (3) Normal or Normal Oblique; (4) Reverse or Reverse Oblique; (5) Combination of (2, 3); (6) Combination of (2,4); (7) Combination of (3,4).
D5-95(sec)	Restrict range of the significant duration of the records, input in the format of [min, max], or leave as blank for no restriction. The duration is defined as the time needed to build up between 5 and 95 percent of the total Arias intensity.
R_JB (km)	Restrict range of Joyner-Boore distance, input in the format of [min, max], or leave as blank for no restriction.
R_rup (km)	Restrict range of closest distance to rupture plane, input in the format of [min, max], or leave as blank for no restriction.
Vs30 (m/s)	Average shear wave velocity of top 30 meters of the site.
Pulse	Restrict the pulse characteristics of the searched record. Options are: (1) Any record; (2) Only pulse-like record; (3) No pulse-like record.

3.2 Peer Database

The source of the database for the PGMD is the PEER Next-Generation Attenuation (NGA) project database of ground motion recordings and supporting information (http://peer.berkeley.edu/nga/). This database was developed as the principal resource for the development of updated attenuation relationships in the NGA research project coordinated by PEER-Lifelines Program (PEER-LL), in partnership with the U.S. Geological Survey (USGS) and the Southern California Earthquake Center (SCEC) (Chiou et al. 2006, 2008; Power et al., 2008). The database represents a comprehensive update and expansion of the pre-existing PEER database (Chiou et al., 2008). The ground motion records are originally from strong motion networks and databases of CGS-CSMIP and USGS and other reliable sources, including selected record sets from international sources. The PEER NGA database includes 3551 three-component recordings from 173 earthquakes and 1456 recording stations. 369 records from the PEER NGA database were not included in the current PEER Ground Motion Database of 3182 records. The records were not included for various reasons including one or more of the following: (a) records considered to be from tectonic environments other than shallow crustal earthquakes in active tectonic regions, e.g. records from subduction zones; (b)earthquakes poorly defined; (c) records obtained in recording stations not considered to be sufficiently close to free-field ground surface conditions, e.g. records obtained in basements or on the ground floors of tall buildings; (d) absence of information on soil/geologic conditions at recording stations; (e) records had only one horizontal component; (f) records had not been rotated to FN and FP directions because of absence of information on sensor orientations or fault strike; (g) records of questionable quality; (h) proprietary data; (i) duplicate records; and (j) other reasons.

Acceleration time series in the PGMD that can be searched for on the basis of record characteristics and other criteria are horizontal components that have been rotated to FN and FP directions. The use of rotated time series in the PGMD does not imply that they are for use in time series analyses in FN and FP directions only, and they can be used in time series sets in the same manner as time series in the as-recorded orientations in other databases. The rotation to FN and FP directions does, however, provide additional information with respect to the seismological conditions under which the recordings were obtained, records in the FN direction have been found to

often contain strong velocity pulses that may be associated with rupture directivity effects.

Ground motion parameters quantified for time series in the DGML database are response spectra, peak ground acceleration (PGA), peak ground velocity (PGV), peak ground displacement (PGD), significant duration, assessments of the lowest usable frequency (longest usable period) for response spectra, and presence and periods of strong velocity pulses. Significant duration was calculated as the time required to build up from 5% to 95% of the Arias Intensity (a measure of energy) of the acceleration time series (refer, for example, to Kempton and Stewart (2006) for definitions of Arias Intensity and significant duration). The recommended lowest usable frequency is related to filtering of a record by the record processing organization to remove low-frequency (long-period) noise. Filtering results in suppression of ground motion amplitudes and energy at frequencies lower than the lowest usable frequency such that the motion is not representative of the real ground motion at those frequencies. It is a user's choice in PGMD on whether to select or reject a record on the basis of the lowest usable frequency. Because of the suppression of ground motion at frequencies lower than the lowest usable frequency, it is recommended that selected records have lowest usable frequencies equal to or lower than the lowest frequency of interest.

A major effort was made in the PEER-NGA project to systematically evaluate and quantify supporting information (metadata) about the ground motion records, including information about the earthquake, travel path from the earthquake source to the recording station site, and local site conditions. Metadata in the PEER-NGA database are described in the NGA flat file and documentation: http://peer.berkeley.edu/products/nga_flatfiles_dev.html. Every record in the database was assigned a unique record number (NGA#) for identification purposes.

Metadata that have been included for records in the PEER Ground Motion Database are: earthquake name, year, magnitude, and type of faulting; measures of closest distance from earthquake source to recording station site (closest distance to fault rupture surface and Joyner-Boore distance); recording station name; site average shear wave velocity in the upper 30 meters, VS30; and NGA#. The PGMD also provides access to the vertical ground motion time series and their response spectra if

available. The same scale factors developed for their horizontal components scales vertical time series and response spectra, and they can be visualized together with the horizontal components. These features are provided as a convenience to users for developing three-component sets of time series.

3.3 Forming the time series

The formation of data sets based on response spectral shape and other criteria is a three-step process: (1) specification of the design or target response spectrum; (2) specification of criteria and limits for conducting searches for time series records; and (3) search of database and selection and evaluation of records.

3.3.1 Step 1 – Developing the target spectrum

The target spectrum of the source design code is selected and calculated for the base scaling.

3.3.2 Step 2 – Specifying criteria and limits for searches for time series records on the basis of spectral shape

A basic criterion used by the PGMD to select a representative acceleration time series is that the spectrum of the time series provides a "good match" to the user's target spectrum over the spectral period range of interest. The user defines the period range of interest. The quantitative measure used to evaluate how well a time series conforms to the target spectrum is the mean squared error (MSE) of the difference between the spectral accelerations of the record and the target spectrum, computed using the logarithms of spectral period and spectral acceleration. The PGMD web-based tool searches the database for records that satisfy general acceptance criteria provided by the user and then ranks the records in order of increasing MSE, with the best-matching records having the lowest MSE.

The focus of the PGMD is on selecting "as recorded" strong ground motion acceleration time series for use in seismic analyses. (In fact the records do include the effects of processing by the supplying agency, such as filtering and baseline correction.) Therefore, the tool does not provide the capability of altering the frequency content of the recordings to better match a target spectrum. However, it does provide the ability to linearly scale recorded time series to improve their match

to the target spectrum and select time series that have the best spectral match. The user has three options for scaling. One option is to apply a scale factor that minimizes the MSE over the period range of interest. This approach results in selection of records that have spectral shapes that are similar on average to the target over the period range of interest, but whose spectra will oscillate about the target. The second option is to scale the records so that the spectral acceleration at a specific period matches the target spectral acceleration at that period. This provides a set of scaled time series whose spectral accelerations are all equal to the target at the specified period. A third option of not scaling is also available. The choice of scaling approach is up to the user. For all three options, the MSEs of the records are calculated and ranked.

Calculation of MSE. The MSE between the target spectrum and the response spectrum of a recorded time series is computed in terms of the difference in the natural logarithm of spectral acceleration. The period range from 0.01 second to 10 seconds is subdivided into a large number of points equally-spaced in *ln* (period, *Ti*) (100 points/log cycle, therefore 301 points from 0.01 second to 10 seconds, end points included) and the target and record response spectra are interpolated to provide spectral accelerations at each period, $SA_{target}(Ti)$, and $SA_{record}(Ti)$, respectively. The MSE is then computed using Equation 3.1 over periods in the user-specified period range of interest:

$$\mathbf{MSE} = \frac{\Sigma \mathbf{w(Ti)}\{\ln[\mathbf{SA\ target(Ti)}] - \ln[\mathbf{f} * \mathbf{SA\ record\ (Ti)}]\}^2}{\Sigma \mathbf{w(Ti)}} \qquad \textbf{(3.1.)}$$

Parameter *f* in Equation 3.1 is a linear scale factor applied to the entire response spectrum of the recording. Parameter *w*(*Ti*) is a weight function that allows the user to assign relative weights to different parts of the period range of interest, providing greater flexibility in the selection of records. The simplest case is to assign equal weight to all periods in the period range of interest (i.e. *w*(*Ti*) = 1), but the user may wish to emphasize the match over a narrow period range while maintaining a reasonable match over a broad period range.

The PGMD web-based tool allows the user to select recordings for which the geometric mean of the two horizontal components provides a good match to the target spectrum. In this case the MSE is computed over both components using Equation 3.1 with the same value of *f* applied to both components. This process maintains the relative amplitude of the two horizontal components.

Calculation of the Scale Factor. As discussed above, the user has three options for specifying the scale factor *f*. The simplest is to use unscaled records, that is *f* = 1.0. The second approach is to scale the records to match the target spectrum at a specific period, denoted *Ts*. In this case the scale factor is given by:

$$\mathbf{f} = \frac{\mathbf{SA\ target\ (Ts)}}{\mathbf{SA\ record\ (Ts)}} \qquad \mathbf{(3.2)}$$

The third option is to apply a scale factor that minimizes the MSE. This approach produces scaled recordings that provide the best match to the spectral shape of the target spectrum over the user-specified period range of interest. Minimization of the MSE as defined in Equation 3.1 is achieved by a scale factor given by the mean weighted residual in natural logarithm space between the target and the record spectra:

$$\ln f = \frac{\Sigma w(Ti) \ln\left[SA\ target\ (Ti) \Big/ \left(SA\ record\ (Ti)\right]\right)}{\Sigma w(Ti)} \qquad \mathbf{(3.3.)}$$

When record selection is based on simultaneously considering both horizontal components, the scale factor computed using Equation 3.3 minimizes the MSE between the target spectrum and the geometric mean of the spectra for the two horizontal components. The geometric mean (GM) of FN and FP horizontal accelerations is given by:

$$\mathbf{SA\ GM} = \sqrt{SA\ FN.SA\ FP}\ \ or \ln SA\ GM = \left(\frac{\ln[SA\ FN + lnSA\ FP)}{\mathbf{2}}\right] \qquad \mathbf{(3.4.)}$$

For all three scaling options, the MSE is computed using Equation 3.1. Note that for all options, it is necessary for the user to specify the weight function because it is used to calculate the MSE and order the results with respect to the degree of match between target spectrum and spectra of recordings over the user-specified period range of significance. Specification of Search Criteria for Records. The user specifies the ranges of parameters over which searches are to be conducted and other limits and restrictions on the searches. These may include: event name; NGA number; station name; earthquake magnitude range; type of faulting; distance range; VS30 range; significant duration range; whether records are to exclude, include, or be limited to pulse records; and limits on the scale factor *f*.

3.4. Database

3.4.1 Database for records with pulses

The principal resource used in identifying and characterizing records with velocity pulses for the PGMD has been the research by Baker (2007). Baker analysed all records within the NGA database and identified FN records having strong velocity pulses that may be associated with rupture directivity effects. The basic approach followed by Baker was to use wavelet analysis to identify the largest velocity pulses. General criteria that were used in defining records with pulses were (1) the pulse is large relative to the residual features of the ground motion after the pulse is extracted, (2) the pulse arrives early in the time series, as would be expected for pulses associated with rupture directivity effects, and (3) the absolute velocity amplitudes are large (PGV of record equal to or greater than 30 cm/sec). The detailed criteria and results for the FN components are described by Baker (2007). The same criteria were applied by Baker for the FP component and those results as well as more detailed results and documentation of analyses for both components are contained on the website http://www.stanford.edu/~bakerjw/pulse-classification.html. Note that there can be no assurance that velocity pulses of records in the database are due to directivity effects without more detailed seismological study of individual records. It is likely that other seismological factors may have caused or contributed to the velocity pulses of some records. However, while the causative mechanisms for the pulses are uncertain, it is expected that the

pulses are similar to those caused by directivity and therefore suitable for use in modelling effects of directivity pulses on structures.

Somerville (2003), Mavroeidis and Papageorgiou (2003), Bray and Rodriguez-Marek (2004), and Fu and Menon (2004) also prepared lists of near-fault records considered to have strong ground motion pulses. The focus of these researchers was on identifying pulses on the FN components and only a few FP pulse records were identified. From examination of these data sets, several additional records having FN pulses were identified. In determining the additional records, we used the criteria that PGV for the records was equal to or greater than 30 cm/sec (same as Baker's criterion) and the records had been identified as pulse records in at least two studies.

All of the researchers mentioned above found a trend for pulse period to increase with magnitude, and this trend is expected based on the physics of fault rupture (Somerville, 2003). Figure 8 shows the individual record estimates of FN pulse period and the mean correlation between pulse period and magnitude of Baker (2007). Although the correlation for pulse period to increase with magnitude is clear, considerable data scatter can also be noted. The standard deviation of the natural logarithm of pulse period determined from Baker's regression was 0.55, corresponding to a factor of about 1.7 between the median regression estimates and median-plus-or-minus one standard deviation estimates. Figure 9 shows mean correlations of pulse period with magnitude by different investigators. All the correlations show a similar trend for pulse period to increase with magnitude.

3.4.2 Selecting Records with Pulses within the PGMD

If desired, a user of the PGMD can limit searches of records to those having pulses through options available on the user interface. Searches can be made for records having FN pulses, FP pulses, or both FN and FP pulses. Similar to other searches for records in the PGMD, a user can specify criteria and limits in searches for pulse records. Pulse records can be scaled and ranked for spectral match.

It is thought that the effects of type of faulting on pulse period may be significant for large magnitude earthquakes, although the effect is not well defined. Therefore it is suggested that for earthquakes greater than magnitude 6.5, records from strike-slip

earthquakes not be used for reverse-slip or normal-slip earthquakes and vice versa. Few pulse records from normal-slip earthquakes are in the database, and records from reverse-slip earthquakes are suggested to be used for normal slip earthquakes. In order to obtain a more detailed understanding of the nature of pulses in time series records considered for analysis, it is suggested that the velocity time series of candidate time series be displayed and examined. This can be readily done through the PGMD graphic interface.

3.5. Demand versus capacity

Both the dynamic analysis results and observed minaret failures indicate that the bottom of the cylindrical body or the top of the transition segment is the most vulnerable section in RC minarets.

These maximum elastic moment and shear force demands will be compared with the predicted moment and shear strengths here. During the post-earthquake reconnaissance visits, the authors observed that the most common steel rebar used inthe earthquake affected region was S220 with a yield strength of 220 MPa. For easy workmanship, small size bars with diameters of 12 or 14 mm were commonly used. In many cases, it was found that the longitudinal reinforcement ratio was close to or smaller than the minimum code specified ratio of 0.01. Many studies carried out after the 1999 earthquakes found that the concrete strength could be as low as 10 MPa.

In this study, a concrete design strength of 50 MPa is used. It should be noted that according to the current Turkish building code, the minimum concrete strength is 20 MPa and in this particular case the concrete strength was high because of the criticality of the structure although the critical section includes two layers of longitudinal rebar, a single layer of steel is assumed at the centreline of the section. The calculated axial load–moment interaction diagram is plotted in for a typical reinforced concrete ring section with a 0.18 m thickness and 1.76 m outer diameter (do) and 1.40 m inner diameter with a corresponding cross sectional area, Ac of 0.9 m2. The diagram also shows the elastic axial load–moment demands calculated from the dynamic time history analysis and code design spectrum. The axial load, N is assumed to be 592 kN (N/Ac fc = 0.06).

The normalized moment demands (M/Acdo f_c) are 0.14, 0.27,and 0.19 for the code design spectrum and dynamic response with Duzce and Kocaeli motions, respectively. The comparison of axial load–moment demands and the capacity curve suggests that the flexural capacity of the minaret model considered here is not sufficient, and smaller than the inelastic demands calculated using the code design spectrum and elastic demands from the dynamic time history analysis. It should be notedthat the flexural demand calculated from the code design spectra is significantly lower than the demand imposed on the minaret during the two earthquakes. This, and the displacement response, imply that the strength and displacement capacity required by the code design spectra may

$$V\,cap = 0.8\left(0.65\,f\,ctd\,Ac\,\left(1 + 0.007\frac{N}{Ac}\right)\right) + \frac{Asw\,fywd\,.d}{s} \qquad \textbf{(3.5)}$$

where Ac is the gross cross-sectional area, f_{ctd} is design tensile strength of concrete, N is the factored axial force calculated under simultaneous action of seismic lateral and axial loads, A_{sw} is the transverse steel area, f_{ywd} is the design yield strength of transverse reinforcement, d is the effective depth of the section, and s is the transverse reinforcement spacing.

Ignoring the contribution of shear reinforcement, the shear capacity of a typical minaret cross section is estimated as V_{cap} = 423 kN with Ac = 900 000 mm2, f_{ctd} = 0.9 N/mm2,N = 592 kN. The predicted shear strength, even without thestrength contribution from transverse steel, appears to be much larger than the calculated shear force demands.

3.6 Linear time-history analysis

Both the interstorey drifts and the story shears, as well as their dispersions, depend significantly on the selection and the scaling of the seismic excitations. The largest values for the responses and their dispersions are for the excitation sets that are characterized by largest *spectral* dispersions (i.e., the set of scaled real accelerograms, and the set of simulated accelerograms;).The drifts based on the Equivalent Static Force Method are larger than the mean drifts from linear time-history analysis by factors ranging from 1.02 to 1.16. This indicates that the

Equivalent Static Force Method provides slightly conservative design interms of interstorey drift.

The mean base shears resulting from the linear time-history analysis are larger than those from the Equivalent Static Force Method by factors of 1.02 to 1.35 (i.e., the design according to the Equivalent Static Force Method is *not* conservative in terms of base shear forces).

3.7 Nonlinear time-history analysis

3.7.1 Interstorey drifts

The largest values for drifts (at any node of the frames) obtained from the nonlinear analyses NLTH1 and NLTH2 are comparable to those from the linear analysis. Inmost cases, the differences between the mean values of the largest drifts from the nonlinear analyses and those from the linear analyses are within the range of about 20%. This shows that the "equal displacement principle" is applicable not only tomaximum displacements but also to maximum drifts.

The shapes of the distributions of the mean and the mean plus one standard deviation values for interstorey drifts along the height of the frames, obtained from the NLTH1and NLTH2 analyses are relatively similar. The largest values for the mean drifts are either from the set of simulated accelerograms or from the set of artificial accelerograms for large events. These two sets have very different spectral dispersions.

The ratios of the mean interstorey drifts from NLTH1 to those from NLTH2 analyses for all excitation sets range approximately between 0.9 and 1.2, with the exception of the drifts for the 4S frame for the set of artificial accelerograms – small events, for which the ratios are between 0.8 and 1.4. This indicates that with the exception of some specific cases (such as the results for the 4S frame subjected to artificial accelerograms for small events), in general one would expect maximum differences of about 20% in the interstorey drifts from the two types of analyses used in this study.

The results show that the dispersion of the drifts from the nonlinear analyses is nonrelated to the dispersion of the spectra of the excitation sets (i.e., in many cases,

sets with small spectral dispersion produce large response dispersion). It is believed that the dispersion of the drifts from the nonlinear analyses is due to the differences in the strong-motion duration of the ground motions. Note that the effects of strong-motion duration were not investigated in this study.

3.7.2 Shear forces

The influence of the type of excitation and the type of analysis on the mean storeyshears is much smaller than that on the mean interstorey drifts. For all three frames and for all excitation sets, the differences between the mean shear forces from the
NLTH1 and NLTH2 analyses are less than 12%.

The dispersions of the storey shears from both analyses (NLTH1 and NLTH2) and forall excitation sets are very small (i.e., the dispersions of storey shears are approximately three times smaller than those of interstorey drifts).As for the drifts, the dispersion of the shear forces from the nonlinear analyses is not related to the dispersion of the spectra of the excitation sets. Based on the results from this study, sets of scaled real records are preferred for use in time-history analysis of building structures. If such records are not available, then sets of simulated accelerograms should be used. This is because the scaled real records and the simulated accelerograms provide realistic spectra of ground motions. On the other hand the spectra of the artificial accelerograms have very smoothed spectra which are very close to the design spectrum (i.e. such spectra cannot be seen from actual records).

4. RESULTS

The result of the FEM analysis with SAP 2000 software is share through tables 4.1, 4.2 and 4.3. The translation of the top node, the frame resultant forces of the mid support of the minaret and the joint reactions of the base are shared and compared with 4 different scaled real ground motions. The Details of the chosen and scaled strong motions can be seen in appendix A and B.

Four different models are used for the comparison. Model 1 is the +90.00 Meter minaret with a mid support that is restricted in u1 and u2. Model 2 is +71.00 with the same support conditions and restrictions. Model 3 is the same model as the number one except the mid support and finally model 4 is alike the model number 2 without the mid support to determine the effect it has on the structure.

Table 4.1: The Translation of the Top Node of the Minaret for TEC 2007 Code spectra and four different scaled Real Strong Motions.

Sap 2000 Models	Load Cases	Translation (cm)
Model 1 (+90.00 mt)	TEC-R2Z2	17.632
	BAM	19.775
	DUZCE	31.393
	KOCAELI	26.775
	MANJIIL	20.25
Model 2 (+71.00 mt)	TEC-R2Z2	8.31575
	BAM	4.714
	DUZCE	3.773
	KOCAELI	4.349
	MANJIIL	4.336
Model 3 (+90.00 mt)	TEC-R2Z2	21.527
	BAM	25.204
	DUZCE	48.889
	KOCAELI	35.683
	MANJIIL	31.948
Model 4 (+71.00 mt)	TEC-R2Z2	11.864
	BAM	9.794
	DUZCE	6.912
	KOCAELI	9.289
	MANJIIL	7.038

Table 4.2: Frame resultant forces of the mid support of the minaret (Model No 1)

Sap 2000 Models	Load Cases	Results	Frame Forces (KN,m)
Model 1 (+90.00 mt)	TEC-R2Z2	Shear V2	8321.96
		Moment M3	114531.6
	BAM	Shear V2	8047.83
		Moment M3	110491.15
	DUZCE	Shear V2	12793.31
		Moment M3	175646.98
	KOCAELI	Shear V2	10918.646
		Moment M3	149910.34
	MANJIIL	Shear V2	8247.37
		Moment M3	113231.961

Table 4.3: Frame resultant forces of the mid support of the minaret (Model No2)

Sap 2000 Models	Load Cases	Results	Frame Forces (KN,m)
Model 2 (+71.00 mt)	TEC-R2Z2	Shear V2	8535.394
		Moment M3	117476.25
	BAM	Shear V2	4560.27
		Moment M3	62669.34
	DUZCE	Shear V2	3660.56
		Moment M3	50311.47
	KOCAELI	Shear V2	4217.935
		Moment M3	57971.33
	MANJIIL	Shear V2	4196.44
		Moment M3	57670.89

Table 4.4: The joint reactions of the base of Minaret (Model No 1)

Sap 2000 Models	Load Cases	Results	Joint Reactions (KN,m)	
Model 1 (+90.00 mt)	TEC-R2Z2	Force	X	8376.917
			Y	1.55E-03
		Moment	X	1.76E-03
			Y	24109.32
	BAM	Force	X	8054.78
			Y	1.41E-05
		Moment	X	1.66E-05
			Y	23166.048
	DUZCE	Force	X	12804.98
			Y	7.10E-05
		Moment	X	8.38E-05
			Y	36828.14
	KOCAELI	Force	X	10928.91
			Y	1.17E-04
		Moment	X	1.37E-04
			Y	31432.53
	MANJIIL	Force	X	8254.713
			Y	3.44E-05
		Moment	X	4.06E-05
			Y	23741.142

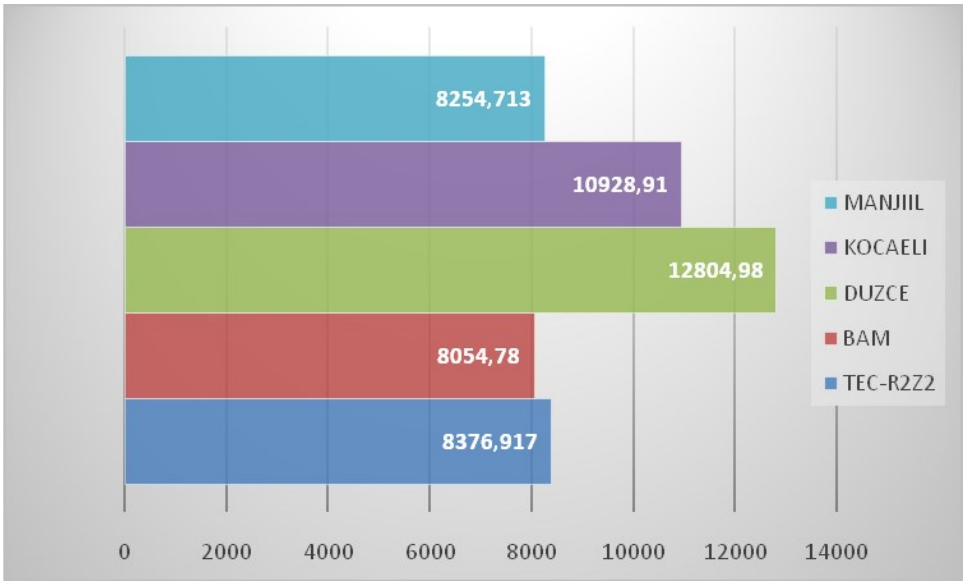

Figure 4.1: Resultant Joint Reaction Forces on the Base node (Model No1.)(KN)

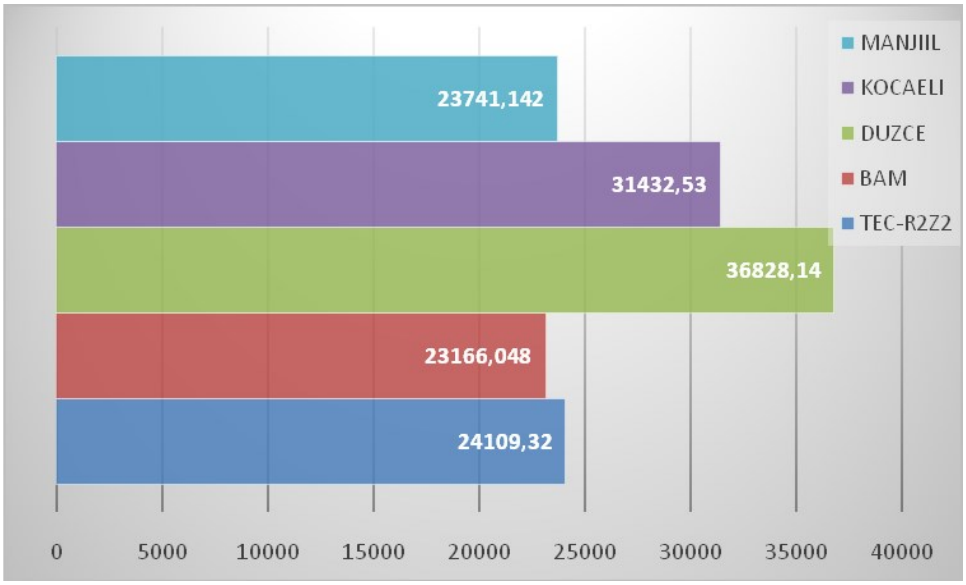

Figure 4.2: Resultant Joint Reaction Moments on the Base node (Model No1.) (KN,m)

Table 4.5: The joint reactions of the base of Minaret (Model No 2)

Sap 2000 Models	Load Cases	Results	Joint Reactions (KN,m)	
Model 2 (+71.00 mt)	TEC-R2Z2	Force	X	8619.94
			Y	4.75E-04
		Moment	X	3.98E-04
			Y	24833.641
	BAM	Force	X	4574.421
			Y	1.79E-05
		Moment	X	1.99E-05
			Y	13159.834
	DUZCE	Force	X	3673.02
			Y	1.70E-05
		Moment	X	1.88E-05
			Y	10567.047
	KOCAELI	Force	X	4232.194
			Y	2.29E-05
		Moment	X	2.38E-05
			Y	12175.74
	MANJIIL	Force	X	4209.717
			Y	1.72E-05
		Moment	X	1.90E-05
			Y	12110.73

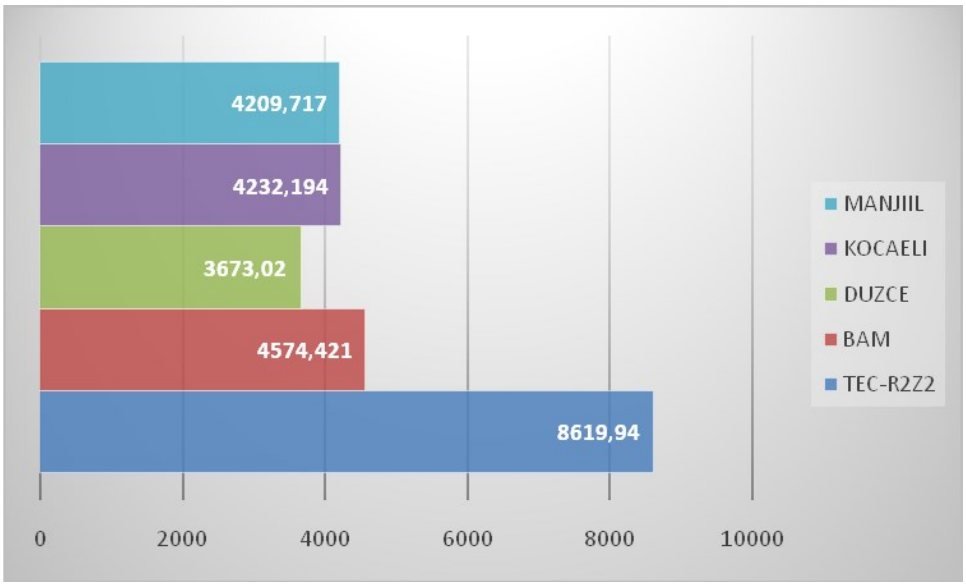

Figure 4.3: Resultant Joint Reaction Forces on the Base node (Model No 2.)(KN)

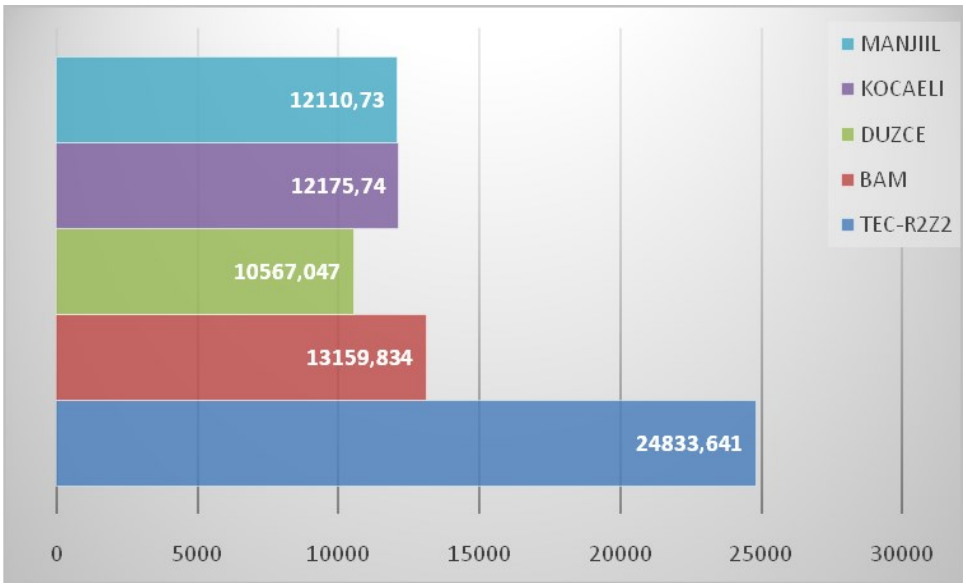

Figure 4.4: Resultant Joint Reaction Moments on the Base node

(Model No2.)(KN,m)

Table 4.6: The joint reactions of the base of Minaret (Model No 3)

Sap 2000 Models	Load Cases	Results	Joint Reactions (KN,m)	
Model 3 (+90.00 mt)	TEC-R2Z2	Force	X	6920.615
			Y	8.27E+01
		Moment	X	4.02E+02
			Y	221402.1
	BAM	Force	X	2724.974
			Y	1.33E+00
		Moment	X	2.74E-01
			Y	170964.75
	DUZCE	Force	X	5284.049
			Y	7.59E-01
		Moment	X	3.70E+00
			Y	331557
	KOCAELI	Force	X	4031.84
			Y	2.25E+00
		Moment	X	1.10E+01
			Y	244092.89
	MANJIIL	Force	X	3537.056
			Y	4.98E-01
		Moment	X	2.42E+00
			Y	217694.69

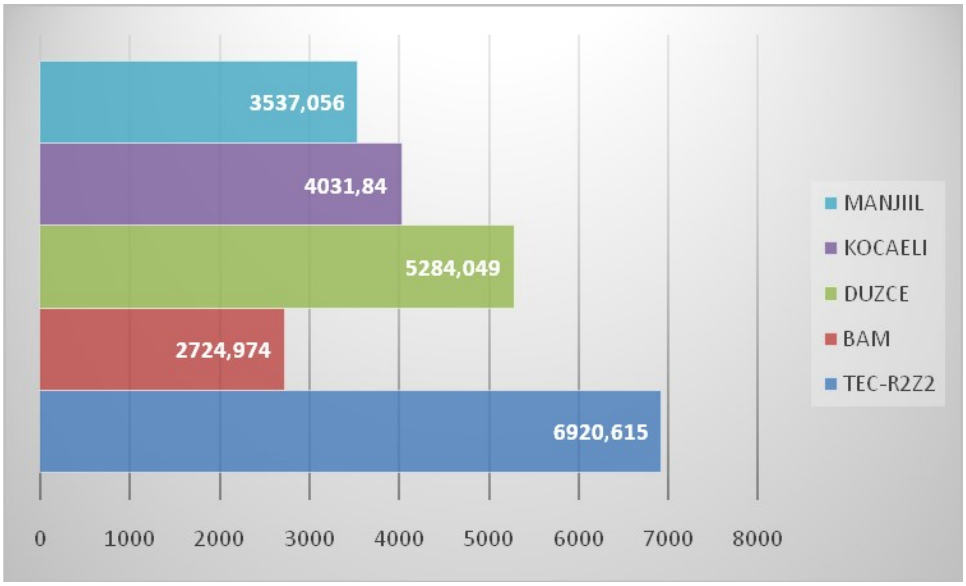

Figure 4.5: Resultant Joint Reaction Forces on the Base node (Model No 3.)(KN)

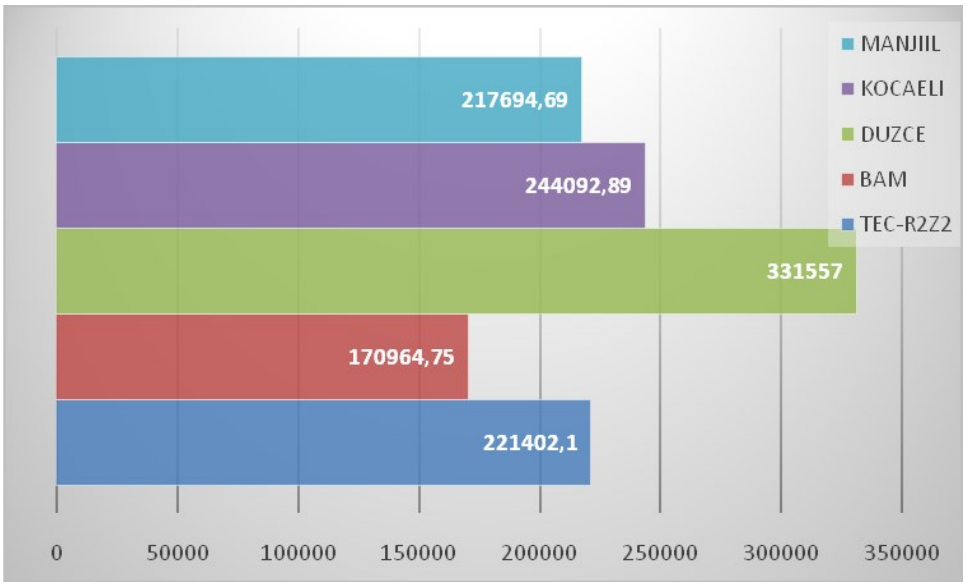

Figure 4.6: Resultant Joint Reaction Moments on the Base node (Model No3.)(KN,m)

Table 4.7: The joint reactions of the base of Minaret (Model No 4)

Sap 2000 Models	Load Cases	Results	Joint Reactions (KN,m)	
Model 4 (+71.00 mt)	TEC-R2Z2	Force	X	6839.052
			Y	4.18E-04
		Moment	X	4.07E-04
			Y	221842.55
	BAM	Force	X	3315.876
			Y	8.43E-06
		Moment	X	8.09E-06
			Y	159202.24
	DUZCE	Force	X	2552.537
			Y	1.62E-05
		Moment	X	1.54E-05
			Y	114301.72
	KOCAELI	Force	X	3257.228
			Y	3.39E-05
		Moment	X	3.25E-05
			Y	152010.8
	MANJIIL	Force	X	2423.144
			Y	9.88E-06
		Moment	X	9.50E-06
			Y	114773.17

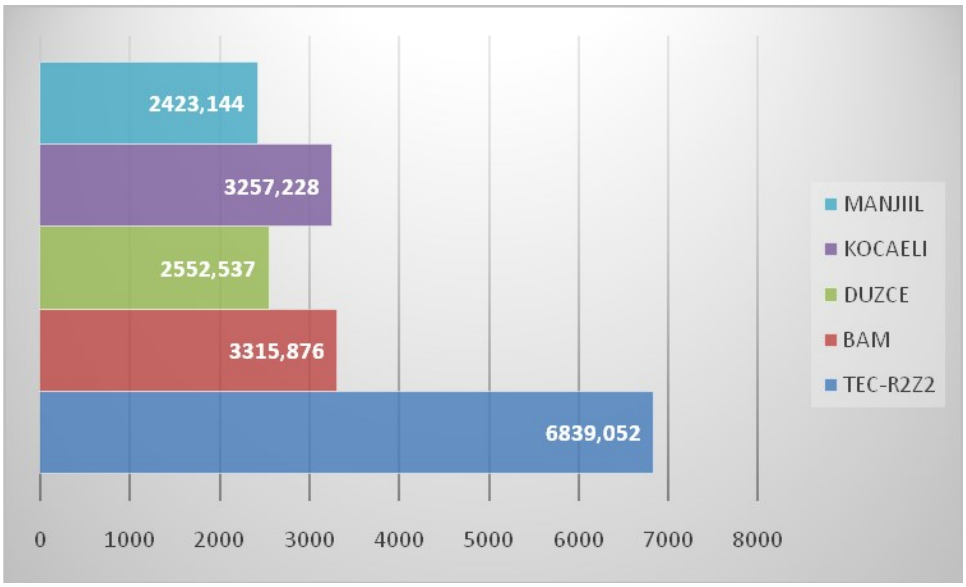

Figure 4.7: Resultant Joint Reaction Forces on the Base node (Model No 4.)(KN)

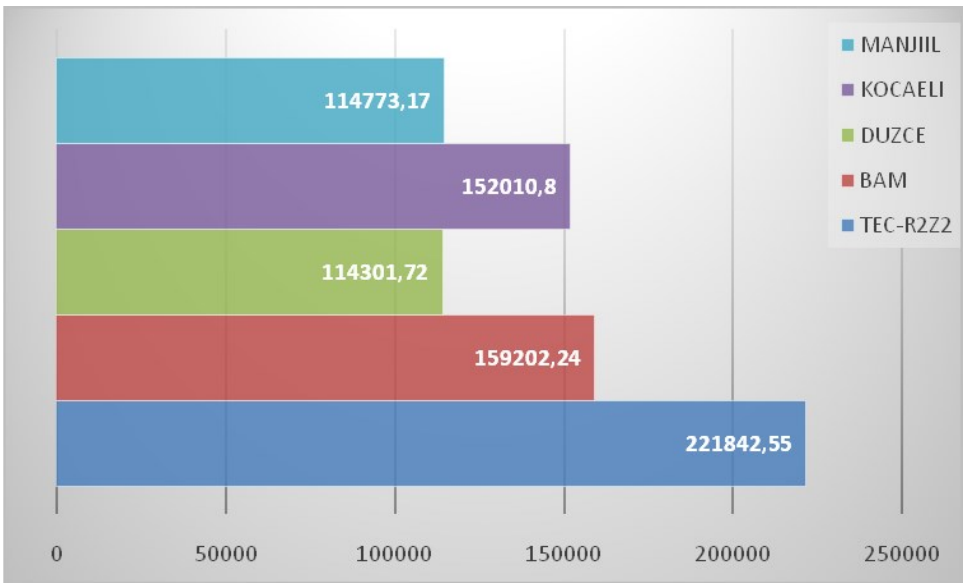

Figure 4.8: Resultant Joint Reaction Moments on the Base node (Model No4.)(KN,m)

5. CONCLUSIONS

Observations from the minarets that collapsed during recent earthquakes and the analyses of a representative minaret showed that the bottom of the cylindrical minaret body immediately above the transition segment is the most vulnerable section under seismic loading. The poor design practices include the use of these items:

(1) Smooth steel rebar,

(2) 180_end hooks at the ends of both the transverse and longitudinal reinforcements,

(3) Unstaggered and short longitudinal lap splices,

(4) Inadequate transverse hoops instead of a spiral reinforcement, and

(5) A short transition length between the square boot and cylindrical body.

These practices exacerbated the problem of insufficient bending strength and deformation capacity near the bottom of cylindrical part and increased the susceptibility of this section to failure. Practicing engineers and contractors can improve the design of minarets by providing a more gradual change from a square or polygonal section to a smaller circular section using a longer transition segment and by eliminating lap splices near the critical section and using instead staggered lap splices over the height of the minaret body. When either stairs or balconies are ignored in the analysis, the maximum shear and flexural demands were underestimated by approximately 20%.

For minarets with the base or boot attached to the mosque structure (TypeI), additional rigidity and stiffness provided by the mosque prevents deformation and damage within the base. In such cases, the failure mostly occurs just above the transition region or base of the cylindrical body.

It was found that the shear strength of the minaret was larger than the maximum shear demands calculated from the dynamic analysis, indicating that shear was not the likely cause of failure. In addition, the shear stress demands were reduced at locations where spiral stairs existed. The results of the elastic time history analyses have shown that the flexural capacity at the critical section would be exceeded when

the representative minaret is subjected to ground motions recorded during recent earthquakes. This is partially because the flexural strength is smaller under relatively small axial loads. The strength and displacement capacities calculated using the inelastic code design spectra may be much lower than the elastic demands imposed during large seismic events such as the Kocaeli and Duzce earthquakes. Almost all minarets surveyed after the recent earthquakes either behaved elastically or collapsed.

Depending on the design code of the TEC 2007 for minarets could be misleading after analysing the results. It can be seen that by over-designing the study cases the real behaviour is within the safe parameters of the design but there is not any safe and specific regulations for the tall pipe-like structures.

The existing design and construction practices should be improved to provide sufficient ductility. Otherwise, it will be misleading to use the inelastic response spectrum analysis prescribed by the current code.

REFERENCES

Abrahamson, N. A., Non-Stationary Spectral Matching Program RSPMATCH, User Manual, July 16, 1993.

Acar R, Livaoglu R, Dogangun A, Sezen H. The effects of subsoils on the seismic response of reinforced concrete cylindrical minarets. In: Fifth international conference on seismology and earthquake engineering. 2007. SE-24.

Boore, D. M., SMSIM - Fortran Programs for Simulating Ground Motions from Earthquakes: Version 2.0 - A Revision of OFR 96-80-A, USGS Open File Report OF 00-509, 2000.

Duzcedamla. Mosques expose the effects of earthquake. http://www.duzcedamla.com/text/index.dwx?TextID=2811; 2006 [in Turkish].

Dogangun A, Sezen H, Tuluk OI, Livaoglu R, Acar R. Traditional Turkish monumental structures and their earthquake response. International Journal of Architectural Heritage 2007;3(1):251–71.

Dogangun A, Tuluk O¨ I, Livaoglu R, Acar R. Traditional Turkish minarets on the basis of architectural and engineering concepts. In: Proceedings of the first international conference on restoration of heritage masonry structures. 2006. P34, p. 1–10.

Dogangun A, Acar R, Livaoglu R, Tuluk OI. Performance of masonry minarets against earthquakes and winds in Turkey. In: Proceedings of the first international conference on restoration of heritage masonry structures. 2006. P32, p. 1–10.

El-Attar AG, Saleh AM, Osman A. Seismic response of a historical Mamluk style minaret. In: Earthquake resistant engineering structures III. WIT; 2001. p. 745–54.

Firat YG. A study of the structural response of minarets in the 1999 Anatolian earthquakes. M.S. thesis. West Lafayette (IN): Purdue University; 2001. Also, http://cobweb.ecn.purdue.edu/_anatolia/FIRAT/ 5adapazari/adapazari2.ppt#257,2,Slide2.

Kramer, S. L., Geotechnical Earthquake Engineering, Prentice Hall, 1996.

Menon A, Lai CG, Macchi G. Seismic hazard assessment of the historical site of Jam in Afghanistan and stability analysis of the minaret. Journal of Earthquake Engineering 2004;8(1):251–94.

Sezen H, Fırat GY, Sozen MA. Investigation of the performance of monumental structures during the 1999 Kocaeli and Duzce earthquakes. Paper no: AE-020. In: Fifth national conference on earthquake engineering. 2003.

Scawthorn C. Preliminary Report Kocaeli (Izmit) Earthquake of 17 August 1999. http://mceer.buffalo.edu/research/Reconnaissance/ turkey8-79/ScawPrelim.pdf; 1999.

Sezen H, Fırat GY, Sozen MA. Investigation of the performance of monumental structures during the 1999 Kocaeli and Duzce earthquakes. Paper no: AE-020. In: Fifth national conference on earthquake engineering. 2003.

Sykora D, Look D, Groci G, Karaesmen E, Karaesmen E. Reconnaissance report of damage to historic monuments in Cairo. Egypt following the October 12, 1992 Dahshur earthquake. Technical report NCEER-93-0016. National Center for Earthquake Engineering Research, State University of New York at Buffalo; 1993.

Syrmakezis CA. Seismic protection of historical structures and monuments. Structural Control and Health Monitoring 2006;13:958–79.

TEC. Turkish code. Ministry of Public Works and Settlement. 2007. Specification for structures to be built in disaster areas; Part III-earthquake disaster prevention, Government of Republic of Turkey; 2007. http://www.deprem.gov.tr, 2007.

http://ngawest2.berkeley.edu/ Feb.2015

https://en.wikipedia.org/wiki/Hassan_II_Mosque Jan. 2015

APPENDICES

APPENDIX A: Regional maps For Strong motion records

Figure A.1: Record for Duzce, Turkey

Figure A.2: Record for Bam, Iran

Figure A.3: Record for Kocaeli, Turkey

Figure A.4: Record for Manjil, Iran

APPENDIX B: Records

-- Summary of Metadata of Selected Records --		Spectral Ordinate	Record Sequence Number	Mean Squared Error	Scale Factor	Tp-Pulse Period (sec)	5-75% Duration (sec)	5-95% Duration (sec)	Arias Intensity (m/sec)
		SRSS	4040	0.162	1.2489	2.023	5.6	9.6	8
Earthquake name	Year	Station Name	Magnitude	Mechanism	Rjb (km)	Rrup (km)	Vs30 (m/sec)	Lowest Useable Frequency (Hz)	
"Bam Iran"	2003	"Bam"	6.6	strike slip	0.05	1.7	487.4	0.0625	
These records were obtained from the NGA-West2 On-Line Ground-Motion Database Tool									
These records are UNSCALED	AT2 = Acceleration		DT2 = Displacement		VT2 = Velocity				
	Models and reports are requested to acknowledge the Pacific Earthquake Engineering Research Center (PEER) in their work and publications.								

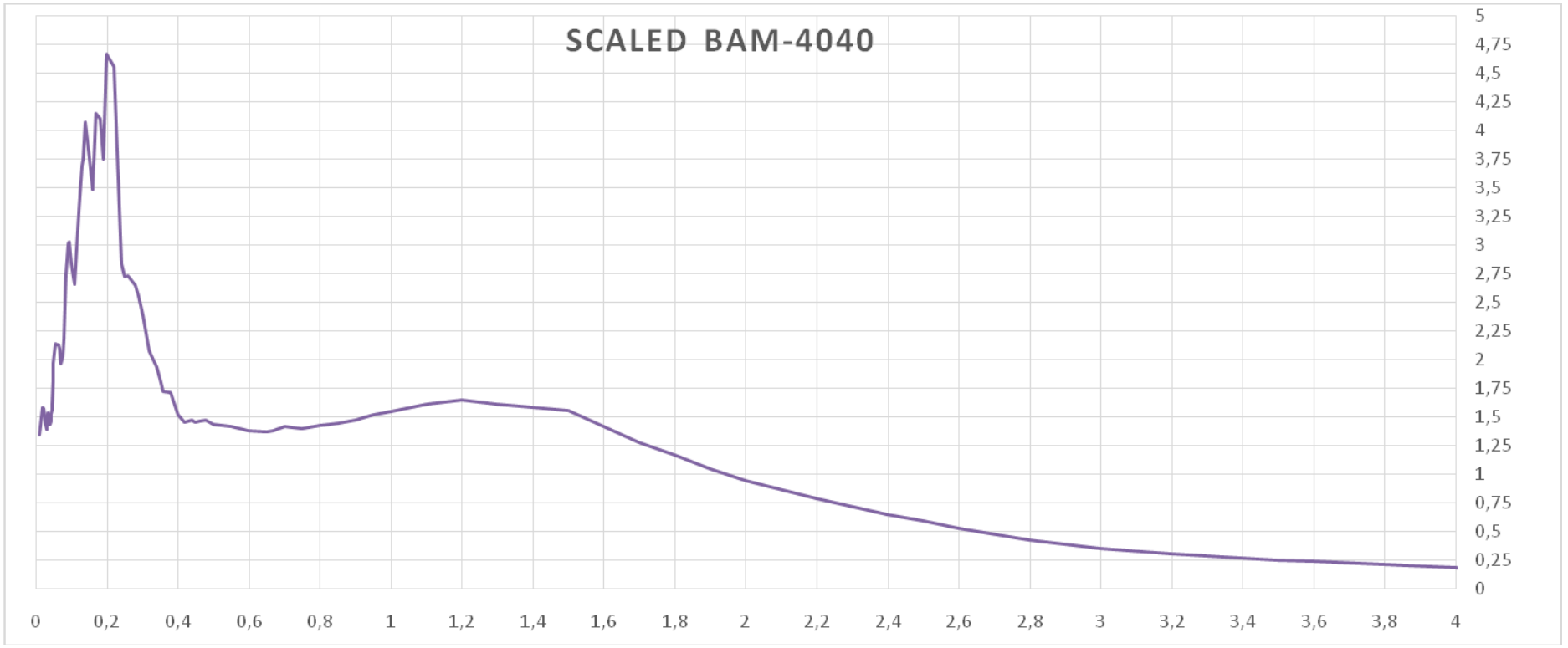
SCALED BAM-4040
5
4,75
4,5
4,25
4
3,75
3,5
3,25
3
2,75
2,5
2,25
2
1,75
1,5
1,25
1
0,75
0,5
0,25
0
0
0,2
0,4
0,6
0,8
1
1,2
1,4
1,6
1,8
2
2,2
2,4
2,6
2,8
3
3,2
3,4
3,6
3,8
4

-- Scaled Spectra used in Search & Scaling --					
Period (sec)	Target pSa (g)	Arithmetic Mean pSa (g)	Arithmetic Mean + Sigma pSa (g)	Arithmetic Mean - Sigma pSa (g)	RSN-4040 SRSS pSa (g)
0.01	1.68179283	1.3370148	1.3370148	1.3370148	1.3370148
0.02	1.77185126	1.57899254	1.57899254	1.57899254	1.57899254
0.022	1.78460609	1.56928816	1.56928816	1.56928816	1.56928816
0.025	1.8018576	1.50405305	1.50405305	1.50405305	1.50405305
0.029	1.82209667	1.4226531	1.4226531	1.4226531	1.4226531
0.03	1.8267514	1.38648041	1.38648041	1.38648041	1.38648041
0.032	1.83564553	1.40990183	1.40990183	1.40990183	1.40990183
0.035	1.84806694	1.53085943	1.53085943	1.53085943	1.53085943
0.036	1.85198912	1.43525932	1.43525932	1.43525932	1.43525932
0.04	1.86673223	1.43556441	1.43556441	1.43556441	1.43556441
0.042	1.87359915	1.4610549	1.4610549	1.4610549	1.4610549
0.044	1.88017007	1.52602283	1.52602283	1.52602283	1.52602283
0.045	1.8833526	1.55855059	1.55855059	1.55855059	1.55855059
0.046	1.88647039	1.61667086	1.61667086	1.61667086	1.61667086
0.048	1.89252231	1.81979935	1.81979935	1.81979935	1.81979935
0.05	1.89834539	1.9702477	1.9702477	1.9702477	1.9702477
0.055	1.9120108	2.13563005	2.13563005	2.13563005	2.13563005
0.06	1.92457222	2.12402197	2.12402197	2.12402197	2.12402197
0.065	1.93620048	2.12526832	2.12526832	2.12526832	2.12526832
0.067	1.94062142	2.09164413	2.09164413	2.09164413	2.09164413
0.07	1.94702919	1.96485984	1.96485984	1.96485984	1.96485984
0.075	1.9571649	2.02654148	2.02654148	2.02654148	2.02654148
0.08	1.96669399	2.18710168	2.18710168	2.18710168	2.18710168
0.085	1.97568745	2.7440877	2.7440877	2.7440877	2.7440877
0.09	1.98420437	3.00799919	3.00799919	3.00799919	3.00799919
0.095	1.99229447	3.02429659	3.02429659	3.02429659	3.02429659
0.1	2	2.83336036	2.83336036	2.83336036	2.83336036
0.11	2.10770601	2.65267643	2.65267643	2.65267643	2.65267643
0.12	2.21109081	3.29510293	3.29510293	3.29510293	3.29510293
0.13	2.31066799	3.69048335	3.69048335	3.69048335	3.69048335
0.133	2.33986323	3.74956486	3.74956486	3.74956486	3.74956486
0.14	2.40685572	4.07362562	4.07362562	4.07362562	4.07362562
0.15	2.5	3.74919844	3.74919844	3.74919844	3.74919844
0.16	2.5	3.4770237	3.4770237	3.4770237	3.4770237
0.17	2.5	4.14805072	4.14805072	4.14805072	4.14805072
0.18	2.5	4.10511816	4.10511816	4.10511816	4.10511816
0.19	2.5	3.75231508	3.75231508	3.75231508	3.75231508
0.2	2.5	4.6666694	4.6666694	4.6666694	4.6666694
0.22	2.5	4.55420947	4.55420947	4.55420947	4.55420947
0.24	2.5	2.835471	2.835471	2.835471	2.835471
0.25	2.5	2.71777029	2.71777029	2.71777029	2.71777029

-- Unscaled Horizontal & Vertical Spectra			
Period (sec)	RSN-4040 Horizontal-1 pSa (g)	RSN-4040 Horizontal-2 pSa (g)	RSN-4040 Vertical pSa (g)
0.01	0.86052	0.6368083	0.969
0.02	1.065154	0.6810483	1.32
0.022	1.042722	0.7010877	1.48
0.025	0.972913	0.7097191	1.5
0.029	0.876189	0.7278906	1.73
0.03	0.851914	0.7117793	1.75
0.032	0.888407	0.6964983	1.74
0.035	0.993576	0.7177915	1.64
0.036	0.897018	0.7183222	1.83
0.04	0.919699	0.6894516	1.82
0.042	0.953127	0.6782883	1.89
0.044	0.996023	0.7077265	1.92
0.045	0.997496	0.7498429	2.04
0.046	1.038934	0.7721321	2.2
0.048	1.227616	0.784883	2.16
0.05	1.363054	0.7941791	2.19
0.055	1.34992	1.049609	2.35
0.06	1.428723	0.9225042	2.49
0.065	1.403511	0.9621931	2.14
0.067	1.354089	0.9854954	1.94
0.07	1.233041	0.9770641	1.8
0.075	1.154426	1.140254	1.59
0.08	1.301408	1.171726	1.86
0.085	1.689739	1.404354	2.28
0.09	1.955815	1.405496	2.74
0.095	2.130861	1.150256	3.24
0.1	1.983074	1.101841	3.62
0.11	1.814453	1.104048	4.29
0.12	2.13686	1.547452	3.29
0.13	2.465872	1.628166	2.67
0.133	2.611913	1.480258	2.64
0.14	2.716648	1.805094	2.58
0.15	2.490481	1.676006	2.5
0.16	2.173188	1.740072	1.94
0.17	2.828941	1.740091	1.53
0.18	2.825255	1.679762	1.68
0.19	2.265544	1.973269	1.58
0.2	2.85621	2.409071	1.61
0.22	2.698965	2.452009	1.47
0.24	1.574793	1.635339	1.08

-- Summary of Metadata of Selected Records --		Spectral Ordinate	Record Sequence Number	Mean Squared Error	Scale Factor	Tp-Pulse Period (sec)	5-75% Duration (sec)	5-95% Duration (sec)	Arias Intensity (m/sec)
		SRSS	1605	0.069	1.5219	-	7.3	11.1	2.9
Earthquake name	Year	Station Name	Magnitude	Mechanism	Rjb (km)	Rrup (km)	Vs30 (m/sec)	Lowest Useable Frequency (Hz)	
"Duzce Turkey"	1999	"Duzce"	7.14	strike slip	0	6.58	281.86	0.1	1.5219
These records were obtained from the NGA-West2 On-Line Ground-Motion Database Tool									
These records are UNSCALED	DT2 = Displacement AT2 = Acceleration VT2 = Velocity								
	Models and reports are requested to acknowledge the Pacific Earthquake Engineering Research Center (PEER) in their work and publications.								

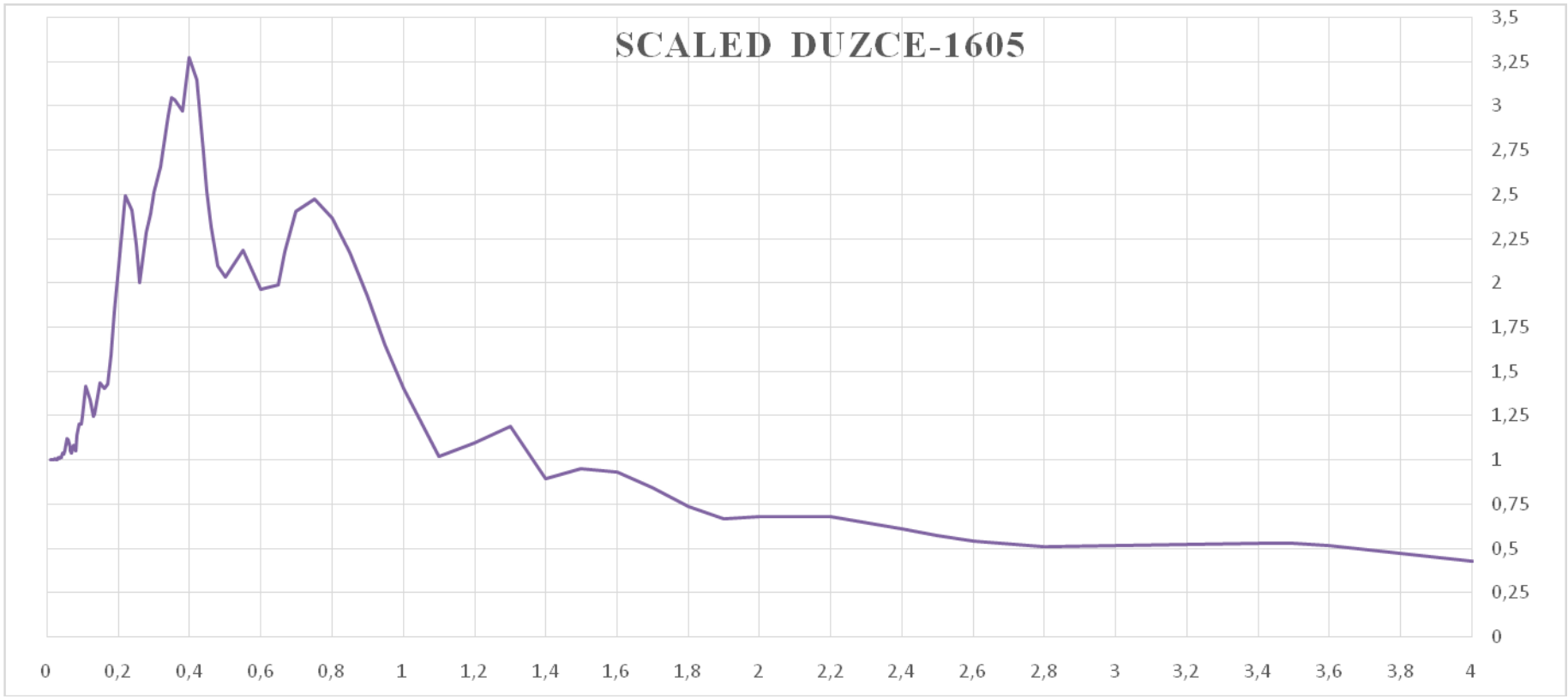
SCALED DUZCE-1605
3,5
3,25
3
2,75
2,5
2,25
2
1,75
1,5
1,25
1
0,75
0,5
0,25
0
0
0,2
0,4
0,6
0,8
1
1,2
1,4
1,6
1,8
2
2,2
2,4
2,6
2,8
3
3,2
3,4
3,6
3,8
4

-- Scaled Spectra used in Search & Scaling --					
Period (sec)	Target pSa (g)	Arithmetic Mean pSa (g)	Arithmetic Mean + Sigma pSa (g)	Arithmetic Mean - Sigma pSa (g)	RSN-1605 SRSS pSa (g)
0.01	1.68179283	0.99716506	0.99716506	0.99716506	0.99716506
0.02	1.77185126	1.00090861	1.00090861	1.00090861	1.00090861
0.022	1.78460609	1.00494802	1.00494802	1.00494802	1.00494802
0.025	1.8018576	1.00050342	1.00050342	1.00050342	1.00050342
0.029	1.82209667	1.00217195	1.00217195	1.00217195	1.00217195
0.03	1.8267514	0.99969373	0.99969373	0.99969373	0.99969373
0.032	1.83564553	1.01092185	1.01092185	1.01092185	1.01092185
0.035	1.84806694	1.00336672	1.00336672	1.00336672	1.00336672
0.036	1.85198912	1.00996192	1.00996192	1.00996192	1.00996192
0.04	1.86673223	1.01293338	1.01293338	1.01293338	1.01293338
0.042	1.87359915	1.02032322	1.02032322	1.02032322	1.02032322
0.044	1.88017007	1.03411755	1.03411755	1.03411755	1.03411755
0.045	1.8833526	1.03573183	1.03573183	1.03573183	1.03573183
0.046	1.88647039	1.03423308	1.03423308	1.03423308	1.03423308
0.048	1.89252231	1.03246723	1.03246723	1.03246723	1.03246723
0.05	1.89834539	1.04683344	1.04683344	1.04683344	1.04683344
0.055	1.9120108	1.11803354	1.11803354	1.11803354	1.11803354
0.06	1.92457222	1.1136442	1.1136442	1.1136442	1.1136442
0.065	1.93620048	1.06783712	1.06783712	1.06783712	1.06783712
0.067	1.94062142	1.05256994	1.05256994	1.05256994	1.05256994
0.07	1.94702919	1.03877451	1.03877451	1.03877451	1.03877451
0.075	1.9571649	1.08035036	1.08035036	1.08035036	1.08035036
0.08	1.96669399	1.04955994	1.04955994	1.04955994	1.04955994
0.085	1.97568745	1.13931866	1.13931866	1.13931866	1.13931866
0.09	1.98420437	1.20089817	1.20089817	1.20089817	1.20089817
0.095	1.99229447	1.20054214	1.20054214	1.20054214	1.20054214
0.1	2	1.24498227	1.24498227	1.24498227	1.24498227
0.11	2.10770601	1.41699177	1.41699177	1.41699177	1.41699177
0.12	2.21109081	1.34086522	1.34086522	1.34086522	1.34086522
0.13	2.31066799	1.24751479	1.24751479	1.24751479	1.24751479
0.133	2.33986323	1.25947943	1.25947943	1.25947943	1.25947943
0.14	2.40685572	1.32829911	1.32829911	1.32829911	1.32829911
0.15	2.5	1.4324441	1.4324441	1.4324441	1.4324441
0.16	2.5	1.39895481	1.39895481	1.39895481	1.39895481
0.17	2.5	1.4260383	1.4260383	1.4260383	1.4260383
0.18	2.5	1.59134838	1.59134838	1.59134838	1.59134838
0.19	2.5	1.83863406	1.83863406	1.83863406	1.83863406
0.2	2.5	2.09197238	2.09197238	2.09197238	2.09197238
0.22	2.5	2.48928548	2.48928548	2.48928548	2.48928548
0.24	2.5	2.40937559	2.40937559	2.40937559	2.40937559
0.25	2.5	2.21527573	2.21527573	2.21527573	2.21527573

-- Unscaled Horizontal & Vertical Spectra			
Period (sec)	RSN-4040 Horizontal-1 pSa (g)	RSN-4040 Horizontal-2 pSa (g)	RSN-4040 Vertical pSa (g)
0.01	0.404449	0.5154821	0.348
0.02	0.406147	0.5172765	0.389
0.022	0.405214	0.5213732	0.399
0.025	0.405759	0.5172428	0.431
0.029	0.408818	0.5162272	0.427
0.03	0.40768	0.5150514	0.439
0.032	0.414284	0.5192267	0.463
0.035	0.409325	0.5168275	0.495
0.036	0.414394	0.5183317	0.519
0.04	0.40954	0.5246544	0.519
0.042	0.404813	0.5344148	0.526
0.044	0.413867	0.5389081	0.599
0.045	0.419032	0.5362492	0.634
0.046	0.42345	0.5315084	0.643
0.048	0.428437	0.5260012	0.668
0.05	0.43043	0.5365285	0.731
0.055	0.424126	0.5998316	0.889
0.06	0.43575	0.5878557	1.21
0.065	0.411671	0.5681867	1.06
0.067	0.417487	0.5513956	0.974
0.07	0.415683	0.5413722	0.986
0.075	0.424339	0.5690792	1.13
0.08	0.436028	0.5343028	1.08
0.085	0.499856	0.5572881	0.873
0.09	0.508231	0.6036101	0.686
0.095	0.549037	0.5664219	0.727
0.1	0.578201	0.5786883	0.87
0.11	0.495335	0.7883717	0.922
0.12	0.502868	0.7234411	0.91
0.13	0.593151	0.5657689	0.776
0.133	0.619676	0.5485201	0.781
0.14	0.65999	0.5711171	0.924
0.15	0.719405	0.6069214	0.822
0.16	0.605086	0.6919746	0.756
0.17	0.577403	0.7379681	0.711
0.18	0.550228	0.889155	0.698
0.19	0.566473	1.067078	0.607
0.2	0.549893	1.259796	0.652
0.22	0.730756	1.463326	0.719
0.24	0.87849	1.317033	0.41
0.25	0.877587	1.161296	0.446

-- Summary of Metadata of Selected Records --		Spectral Ordinate	Record Sequence Number	Mean Squared Error	Scale Factor	Tp-Pulse Period (sec)	5-75% Duration (sec)	5-95% Duration (sec)	Arias Intensity (m/sec)
		SRSS	1164	0.0381	15.2912	-	18.8	38	0
Earthquake name	Year	Station Name	Magnitude	Mechanism	Rjb (km)	Rrup (km)	Vs30 (m/sec)	Lowest Useable Frequency (Hz)	
"Kocaeli Turkey"	1999	"Istanbul"	7.51	strike slip	49.66	49.66	51.95	595.2	16.8842
These records were obtained from the NGA-West2 On-Line Ground-Motion Database Tool									
These records are UNSCALED	Models and reports are requested to acknowledge the Pacific Earthquake Engineering Research Center (PEER) in their work and publications.								
	AT2 = Acceleration DT2 = Displacement VT2 = Velocity								

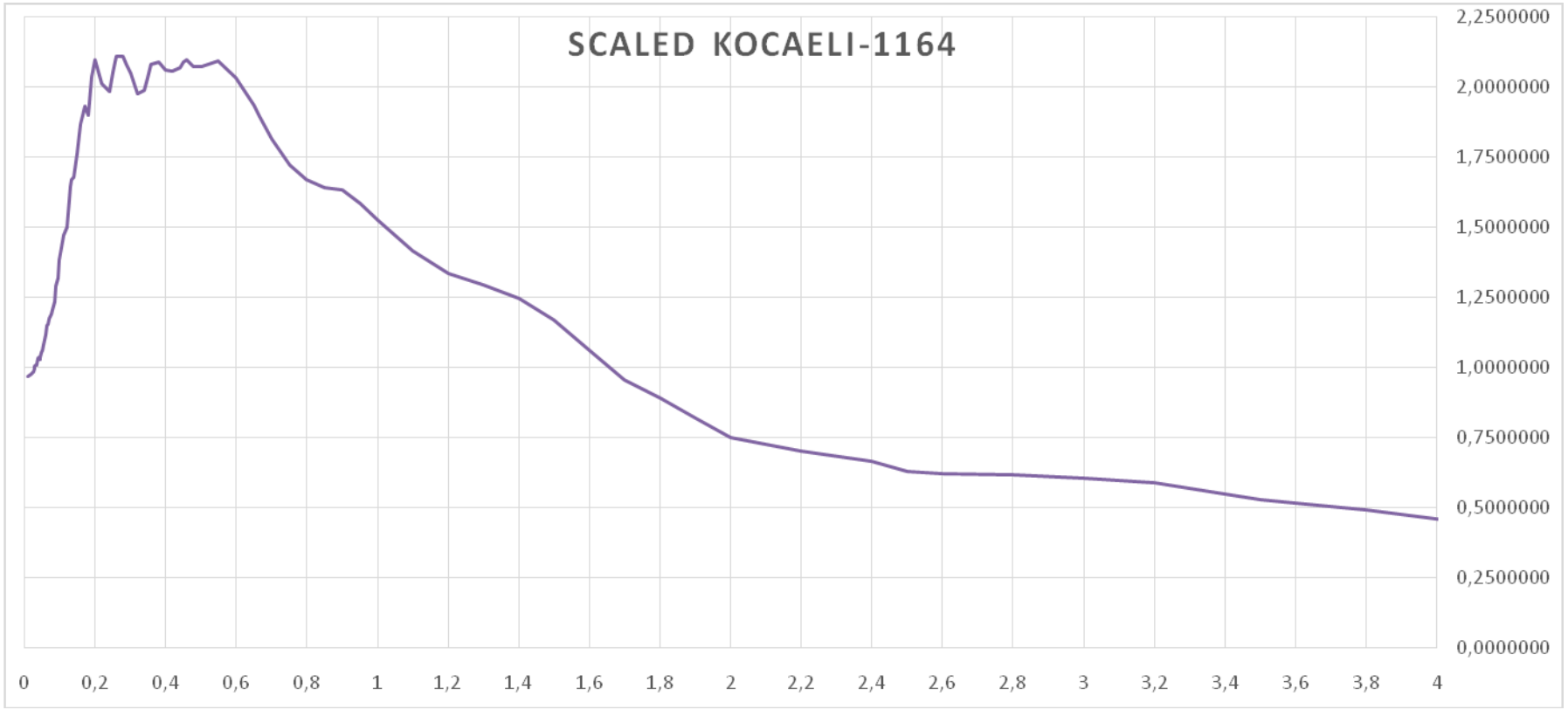
SCALED KOCAELI-1164
2,2500000
2,0000000
1,7500000
1,5000000
1,2500000
1,0000000
0,7500000
0,5000000
0,2500000
0,0000000
0
0,2
0,4
0,6
0,8
1
1,2
1,4
1,6
1,8
2
2,2
2,4
2,6
2,8
3
3,2
3,4
3,6
3,8
4

-- Scaled Spectra used in Search & Scaling --

-- Scaled Spectra used in Search & Scaling --

Period (sec)	Target pSa (g)	Arithmetic Mean pSa (g)	Arithmetic Mean + Sigma pSa (g)	Arithmetic Mean - Sigma pSa (g)	RSN-1164 SRSS pSa (g)
0.01	1.6817928	0.9656627	1.2603617	0.7398704	1.1456833
0.02	1.7718513	0.9727138	1.2824621	0.7377779	1.1404455
0.022	1.7846061	0.9795307	1.3025941	0.7365921	1.1491041
0.025	1.8018576	0.9814039	1.3072223	0.7367941	1.1486344
0.029	1.8220967	0.9951499	1.3548704	0.7309359	1.1430965
0.03	1.8267514	1.0025955	1.3817473	0.7274830	1.1296396
0.032	1.8356455	1.0079626	1.3887883	0.7315648	1.1803484
0.035	1.8480669	1.0060067	1.3712736	0.7380361	1.1600948
0.036	1.8519891	1.0089851	1.3787722	0.7383751	1.1583915
0.04	1.8667322	1.0294822	1.4459241	0.7329801	1.2776790
0.042	1.8735992	1.0326318	1.4538439	0.7334545	1.2881655
0.044	1.8801701	1.0254223	1.4202063	0.7403789	1.3094409
0.045	1.8833526	1.0297329	1.4260639	0.7435500	1.3349453
0.046	1.8864704	1.0358246	1.4430579	0.7435133	1.3494799
0.048	1.8925223	1.0510964	1.4965987	0.7382096	1.3696926
0.05	1.8983454	1.0596524	1.5357805	0.7311352	1.3580310
0.055	1.9120108	1.0778575	1.6170538	0.7184528	1.2389240
0.06	1.9245722	1.1133303	1.6893562	0.7337140	1.3476347
0.065	1.9362005	1.1460148	1.7769875	0.7390879	1.3936245
0.067	1.9406214	1.1517244	1.7871431	0.7422288	1.4486338
0.07	1.9470292	1.1698831	1.8512319	0.7393058	1.4982676
0.075	1.9571649	1.1880774	1.8714237	0.7542535	1.5323066
0.08	1.9666940	1.2050769	1.8936093	0.7669007	1.3849953
0.085	1.9756875	1.2319114	1.9132531	0.7932070	1.4958625
0.09	1.9842044	1.2886973	2.0767348	0.7996884	1.8031088
0.095	1.9922945	1.3181187	2.1045796	0.8255506	1.9775901
0.1	2.0000000	1.3816927	2.2527604	0.8474379	2.2001320
0.11	2.1077060	1.4706900	2.4261320	0.8915134	1.9702039
0.12	2.2110908	1.4996295	2.5149716	0.8942004	1.9209007
0.13	2.3106680	1.6434240	2.9612799	0.9120524	2.0977236
0.133	2.3398632	1.6680982	3.0404888	0.9151659	2.2588207
0.14	2.4068557	1.6740532	3.0278835	0.9255489	2.1941915
0.15	2.5000000	1.7605108	3.2716556	0.9473486	2.2935916
0.16	2.5000000	1.8637098	3.6862497	0.9422623	2.5114825
0.17	2.5000000	1.9293500	3.8573512	0.9650124	2.4170268
0.18	2.5000000	1.8981923	3.5912955	1.0032964	2.5687619
0.19	2.5000000	2.0346478	4.0347123	1.0260438	2.7712208
0.2	2.5000000	2.0929982	4.3719421	1.0019898	2.8420184

-- Scaled Spectra used in Search & Scaling --					
Period (sec)	Target pSa (g)	Arithmetic Mean pSa (g)	Arithmetic Mean + Sigma pSa (g)	Arithmetic Mean - Sigma pSa (g)	RSN-1164 SRSS pSa (g)
0.22	2.5000000	2.0094718	3.6035762	1.1205471	2.9262505
0.24	2.5000000	1.9810782	3.2424363	1.2104080	2.6220665
0.25	2.5000000	2.0487180	3.2930256	1.2745863	2.6103032
0.26	2.5000000	2.1048797	3.3045381	1.3407377	2.4821818
0.28	2.5000000	2.1068023	3.2383068	1.3706595	1.9532885
0.29	2.5000000	2.0795674	3.1612427	1.3680065	1.9014931
0.3	2.5000000	2.0462015	3.0532605	1.3713014	1.8565486
0.32	2.5000000	1.9745213	2.7611511	1.4119959	2.0762674
0.34	2.5000000	1.9839896	2.7304625	1.4415927	2.0533379
0.35	2.5000000	2.0289448	2.8240803	1.4576841	2.2467520
0.36	2.5000000	2.0782287	2.9556363	1.4612875	2.3623478
0.38	2.5000000	2.0858258	2.9629577	1.4683535	2.0677141
0.4	2.5000000	2.0577222	2.8743079	1.4731270	1.7406915
0.42	2.4047070	2.0550920	2.8038388	1.5062932	1.6475499
0.44	2.3172325	2.0649362	2.8409295	1.5009037	1.7280984
0.45	2.2761226	2.0861970	2.8627425	1.5202967	1.6679395
0.46	2.2366218	2.0944605	2.9000051	1.5126749	1.6426683
0.48	2.1620713	2.0722555	2.9998935	1.4314652	1.4807344
0.5	2.0929005	2.0718227	3.0924844	1.3880261	1.3691912
0.55	1.9398948	2.0904037	3.3353478	1.3101445	1.3372384
0.6	1.8100000	2.0306626	3.0231865	1.3639881	1.2269483
0.65	1.6984218	1.9315275	2.7814204	1.3413285	1.1239180
0.667	1.6639204	1.8922327	2.6879310	1.3320821	1.1128017
0.7	1.6012581	1.8118973	2.4870055	1.3200501	1.2179748
0.75	1.5158040	1.7191638	2.2434360	1.3174096	1.1791135
0.8	1.4400000	1.6686718	2.1018675	1.3247579	1.2838014
0.85	1.3715520	1.6408413	2.1289084	1.2646670	1.3892116
0.9	1.3100000	1.6291590	2.1888449	1.2125843	1.3886335
0.95	1.2523475	1.5827030	2.1647090	1.1571758	1.2980783
1	1.2000000	1.5208778	2.1800764	1.0610037	1.1713776
1.1	1.1135068	1.4121451	2.1084096	0.9458094	0.8621497
1.2	1.0400000	1.3309637	1.9679012	0.9001795	0.7797123
1.3	0.9755031	1.2903945	1.9245786	0.8651858	0.8955396
1.4	0.9193598	1.2423444	1.8386895	0.8394128	1.0557711
1.5	0.8700000	1.1679404	1.7650808	0.7728172	1.0694874
1.6	0.8259142	1.0600922	1.6278407	0.6903596	0.9388486
1.7	0.7865389	0.9550364	1.4711420	0.6199908	0.7284576
1.8	0.7511358	0.8883665	1.4161533	0.5572807	0.5643052
1.9	0.7191151	0.8154628	1.3098314	0.5076834	0.5138254
2	0.6900000	0.7470079	1.1928470	0.4678058	0.4652903

-- Scaled Spectra used in Search & Scaling --

-- Scaled Spectra used in Search & Scaling --

Period (sec)	Target pSa (g)	Arithmetic Mean pSa (g)	Arithmetic Mean + Sigma pSa (g)	Arithmetic Mean - Sigma pSa (g)	RSN-1164 SRSS pSa (g)
2.2	0.6406707	0.7001310	1.1454441	0.4279419	0.5034325
2.4	0.5987225	0.6622631	1.1283905	0.3886886	0.4473622
2.5	0.5800000	0.6279277	1.0510513	0.3751417	0.4455235

-- Unscaled Horizontal & Vertical Spectra			
Period (sec)	RSN-1164 Horizontal-1 pSa (g)	RSN-1164 Horizontal-2 pSa (g)	RSN-1164 Vertical pSa (g)
0.01	0.04363989	0.06090311	0.0365
0.02	0.04340328	0.06065124	0.0365
0.022	0.04351963	0.06126372	0.0366
0.025	0.04340621	0.0613065	0.0362
0.029	0.04354159	0.06076543	0.0382
0.03	0.04343943	0.05975386	0.0388
0.032	0.04467233	0.06295122	0.0421
0.035	0.04240064	0.06291208	0.0381
0.036	0.04296567	0.06239236	0.0382
0.04	0.04645398	0.0694527	0.0414
0.042	0.04606606	0.07053114	0.0455
0.044	0.04568162	0.07243113	0.0495
0.045	0.04748499	0.07325772	0.0524
0.046	0.04962533	0.07297747	0.0542
0.048	0.05372645	0.07167225	0.0508
0.05	0.05526829	0.06951846	0.0489
0.055	0.05394961	0.0604481	0.0498
0.06	0.05999991	0.06455316	0.0606
0.065	0.05322154	0.07398472	0.0612
0.067	0.0567456	0.07586093	0.0611
0.07	0.05875276	0.07841302	0.0634
0.075	0.06065676	0.07976482	0.0621
0.08	0.06150592	0.0664887	0.0496
0.085	0.06414933	0.07385495	0.0529
0.09	0.07390662	0.09188258	0.0501
0.095	0.08008222	0.1015512	0.0522
0.1	0.08418678	0.1166815	0.0498
0.11	0.07637715	0.1037672	0.0442
0.12	0.08230955	0.09489873	0.0453
0.13	0.1052431	0.08799727	0.0578

Period (sec)	RSN-1164 Horizontal-1 pSa (g)	RSN-1164 Horizontal-2 pSa (g)	RSN-1164 Vertical pSa (g)
0.14	0.107514	0.09503201	0.0692
0.15	0.1018538	0.1101088	0.0759
0.16	0.1068859	0.1247046	0.069
0.17	0.1079726	0.1154418	0.0787
0.18	0.1128865	0.1244065	0.0867
0.19	0.1355126	0.1203345	0.09
0.2	0.1441514	0.1173202	0.0881
0.22	0.1244164	0.1454035	0.0712
0.24	0.105724	0.1350042	0.103
0.25	0.1024095	0.1365751	0.0994
0.26	0.1106765	0.1187467	0.0806
0.28	0.09158951	0.08904283	0.0845
0.29	0.08548644	0.09030745	0.0918
0.3	0.08629274	0.08540826	0.0908
0.32	0.1050846	0.08598743	0.0868
0.34	0.09637914	0.09350245	0.0791
0.35	0.1107277	0.09658153	0.0741
0.36	0.1254554	0.09015644	0.0684
0.38	0.1166394	0.06841253	0.0561
0.4	0.09530476	0.06225436	0.0524
0.42	0.07970691	0.07249638	0.0608
0.44	0.0829711	0.07673055	0.0658
0.45	0.08355547	0.07011787	0.0633
0.46	0.08521449	0.0654119	0.0582
0.48	0.08060485	0.05366531	0.0502
0.5	0.07714354	0.04545816	0.054
0.55	0.07674555	0.04192666	0.059
0.6	0.06638963	0.04506279	0.0537
0.65	0.04606863	0.05727167	0.0528
0.667	0.04367904	0.05820797	0.0578
0.7	0.05034074	0.06172697	0.057
0.75	0.05329721	0.05572629	0.0494
0.8	0.05723855	0.06142042	0.0416
0.85	0.06416012	0.0643213	0.0322
0.9	0.06065817	0.06758305	0.0365
0.95	0.05390678	0.06557763	0.0344
1	0.04827995	0.05947515	0.0393
1.1	0.03857284	0.04112248	0.0343
1.2	0.03714543	0.03493246	0.0317
1.3	0.04238298	0.04041787	0.0365
1.4	0.04632113	0.05120011	0.0345
1.5	0.04192888	0.05597979	0.0298

Period (sec)	RSN-1164 Horizontal-1 pSa (g)	RSN-1164 Horizontal-2 pSa (g)	RSN-1164 Vertical pSa (g)
1.6	0.0339517	0.05115635	0.0252
1.7	0.02552997	0.04022044	0.0222
1.8	0.02486398	0.02727039	0.0173
1.9	0.02473819	0.02274107	0.0157
2	0.02338204	0.01947246	0.0136
2.2	0.0282332	0.01693534	0.0135
2.4	0.02409532	0.01659323	0.0178
2.5	0.02461729	0.01558485	0.0173
2.6	0.02879616	0.01788869	0.0165
2.8	0.03418195	0.02107217	0.0188
3	0.03023983	0.02283852	0.0199
3.2	0.02439961	0.02376078	0.0189
3.4	0.02002182	0.02321263	0.0208
3.5	0.01988167	0.02505952	0.0211
3.6	0.02109892	0.02525184	0.0209
3.8	0.02516061	0.02264414	0.0191
4	0.02657189	0.02061379	0.017
4.2	0.02478856	0.02031052	0.0159
4.4	0.02146575	0.02182569	0.0161
4.6	0.01846828	0.0226541	0.0167
4.8	0.01639321	0.02227678	0.017
5	0.01468104	0.02177114	0.0168
5.5	0.01269692	0.02018521	0.0149
6	0.01117032	0.01887939	0.0132
6.5	0.01034432	0.01895062	0.0112
7	0.00927419	0.01853455	0.00967
7.5	0.00758001	0.01718566	0.00848
8	0.00610675	0.01507309	0.00735
8.5	0.00520568	0.01270636	0.00684
9	0.00428903	0.01117401	0.00641
9.5	0.0036173	0.00999795	0.00583
10	0.00324578	0.00876979	0.00509

-- Summary of Metadata of Selected Records --		Spectral Ordinate	Record Sequence Number	Mean Squared Error	Scale Factor	Tp-Pulse Period (sec)	5-75% Duration (sec)	5-95% Duration (sec)	Arias Intensity (m/sec)
		SRSS	1633	0.0904	1.7227	-	10.8	29.1	7.5
Earthquake name	Year	Station Name	Magnitude	Mechanism	Rjb (km)	Rrup (km)	Vs30 (m/sec)	Lowest Useable Frequency (Hz)	
"Manjiil Iran"	1990	"Abbar"	7.37	strike slip	12.55	12.55	723.95	0.13	1.7227
These records were obtained from the NGA-West2 On-Line Ground-Motion Database Tool									
These records are UNSCALED	Models and reports are requested to acknowledge the Pacific Earthquake Engineering Research Center (PEER) in their work and publications.								
	AT2 = Acceleration DT2 = Displacement VT2 = Velocity								

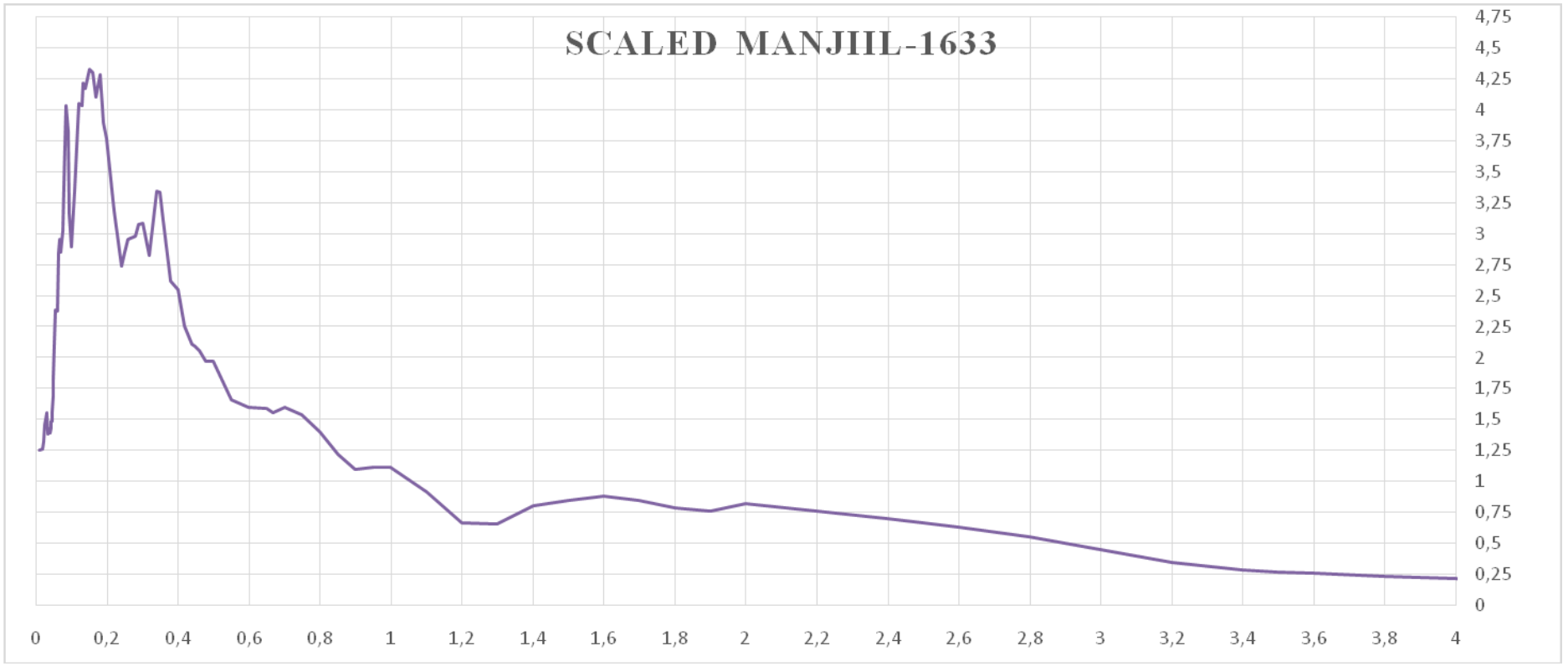
SCALED MANJIIL-1633
4,75
4,5
4,25
4
3,75
3,5
3,25
3
2,75
2,5
2,25
2
1,75
1,5
1,25
1
0,75
0,5
0,25
0
0
0,2
0,4
0,6
0,8
1
1,2
1,4
1,6
1,8
2
2,2
2,4
2,6
2,8
3
3,2
3,4
3,6
3,8
4

-- Scaled Spectra used in Search & Scaling --

-- Scaled Spectra used in Search & Scaling --

Period (sec)	Target pSa (g)	Arithmetic Mean pSa (g)	Arithmetic Mean + Sigma pSa (g)	Arithmetic Mean - Sigma pSa (g)	RSN-1633 SRSS pSa (g)
0.01	1.68179283	1.25204693	1.25204693	1.25204693	1.25204693
0.02	1.77185126	1.25794684	1.25794684	1.25794684	1.25794684
0.022	1.78460609	1.32177469	1.32177469	1.32177469	1.32177469
0.025	1.8018576	1.45484069	1.45484069	1.45484069	1.45484069
0.029	1.82209667	1.50214662	1.50214662	1.50214662	1.50214662
0.03	1.8267514	1.55531855	1.55531855	1.55531855	1.55531855
0.032	1.83564553	1.54295016	1.54295016	1.54295016	1.54295016
0.035	1.84806694	1.38227155	1.38227155	1.38227155	1.38227155
0.036	1.85198912	1.42237752	1.42237752	1.42237752	1.42237752
0.04	1.86673223	1.38903163	1.38903163	1.38903163	1.38903163
0.042	1.87359915	1.43208703	1.43208703	1.43208703	1.43208703
0.044	1.88017007	1.48651557	1.48651557	1.48651557	1.48651557
0.045	1.8833526	1.48635089	1.48635089	1.48635089	1.48635089
0.046	1.88647039	1.56397413	1.56397413	1.56397413	1.56397413
0.048	1.89252231	1.68903917	1.68903917	1.68903917	1.68903917
0.05	1.89834539	1.82252968	1.82252968	1.82252968	1.82252968
0.055	1.9120108	2.37873707	2.37873707	2.37873707	2.37873707
0.06	1.92457222	2.37259491	2.37259491	2.37259491	2.37259491
0.065	1.93620048	2.83676705	2.83676705	2.83676705	2.83676705
0.067	1.94062142	2.95015414	2.95015414	2.95015414	2.95015414
0.07	1.94702919	2.84730572	2.84730572	2.84730572	2.84730572
0.075	1.9571649	3.02360494	3.02360494	3.02360494	3.02360494
0.08	1.96669399	3.38093239	3.38093239	3.38093239	3.38093239
0.085	1.97568745	4.03022669	4.03022669	4.03022669	4.03022669
0.09	1.98420437	3.82392004	3.82392004	3.82392004	3.82392004
0.095	1.99229447	3.15809367	3.15809367	3.15809367	3.15809367
0.1	2	2.88980868	2.88980868	2.88980868	2.88980868
0.11	2.10770601	3.34296181	3.34296181	3.34296181	3.34296181
0.12	2.21109081	4.05259497	4.05259497	4.05259497	4.05259497
0.13	2.31066799	4.02945275	4.02945275	4.02945275	4.02945275
0.133	2.33986323	4.2171018	4.2171018	4.2171018	4.2171018
0.14	2.40685572	4.17233854	4.17233854	4.17233854	4.17233854
0.15	2.5	4.32507521	4.32507521	4.32507521	4.32507521
0.16	2.5	4.29840564	4.29840564	4.29840564	4.29840564
0.17	2.5	4.09749434	4.09749434	4.09749434	4.09749434
0.18	2.5	4.28195091	4.28195091	4.28195091	4.28195091
0.19	2.5	3.892	3.892	3.892	3.892
0.2	2.5	3.7677594	3.7677594	3.7677594	3.7677594
0.22	2.5	3.18875404	3.18875404	3.18875404	3.18875404
0.24	2.5	2.73931182	2.73931182	2.73931182	2.73931182

Period (sec)	Target pSa (g)	Arithmetic Mean pSa (g)	Arithmetic Mean + Sigma pSa (g)	Arithmetic Mean - Sigma pSa (g)	RSN-1633 SRSS pSa (g)
0.25	2.5	2.84861589	2.84861589	2.84861589	2.84861589
0.26	2.5	2.95332154	2.95332154	2.95332154	2.95332154
0.28	2.5	2.97632609	2.97632609	2.97632609	2.97632609
0.29	2.5	3.07360527	3.07360527	3.07360527	3.07360527
0.3	2.5	3.0848503	3.0848503	3.0848503	3.0848503
0.32	2.5	2.82210157	2.82210157	2.82210157	2.82210157
0.34	2.5	3.33639585	3.33639585	3.33639585	3.33639585
0.35	2.5	3.32777739	3.32777739	3.32777739	3.32777739
0.36	2.5	3.1081946	3.1081946	3.1081946	3.1081946
0.38	2.5	2.61891456	2.61891456	2.61891456	2.61891456
0.4	2.5	2.54178163	2.54178163	2.54178163	2.54178163
0.42	2.40470696	2.24975609	2.24975609	2.24975609	2.24975609
0.44	2.31723254	2.10477923	2.10477923	2.10477923	2.10477923
0.45	2.27612257	2.08734266	2.08734266	2.08734266	2.08734266
0.46	2.23662175	2.0527047	2.0527047	2.0527047	2.0527047
0.48	2.1620713	1.96386973	1.96386973	1.96386973	1.96386973
0.5	2.09290045	1.96631845	1.96631845	1.96631845	1.96631845
0.55	1.93989481	1.65830169	1.65830169	1.65830169	1.65830169
0.6	1.81	1.59517471	1.59517471	1.59517471	1.59517471
0.65	1.69842175	1.58327352	1.58327352	1.58327352	1.58327352
0.667	1.66392037	1.55195231	1.55195231	1.55195231	1.55195231
0.7	1.60125814	1.59398936	1.59398936	1.59398936	1.59398936
0.75	1.51580396	1.5331979	1.5331979	1.5331979	1.5331979
0.8	1.44	1.39899609	1.39899609	1.39899609	1.39899609
0.85	1.37155195	1.21304431	1.21304431	1.21304431	1.21304431
0.9	1.31	1.09267944	1.09267944	1.09267944	1.09267944
0.95	1.2523475	1.11313436	1.11313436	1.11313436	1.11313436
1	1.2	1.11433503	1.11433503	1.11433503	1.11433503

-- Unscaled Horizontal & Vertical Spectra			
Period (sec)	RSN-1633 Horizontal-1 pSa (g)	RSN-1633 Horizontal-2 pSa (g)	RSN-1633 Vertical pSa (g)
0.01	0.5260827	0.5014857	0.545
0.02	0.5300136	0.5023213	0.546
0.022	0.5559552	0.5288107	0.566
0.025	0.5939077	0.60042	0.644
0.029	0.5918179	0.6404056	0.575
0.03	0.6432602	0.6335351	0.599
0.032	0.6384428	0.6281943	0.612
0.035	0.5903909	0.5434061	0.603
0.036	0.596225	0.5712018	0.589
0.04	0.5867854	0.5530348	0.59
0.042	0.5940158	0.5815844	0.597
0.044	0.6121947	0.6081474	0.612
0.045	0.6303685	0.5891487	0.63
0.046	0.6759795	0.606053	0.653
0.048	0.6891776	0.6974077	0.701
0.05	0.7611849	0.7347803	0.723
0.055	1.063649	0.8805639	0.828
0.06	0.9482766	0.998839	0.9
0.065	0.9775038	1.325223	0.979
0.067	0.9476262	1.42648	0.971
0.07	0.9383732	1.360651	1.09
0.075	1.054981	1.402752	1.26
0.08	1.031385	1.669766	1.46
0.085	1.063287	2.083946	1.33
0.09	1.05372	1.95373	1.18
0.095	1.193933	1.391177	1.47
0.1	1.1269	1.242651	1.37
0.11	1.26118	1.474878	1.45
0.12	1.469658	1.836965	1.5
0.13	1.390896	1.880616	1.75
0.133	1.608433	1.845456	1.73
0.14	1.79725	1.62361	1.49
0.15	1.979883	1.543901	1.44
0.16	2.079983	1.37831	1.74
0.17	1.881151	1.45565	1.97
0.18	1.973588	1.511106	1.76
0.19	1.767726	1.406963	1.45
0.2	1.68392	1.395754	1.25
0.22	1.30813	1.309664	1.08
0.24	1.209944	1.031817	0.899

Period (sec)	RSN-1633 Horizontal-1 pSa (g)	RSN-1633 Horizontal-2 pSa (g)	RSN-1633 Vertical pSa (g)
0.25	1.219363	1.116953	0.936
0.26	1.210658	1.213857	1.09
0.28	1.118014	1.317252	1.18
0.29	1.129317	1.38133	1.25
0.3	1.135605	1.384618	1.19
0.32	1.134263	1.182037	1.04
0.34	1.203122	1.517748	0.807
0.35	1.234424	1.485902	0.791
0.36	1.213422	1.335324	0.819
0.38	1.144373	1.000816	0.732
0.4	1.078269	1.007185	0.679
0.42	0.9657459	0.8791509	0.659
0.44	0.8586475	0.8692299	0.62
0.45	0.7957623	0.9137652	0.59
0.46	0.7325432	0.93982	0.543
0.48	0.6765237	0.9175836	0.505
0.5	0.6362801	0.9476469	0.513
0.55	0.5592761	0.7835065	0.577
0.6	0.6768752	0.6319045	0.517
0.65	0.7492633	0.532279	0.432
0.667	0.7615529	0.4813137	0.475
0.7	0.8134103	0.4410818	0.477
0.75	0.6683314	0.5877596	0.45
0.8	0.6400973	0.4998016	0.427
0.85	0.5773455	0.4031433	0.331
0.9	0.4543637	0.4425897	0.301
0.95	0.3875226	0.5170711	0.327
1	0.354223	0.5412611	0.371
1.1	0.226424	0.4771459	0.393
1.2	0.1622998	0.3498027	0.332
1.3	0.211613	0.3149995	0.363
1.4	0.2162782	0.4136255	0.345

CURRICULUM VITAE

Name Surname: Keyvan Dehghanian

Place and Date of Birth: Tabriz-1988

E-Mail: Dehghanian@outlook.com

EDUCATION: B.Sc in civil engineering

B.Sc.: Tabriz Azad University